Ministry of Higher Education

& Scientific Research

University of Technology

Chemical Engineering Department

Fabrication And Performance Of Pol-phenyl Sulfone Forward osmosis Hollow Fiber Membrane For Desalinate Saline Water

A Thesis

Submitted to the

Department of Chemical Engineering at the University of Technology

in a Partial Fulfillment of the Requirements for the Degree of Master of Science in Chemical Engineering / Chemical Processing Engineering

By

Mariam Jbor Jaafer

Supervised By

Prof. Dr.Qusay F. Alsalhy ***Asst. prof. Dr.Jenan A. Al-Najar***

1439 ***2018***

Acknowledgments

First of all I thank the Almighty "Allah", whose Grace enabled me to continue this work and overcome all difficulties.

I would like to express my deepest appreciation to my supervisors, ***Prof. Dr. Qusay. F. Alsalhy and Asst. prof. Dr.Jenan A. Al-Najar*** *for their invaluable supervision, mentorship, and support, which were instrumental in completing this research.*

I wish to express my gratefulness to the head of the Chemical Engineering Department ***Asst Prof. Dr. Jamal M. Ali*** *for his help throughout the work.*

I would like to convey my sincere appreciation to all staff of Chemical Engineering Department at University of Technology, especially ***Mr. Basheer Ahmed*** *and all others who have helped me.*

Abstract

In this study the factors affecting the performance of the forward osmosis (FO) process for saline water desalination through the utilized three different concentration of hollow membranes was investigated. Three Poly (phenyl sulfone) (PPSU) hollow fibers with different polymer contents were fabricated using a method of phase inversion used in forward osmosis (FO) process. Various characteristics such as surface and cross-sectional structure, membrane thickness, surface roughness, mean pore size and pore size distribution were measured using scanning electron microscopy (SEM) and Atomic Force Microscope (AFM) as well as the porosity of the hollow fibers was also measured. The effect of operating conditions such as draw solutions (DS) concentration which was Sodium chloride (NaCl) solution of (1–3M) , feed solutions (FS) concentration, i.e., deionized water (DI) and 0.5 M of Sodium chloride (NaCl) , draw solutions flow rate of (0.1- 1.0 l/min), feed solutions flow rate of (0.1- 1.0 l/min) on the FO performance were studied at constant pressure (atmospheric pressure) and temperature of 25±5 ºC. It was observed that as the draw solution (DS) content and flow rate of the feed increased, the water flux increased, while with increasing of content of the feed and draw solution DS flow rate resulted to decrease the water flux. Poly (phenyl sulfone) PPSU 25% hollow fiber membrane showed a forward osmosis (FO) flux of (13.48 L m^{-2} h^{-1}) when tested in the active layer facing to feed solution mode using 0.5 M and 3 M sodium chloride as feed and draw solutions respectively. the increasing in the water flux for the concentration 1.0−1.5 M is between 43− 55%, while for concentration 1.5−2.0 M, 2.0−2.5

M, and 2.5−3.0 M were 21−39%, 24− 23%, and 18− 23% respectively for three hollow fiber (HFFO) membranes. This outcome reveals that higher water flux obtained with concentration of 1.0−1.5 M., while the reverse salt flux was 7.30 gMH. In addition, pure water permeability (PWP) PPSU 25% membrane showed PWP value (2.25 L m^{-2} h^{-1} bar^{-1}) higher by 29% and 56% respectively than PPSU 29% (PWP 1.59 L m^{-2} h^{-1} bar^{-1}) and PPSU 30% (PWP 0.99 L m^{-2} h^{-1} bar^{-1}) and salt permeability (B) was (0.37 L m^{-2} h^{-1}) for PPSU 25% which was also higher than the other two membranes. The pore size was reduced by about (22.28 and 28.75%) of inner surface, whereas for outer surface was reduced by about (26.88 and 38.78%) with increasing the **PPSU** polymer concentration from 25 wt.% to 29 and 30 wt.%, respectively. The structural parameter (S) displayed lower value for PPSU 25% of (467 µm) which was well corresponding to its performance. In conclusion, the results indicated that the forward osmosis process was an encouraging performance and the Poly (phenyl sulfone) PPSU hollow fiber membrane was able to desalinate saline water with different concentrations and sources.

Nomenclature

Symbol	Definition	Units
A	Water Permeability Coefficient	$l/m^2.h.bar$
A_m	Area of membrane	M^2
B	Salt permeability coefficient	m/s
CF	Feed side concentration	gm/L
CP	Permeate side concentration	gm/L
D	Solute diffusion coefficient	m^2/s
D*	Mean pore size	nm
d_{in} / ID	Inner diameter	cm
d_{out} / OD	Outer diameter	cm
G	measured weight	gm
JS	Salt flux	LMH
J_W	Water flux	l/m^2 hr
K	Mass transfer coefficient	m/s
M	solution molarity	mol/L
P	Pressure	bar
QDS	Draw solution flow rate	L/min
QFS	Feed solution flow rate	L/min
Ra	Mean roughness	nm
R_g	General gas constant	L atm/mol K
R_{rms}	The root mean square	nm

Rs	Rejection Percentage	
RSF	Reverse salt flux	g/m^2 hr
S	structural parameter	μm
SRSF	Specific reverse salt flux	gm/L
T	Temperature	K
t	Membrane thickness	m

GREEK SYMBOLS

Symbol	Definition	Units
ε	Porosity of the support layer	
μw	Water chemical potential	Joule / mole
μ_{wD}	Draw solution chemical potential	Joule / mole
μ_{wF}	Feed solution chemical potential	Joule / mole
π	Osmotic pressure	bar
π_D	Draw solution osmotic pressure	bar
π_F	Feed solution osmotic pressure	bar
σ	reflection coefficient	
τ	Tortuosity of the support layer	
π_{FB}	Feed bulk osmotic pressure	bar
π_{Fm}	Membrane surface osmotic pressure	bar

ABBREVIATION

Symbol	Definition
AFM	Atomic Force Microscopy
AL	Membrane active layer
CA	Cellulose acetate
CASS	carboxyethyl amine sodium salts
CECP	Concentrative external concentration polarization
CP	Concentration polarization
DECP	Dilutive external concentration polarization
DI	Deionized water
DS	Draw solution
ECP	external concentration polarization
ED	Electrodialysis
FO	Forward osmosis
FS	Feed solution
HFFO	Hollow fiber forward osmosis
HTI	Hydration Technologies Innovations
ICP	internal concentration polarization
MED	multiple effect evaporation
MF	Microfiltration
MNPs	Magnetic nanoparticles
MSF	multistage flash desalination
MVC	mechanical vapor compression process
MWCO	Molecular Weight cute off
NF	Nanofiltration

PA	Polyamide
PAI	polyamide–imide
PAN	polyacrylonitrile
PBI	Polybenzimidazole
PEI	polyethyleneimine
PESU	polyethersulfone
PFSA	Perfluorosulfonic acid
PK	porous polyketone
PPSU	polyphenylenesulfone
PRO	pressure rented osmosis
PSF	polysulfone
PSU	polysulfone
PVDF	polyvinylidene fluoride
PVP	polyvinylpyrrolidone
PWP	Pure water permeability
RO	Reverse osmosis
SEM	Scanning Electron Microscopy
SPES	sulphonated polyethersulfone
SPPO	sulfonated poly (phenylene oxide)
SPSf	Sulfonated polysulfone
SWFO	Spiral-wound forward osmosis
TDS	Total Dissolved Solids
TFC	Thin film composite
TFN	Thin film nanocomposite
TMP	transmembrane pressure
TTHP-Na	Triethylenetetramine hexapropionic acid sodium

UF	Ultrafiltration
VCD	Vapour compression distillation

List of Contents

Subject	Page
Acknowledgement ……..	I
Abstract ……..	II
Nomenclature ……..	IV
Greek Symbols …….	V
Abbreviations ……	VI
List of Contents ……	IX
List of Tables ……	XII
List of Figures ……	XIII
Chapter One : Introduction	
1. Introduction …….	1
1.2 Objectives and Scope of this Study …….....	6
Chapter Two : Literature Survey	
2. Introduction …….	8
2.1 Principle work of forward Osmosis ……..……..	10
2.2 Membrane modules and devices ……..	11
2.2.1 Plate-and-frame ……	13
2.2.2 Spiral-wound ……...	14
2.2.3 Tubular and Hollow fiber ..…….	15
2.2.4 Hydration bags ……	17
2.3 Challenges for FO……..……	18
2.3.1. Concentration polarization……	18

2.3.1.1 Internal Concentration Polarization (ICP)…….. 19
2.3.1.2 External Concentration Polarization (ECP)…… 21
2.3.1.3 Impacts of Concentration Polarization…… 21
2.3.2. Membrane Fouling……...…….. 23
2.3.3. Reverse Solute Flux …….. 23
2.3.4. Membrane Cleaning Strategies ……. 25
2.3.5 FO membranes……. 25
2.3.6 Draw solutions……..... 26
2.4 Literature survey…… 27

Chapter Three : Experimental Work

3. Experimental work ……. 41
3.1 Materials ……..... 41
3.1.1 Membranes …….. 42
3.1.1.1 Membrane characterization …… 43
3.1.2 Feed and draw solutions ……. 44
3.2 Forward Osmosis System …… 45
3.3 Measurement of FO performance …… 49
3.3.1 Water permeability coefficient (A) ……... 49
3.3.2 The salt rejection (Rs) …… 50
3.3.3 Salt permeability coefficient (B)……. 50
3.3.4 The structural parameter (*S*)……... 51
3.3.5 Water flux ……... 52
3.3.6 Solute flux…… 52

Chapter Four: Results and Discussion

4 General …… 54
4.1. Hollow fiber forward osmosis analysis 54

4.1.1 Scanning electron microscope (SEM)……. 54
4.1.2. Atomic Force Microscope (AFM) analysis…… 61
4.2 Parameters Affected Membrane Performance …… 67
4.2.1 Porosity and thickness……... 67
4.2.2 Structural parameter (S)…… 69
4.3 Mass transport characteristics of HFFO membranes…… 70
4.3.1 Water permeability coefficient (A)……. 70
4.3.2 Salt rejection (Rs)……... 72
4.3.3 Salt permeability coefficient (B)……... 72
4.4 Effect of Operating Conditions …… 72
4.4.1 Flux variation with time……. 73
4.4.2 Effect of Draw Solution Concentration on Water Flux.. 74
4.4.3 Effect of Draw Solution Flow Rate…… 75
4.4.4 Effect of Feed Solution Flow Rate……. 76
4.4.5 Reverse Salt Flux variation with time ……... 78
4.4.6 Reverse draw solute flux as a function of draw solution concentration……... 78
4.4.7. Specific revers salt flux with draw solution concentration ……..... 80
4.4.8 Specific Salt Flux variation with time……... 80
4.5 Comparison the FO performances in the present work with other research……. 81

Chapter Five: Conclusions and Recommendations

5. Conclusions…….. 84
5.1 Recommendations for Further Work …… 85

References…… 86– 99

A-Table of Experimental Results……...……...…. 100

List of Tables

Table	Page
Table 1.1 Percentage of pure water around the world produced at different rates from varies desalination processes ……	3
Table 2.1 Comparison among RO, FO, and PRO process……..	12
Table 2.2 Summary of notable FO membrane developments….	37
Table 3.1 Sodium chloride (NaCl) solutions chemical specification ……	41
Table 3.2 Spinning parameters of PPSU hollow fiber membranes……	42
Table 3.3 Variables of operating conditions for FO process……	48
Table 4.1 Summary of the Characteristics for three HFFO membranes…….....	55
Table 4.2 Mean Pore Size and pore size distribution, and Roughness of the inner surface of PPSU Hollow Fiber Membranes. ……	67
Table 4.3 Mean Pore Size and pore size distribution, and Roughness of the outer surface of PPSU Hollow Fiber Membranes. ……	67
Table 4.4: Summary of the transport parameters A, B, RS and S, calculated by the RO experiments. With porosity, thickness and length for three HF membranes……	72

List of Figures

Figure	Page
Figure 1.1: Water desalination technologies ……	2
Figure 1.2: Principle of forward Osmosis process ……..	5
Figure 2.1. (A) Shows the ability of different techniques to expel the suspended and dissolved materials, (B) membranes pore size used in different types of desalination processes. ……	9
Figure. 2.2. Water diffuses in FO, PRO, and RO system ……..	11
Figure.2.3. Flat-sheet FO membranes installed in plate and frame modules design ……	14
Figure.2.4. Spiral wound for forward osmosis (SWFO) …..	15
Figure 2.5. Tubular membrane module. ……	16
Figure 2.6. Hollow fiber membrane module …….	16
Figure.2.7. Water purification by hydration bag ……	17
Figure.2.8 Schematic description for (a) dilutive internal concentration polarization, and (b) concentrative internal concentration polarization……..	20
Figure. 2.9 The retarded forward diffusion of feed solutes in the forward osmosis process by the reverse draw Solutes……	24
Figure 3.1 The Scanning Electron Microscope (SEM) device…	43
Figure 3.2 Photograph of FO system ……..	46
Figure 3.3 The schematic diagram of the experimental bench scale FO process……..	46
Figure 3.4 Hollow fiber module…….	48
Figure 3.5 Picture for Membrane Module…….	49
Figure 4.1 Membrane dimensions calculation concentrations…..	55

Figure 4.2. The hollow fibers membranes outer surface SEM images with different PPSU concentrations: (a) 25 wt % , (b) 29 wt % , (c) 30 wt %..... 56
Figure 4.3 The hollow fibers membranes inner surface SEM images with different PPSU concentrations: (a) 25 wt % , (b) 29 wt % , (c) 30 wt %.....…….. 57
Figure 4.4 The PPSU 25 wt% hollow fiber membrane cross section SEM images……. 58
Figure 4.5 The PPSU 29 wt% hollow fiber membrane cross section SEM images……. 59
Figure 4.6 The PPSU 30 wt% hollow fiber membrane cross section SEM images…… 60
Figure 4.7. The inner surfaces of the PPSU hollow fibers topography and three-dimensional AFM images with different PPSU concentrations…….. 64
Figure 4.8. The outer surfaces of the PPSU hollow fibers topography and three-dimensional AFM images with different PPSU concentrations…….. 65
Figure 4.9 The normal distribution chart of pores for the inner and outer surfaces of the PPSU hollow fibers…… 66
Figure.4.10 Relationship between polymer percentage in membrane and porosity…… …….. 68
Figure.4.11 Relationship between polymer percentage in membrane and thickness…….…. 69
Figure. 4.12 Water Flux Change with pressure for PPSU 25% . 70
Figure. 4.13 Water Flux Change with pressure for PPSU 29% . 71

Figure. 4.14 Water Flux Change with pressure for PPSU 30% . 71
Figure .4.15 Water Flux Change with time…….. 74
Figure .4.16 Water Flux Change with Concentration Draw Solutes…….. 75
Figure .4.17 Water Flux Change with DS flow rate…… 76
Figure .4.18 Water Flux Change with FS flow rate …….. 77
Figure 4.19 Reverse Salt Flux with Time…… 78
Figure.4.20 Effect of Draw Solution Concentration on the reverse salt flux……. 79
Figure 4.21 Comparison of Specific Salt Flux with Different concentration of Draw Solutions for three types of membranes... 80
Figure.4.22 Specific salt flux with Time…… 81

CHAPTER ONE
INTRODUCTION

1. Introduction

Water is one of the most important elements of life's living necessities to meet the needs of living beings on Earth. With increasing population growth and demand for water for different needs such as drinking, water shortage has become a global problem of daily life. Therefore, it has been important to search for a wide range of sources to cover the water shortage. One of these reliable methods is desalination of sea water and saltwater in general. There are several techniques applied to mitigate this problem, but the use of energy in water desalination is considered to be somewhat expensive when applying conventional thermal separation techniques **(Xiong et al., 2016; Zhao et al., 2012)**. For distillation process, which can be described as a way to remove salts from water, this technology has become an important clean water source **(Trung et al., 2017; Arkhangelsky et al., 2012)**. Water containing less than 1,000 mg L^{-1} salts or total dissolved solids (TDS) can be called as clean water **(Linares et al., 2014)**. Actually, there are two types of technology currently employed widely for water desalination are generally considered thermal technology or membrane technology **(Trung et al., 2017).** Thermal technologies, as indicated by their name, are based on the principle of using heat in salt water evaporation and collecting steam condensate output from the process of distillation to produce pure water, but the use of this technique in desalination of saline water is considered to be rather expensive in terms of economic cost**(Krishna et al.,2004)**.

In contrast, the technology used in membrane separation is a fast-developing that utilizes many great variety sub-techniques and many materials used in the manufacture of membranes **(Linders et al., 1992)**, the use of membranes in the process of purification has become very

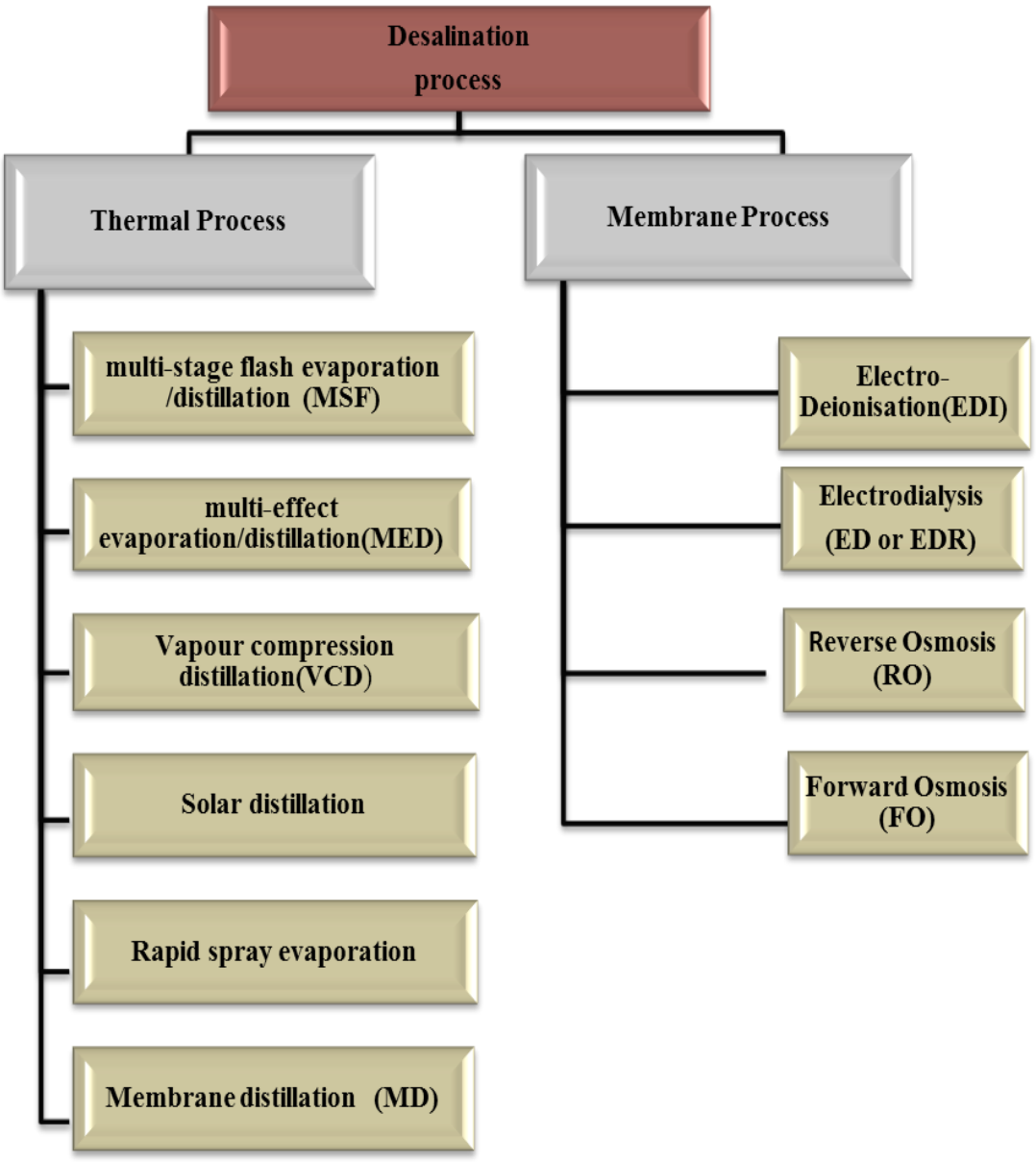

Figure 1.1: Water desalination technologies.

common in recent times due to increasing environmental pollution, not only to the ability to desalinate water, but also to remove the impurities in it **(Shon et al., 2002).** The important types of the two technologies are shown in Figure (1.1) **(Clayton et al., 2015).**

Reverse osmosis has clearly dominated the present time on desalination process, in addition to the multistage flash desalination (MSF) processes. While some thermal desalination processes such as mechanical vapor compression process (MVC) and the multiple effect evaporation (MED), their uses are probably limited **(Subramani et al., 2015)**. Pure water around the world is produced at different rates from various desalination processes. The following Table 1.1 illustrates that.

Table 1.1: Percentage of pure water around the world produced at different rates from various desalination processes **(Alkaisi et al., 2017).**

Desalination process	Contribution to the world water production
Reverse osmosis (RO)	62%
Multi-effect evaporation/distillation(MED)	14%
Multi-stage flash evaporation /distillation (MSF)	10%
Electrodialysis (ED or EDR)	5%
Vapour compression distillation(VCD)	5%
Others	4%

In spite of widespread use of reverse osmosis in desalination processes as described in Table 1.1, the capacitive energy used to exceed the osmotic pressure by generating hydraulic pressure and to drive the process is very high

(Linares et al., 2014; Ong et al., 2012). Energy has an important influence on the cost of desalination. The reduce energy usage makes the desalination process at reasonable prices.

In recent years, the forward osmosis process has become an emerging technology for desalination of saline water, which can be applied in Iraq to filter water of the two rivers from impurities and desalinate the water accompanying the extraction of oil (and it is also known that the country is rich in oil wealth, which must be exploited in all respects).

Which has several advantages compared to reverse osmosis process and other desalination technologies; such as high rejection of contaminants substances, relatively little energy and low membrane fouling **(Darwish et al.,2014).** FO process depends on the chemical potential between two solutions that have different concentrations separated by a semi-permeable membrane. Water transport from feed solution (FS) that has low concentration and osmotic pressure solution (π_F) to draw solution (DS) that has high concentration and osmotic pressure (π_D) solution due to the osmotic pressure gradient as shown in Figure (1.2) **(Hawari et al., 2016)**. Depending on the second law of thermodynamic, the driving force for FO process is the water chemical potential (μ_w) difference between the DS (low $\mu_{w,D}$) and the FS (high $\mu_{w,F}$) **(Darwish et al., 2014; Ge et al., 2013).**

$$\Delta\mu_w = \mu_{W,F} - \mu_{W,D} \qquad 1.1$$

Forward osmosis has made progress and wide performance in various applications, such as desalination, wastewater concentration, resource recovery, wastewater treatment while drawing attention to the fact that it has the ability to increase its water supply by treating the seawater and wastewater

(Korenak et al., 2017). Despite the good performance of the process of osmosis, there are only a few obstacles that must be overcome for a perfect integrated process, such as fouling and internal concentration polarization (ICP) through the search for suitable membranes and draw solution of high efficiency and easy retrieval **(Low et al., 2015; Kim et al., 2015)**.

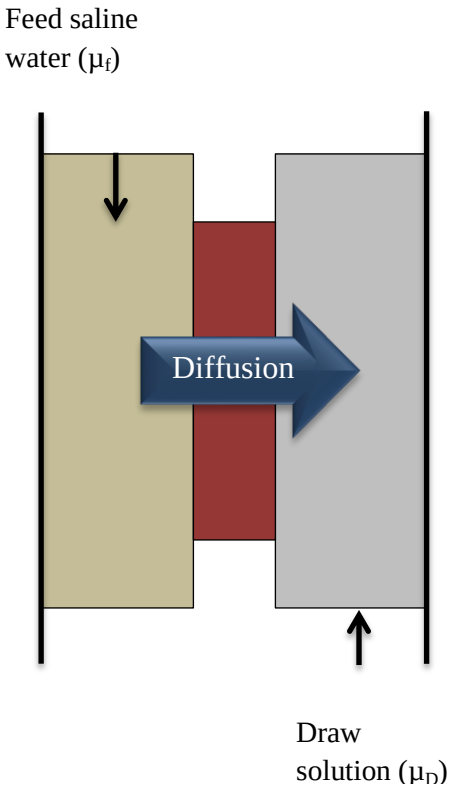

Figure 1.2: Principle of forward Osmosis process

Similar to RO process, the forward osmosis process uses semi-permeable membranes, which must have a high ability to separate water from dissolved solids, provide high permeability of water, high salt rejection, and considerably reduce the internal and external concentration polarization (ICP, ECP), mechanical resistance and a well chemical stability. As well as, a good

draw solution (DS) should have these excellence properties: a high water flux from osmosis cell, lower reverse solute flux (RSF), zero toxicity, a moderately low cost, and easy reclamation. Also it must be compatible with the forward osmosis membrane **(Ge et al., 2013; Wang et al 2012).**

Many polymers were selected and tested in the manufacture of membranes that have a hydrophilic property to use in the forward osmosis process such as polysulfone (PSF), Polybenzimidazole (PBI), polyamide (PA), polyvinylpyrrolidone (PVP), polyvinylidene fluoride (PVDF), polyacrylonitrile (PAN), Poly (phenyl sulfone) (PPSU) and polyethersulfone (PESU) **(Altaee et al., 2014; Lutchmiah et al., 2014; Feng et al., 2016).** One of these polymers used is the polyphenylsulfone (PPSU), which has interesting properties when entering into the manufacture of various membranes such as good resistance to chemical materials, has a good hydrolysis stability, appeared mechanical strength and good glass transition temperature **(Feng et al., 2016).** Depending on the particular manufacturing method, the resulting membranes are divided into three main categories: thin film composite (TFC) membranes, phase inversion-formed cellulosic membranes, and chemically modified membranes **(Zhao et al., 2012)**.

1.2 Objectives and Scope of this Study

- The main aim of this work is to examine the efficiency of forward osmosis (FO) technique as a process for desalination of saline water using three types of PPSU hollow fiber membranes.

- Investigating the effect of PPSU concentration on properties of PPSU HF membranes such as morphological structure, porosity, pore size and thickness

and find the suitability of these membranes for the forward osmosis process applications.

- Study the effect of the different parameters such as concentration of draw solution, and feed and draw solutions flow rate on water flux of PPSU HFs.

CHAPTER TWO

Theoretical concepts and Literature Survey

2. Introduction

The shortage of potable water in countries suffering from a lack of freshwater resources has led to the search for alternative sources of saline water desalination **(McCutcheon et al., 2006)**. Until now, desalination processes related to the membranes such the reverse osmosis process (RO), and nanofiltration (NF), which are considered to have little productivity due to fouling as a result using the hydraulic pressure as a driving force to exceed the osmotic pressure of the feed water which causes an increase in operational costs **(Mi et al., 2010; McCutcheon et al., 2006).**

Although reverse osmosis (RO) has been widely spread, its desalination of saline water is somewhat limited 62% **(McCutcheon et al., 2006; Alkaisi et al., 2017)**. That is related to three obstacles when used, such as hydraulic pressure controlling the process (≈ 60 bar), which causes an increase in energy consumption for desalination process. The primary treatment is necessary to maintain operational units and membranes, as well as membranes fouling which leads to decrease in water permeability and increase feed channel pressure drop **(Linares et al., 2014)**. Therefore, more suitable, economic and suitable production processes have been sought for saline water desalination, such as forward osmosis process, that uses semipermeable polymeric membranes, which can become a sustainable alternative to other desalination

processes **(Mi et al., 2010; McCutcheon et al., 2006)**. The fouling ability of forward osmosis is fairly low due to the low or no hydraulic pressure used to produce water compared to other pressure driven processes **(Yang et al., 2016)**. Figure (2.1) illustrates pore size with principle and ability of pressure-driven membrane processes for water purification.

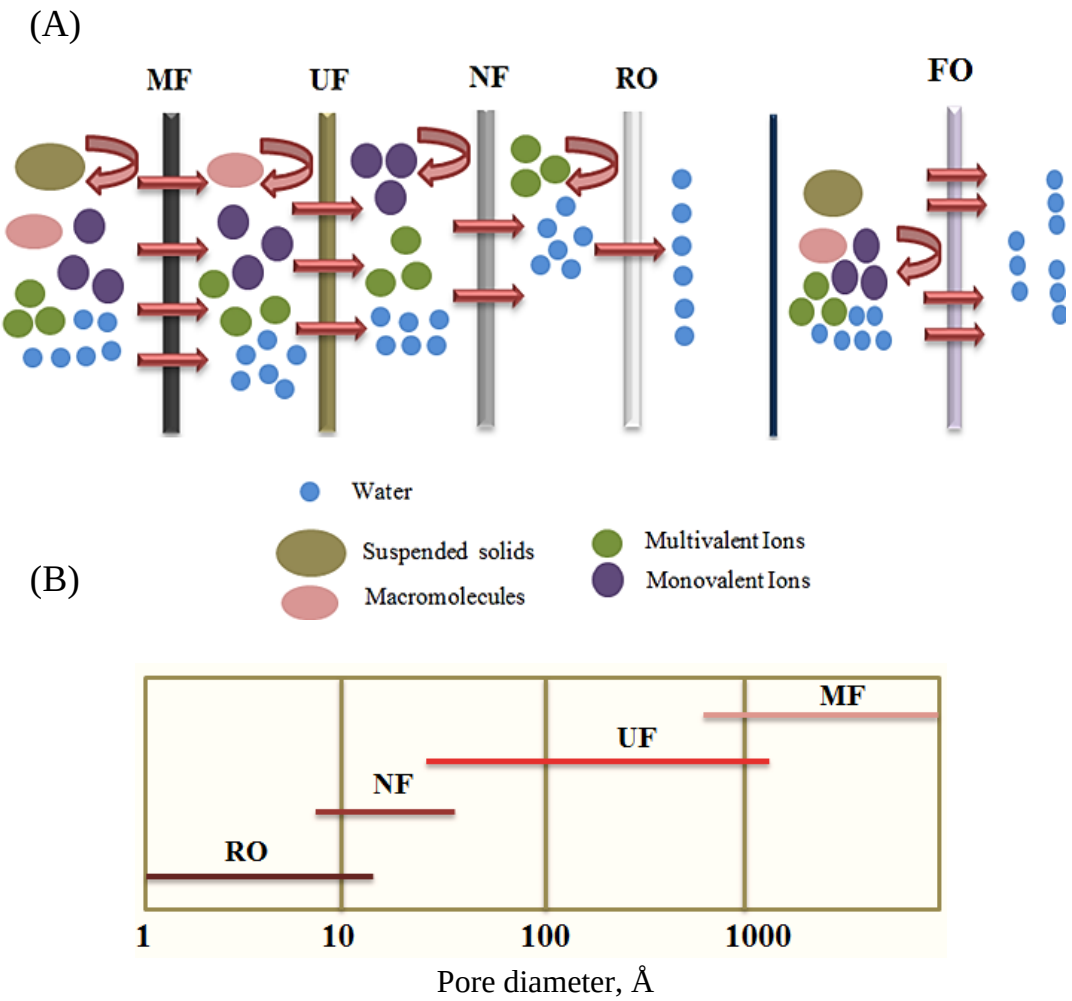

Figure 2.1 (A) Shows the ability of different techniques to expel the suspended and dissolved materials, (B) membranes pore size used in different types of desalination processes **(Sagle et al., 2004; Li et al., 2011).**

2.1 Principle work of forward Osmosis

An osmosis phenomenon is the transport of water across a semipermeable membrane from the low concentration regime to the high concentration regime due to the osmotic pressure difference which is the process driving force. Osmotic pressure (denoted as π) can be found using van't Hoff's law from the concentration of the solution **(Cath et al., 2006; Wallace et al., 2008).**

$$\pi = i.M.R.T \qquad 2.1$$

where (π) is the solution osmotic pressure at (atm); (i) is the ions number and molecules per solute mole; M is the solution molarity (mol/L); T is the solution temperature (K); and R is general gas constant, 0.08206 (L atm/(mol K)). From equation (2.1) it can be seen that the osmotic pressure depends on the salt type (i) and its molar concentration (M).

In the FO process as explained in Figure (2.2), the membrane permeate side contains draw solution (DS) which has higher salt concentration and higher osmotic pressure than feed solution (FS) on the other surface of the membrane **(Yang et al., 2016).** While in the RO process, ΔP is more than Δπ that means the hydraulic pressure applied on the solution that has high concentration is greater than an osmotic pressure difference across semi-permeable membrane, so water moves from the high to low concentration sides. In the Pressure Retarded Osmosis (PRO) process Δπ is greater than ΔP, which shows that the pressure applied on the high concentration solution, but it is less than osmotic pressure difference across a semipermeable membrane, and the flowing of water became from low concentration solution to solution

which has high concentration (as in FO) **(Darwish et al., 2016).** The equation that illustrates the concept of solvent transfer across the membrane in (FO), pressure retarded osmosis (PRO) and reverse osmosis (RO) processes is:

$$Jw = A\ (\sigma\ \Delta\pi - \Delta P) \qquad 2.2$$

where J_w is permeate water flux; A is the constant of water permeability of the membrane; σ is the reflection coefficient; Δπ is the osmotic pressure difference across the semi-permeable membrane, and ΔP is applied pressure. In FO, ΔP = 0; and in RO process ΔP>Δπ **(Lutchmiah et al., 2014)**. Comparison between RO, FO, and PRO systems is provided in Table 2.1.

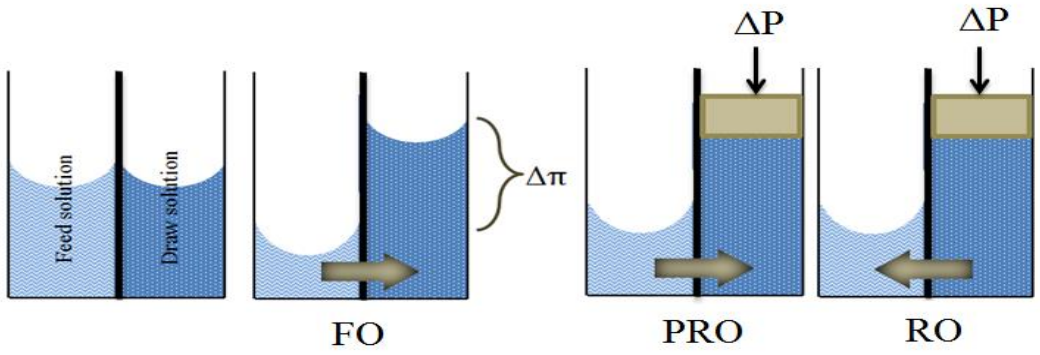

Figure 2.2 Water diffuses in FO, PRO, and RO system. For FO process, ΔP is nearly zero and water transports to a high concentration region of the membrane. In PRO process, water moves to the more concentration region that is under high pressure (Δπ>ΔP). In RO process, water moves to the lower concentration region due to the effect of hydraulic pressure (ΔP>Δπ).

2.2 Membrane modules and devices

The purposes of module design should include the most important is to reduce the cost (energy consumption and cost used in module manufacturing) **(Yang et al., 2013).** The design of the module has become one of the priorities that must be given special importance in the FO process, so it must be designed an ideal module characterized by high compaction density which

Table 2.1 Comparison among RO, FO, and PRO processes **(Klaysom et al., 2013)**

	RO	FO	PRO
Driving force	• External hydraulic pressure (P)	• Osmotic pressure	• Osmotic pressure
Main application	• Water purification process • Desalination	• Water purification process • Desalination	• Power production
Operating condition	• P~ 10–70 bar • Brackish and seawater feed solution • pH 6–7	• P~ atmospheric • Brackish, seawater or some synthetic draw solutions, such as aqueous NH3 • Impaired water, seawater or other feed solution • pH 6 – 11	• P ~ 10–15 bar • River, brackish, seawater, and brine solution • pH 6–7
Desirable membrane property			
(1) Physical morphology	• Dense top layer and porous sub-layer • Good thermal and mechanical stability	• Thin membranes with a dense active layer on porous, low torturous sub-layer	• Thin membranes with a dense active layer on porous, low torturous sub-layer
(2) Chemical property	• Good chemical stability to chloride solution	• Very hydrophilic • Good chemical stability of chloride solution and synthetic draw solution	• Very hydrophilic
(3) Membrane requirement	• High water permeability • High solute retention • Robust for high-pressure operation	• High water permeability • High solute retention • Stable in the synthetic draw solution	• High water permeability • Good solute retention to maintain osmotic pressure driving force • Strong enough for the externally applied pressure
Target performance	• High flux (at around 4–5 mm s^{-1})	• High flux and good water recovery	• High power density (>5W m^{-2})
Challenges	• Energy consumption • Operating cost	• Internal concentration polarization • Suitable draw solution • Draw solution recovery and re-concentration	• Internal concentration polarization • Module design • Membrane cleaning • Feed stream pre-treatment

provides high transport water area and minimal pressure drop while allowing limited External Concentration Polarization (ECP) and fouling **(Blandin et al., 2016)**, There are several different designs for the module used in forward osmosis process to contain the membranes, in general, the four main types of modules are plate-and-frame, spiral wound, tubular and hollow fiber.

2.2.1 Plate-and-frame

Because of its simple design (consisting of two end plates, the flat sheet membrane, and spacers) and ease of use have been widely applied in the industrial and laboratory, including the forward osmosis process. The initial design relies on a simple filters have a flat sheet membranes confined in a filter press called "plate-and-frame" modules **(Yang et al., 2013; Wallace et al., 2008)**. It can be used in various shapes and sizes in range from small laboratory equipment containing one small membrane to a large system containing more than 1,700 membranes. Despite the good design of the large panels and frames that have been installed well, but with the increasing size of the system becomes more complicated. the obstacles greatly affect the performance of the plate and frame module in the membrane processes are the lack of suitable membrane support with a relatively small density of packing. Other problems include difficulty in determining the damage to the membrane and low range of operating conditions such as flow velocity and pressure in addition to internal and external concentration polarization problems **(Cath et al., 2006)**.

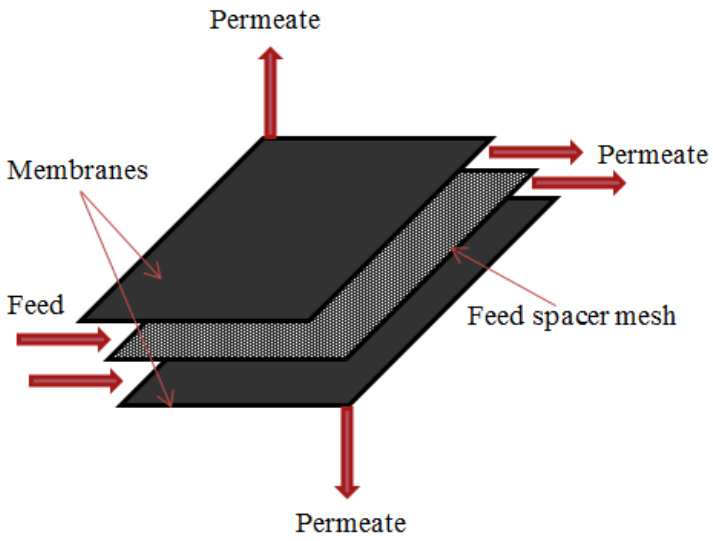

Figure 2.3 Flat-sheet FO membranes installed in plate and frame modules design.

2.2.2 Spiral-wound

The most common and used type in applications related to the membrane processes such as nanofiltration (NF) or reverse osmosis (RO) membranes is the spiral wound module. The unit contains a flat membrane enveloped around a perforated assembly pipe **(Darwish et al., 2016)**. In the forward osmosis process FO, SWFO has been significantly developed to be suitable for use in the process, especially with the draw solution flow rate. Taking into account backwash for SWFO membranes to a removal of fouling from the surface of the membranes and the carrier ducts for feed and draw solutions **(Lutchmiah et al., 2014)**. In spite of these efforts to improve the performance of spiral-wound in FO , however, the pressure drop on the draw solution (DS) due to the spiral circular flow on the shell side of the membrane and which uses the series of connected elements is not very suitable for large-scale operations **(Cath et al., 2006)**.

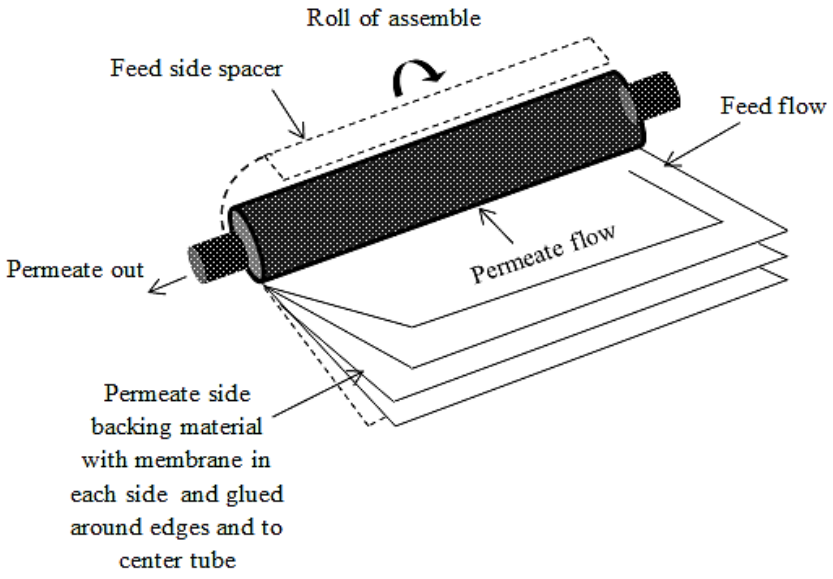

Figure 2.4: Spiral wound for forward osmosis (SWFO).

2.2.3 Tubular and Hollow fiber

The tubular membranes (hollow or tubes fibers) are characterized by several properties which make them highly suitable for use in the forward osmosis process, including that the tubular membranes are self-supporting and that mean they bear a high hydraulic pressure (especially when used in PRO mode) without the fears of membrane deformation. It is also easy to fill in packages inside the module, where with the density of the packaging can be high and which leads to an increased surface area for water transport on both surfaces of the membrane; a flow mode is suitable for FO process **(Cath et al., 2006)**. There is an important difference between tubular and hollow fiber membranes in terms of the flow system that can be achieved through bore side. In the hollow fiber membranes (internal diameter <1 mm), laminar flow can be achieved, and so, mixing at the membrane surface is limited.

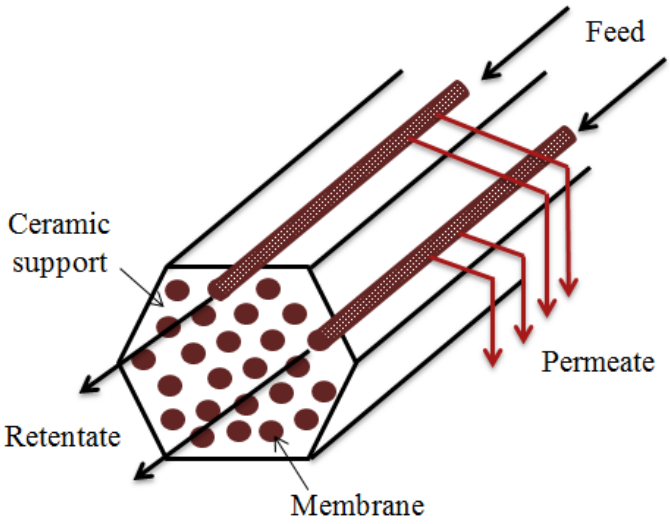

Figure 2.5: Tubular membrane module.

External CP, fouling, and scaling caused reduce mass transport across the membrane at these conditions. In tubular membranes (internal diameter ≥2 mm), turbulence can be easily achieved and CP, fouling, and scaling decreased **(Cath et al., 2006)**.

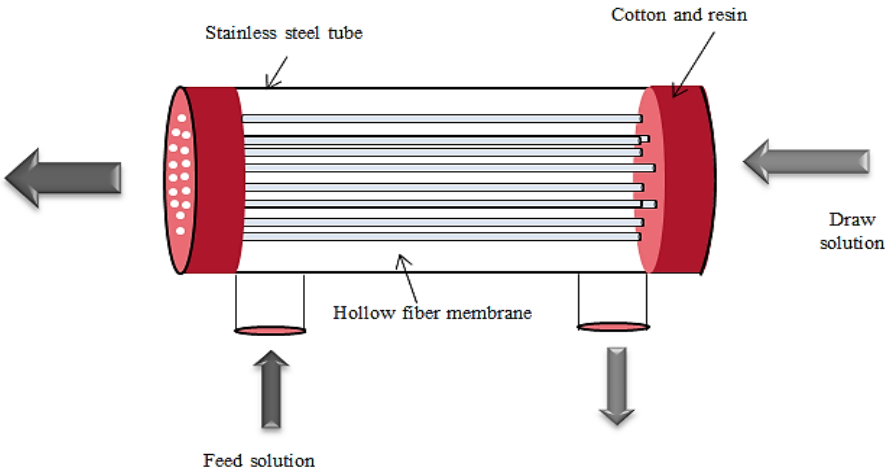

Figure 2.6: Hollow fiber membrane module.

2.2.4 Hydration bags

This new technology is considered to be one of the most promising in the field of water production and recycling, and redefines the field of membrane separation technology in a literal manner. It is considered an important application in the forward osmosis process which developed by Hydration Technology Innovations. It consists of a small water purifier bag, most often used by the military **(Duranceau et al., 2012)**. One of the famous applications on the osmosis process is the hydration bag, which consists of two lined bag, the outer one is sealed plastic bag filled with water to be distilled as feed solution. While the internal bag is made from the membrane of forward osmosis and it filled with the suitable draw solution (such as solid glucose) **(Cath et al., 2006).** Although the process very slow it is distinguished from the other desalination techniques as they do not need the energy to transfer water (as in the principle of the FO process) and it is minimal fouling occurs especially when using muddy water as FS **(Jacob et al., 2006)**.

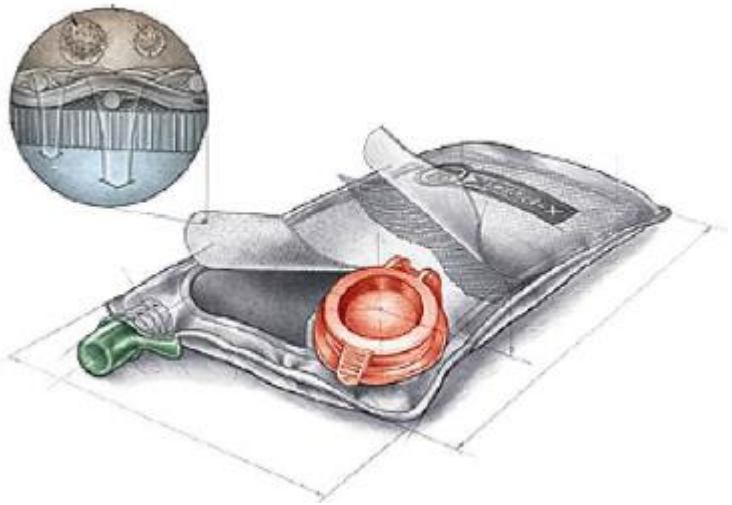

Figure 2.7. Water purification by hydration bag **(Duranceau et al., 2012)**.

2.3 Challenges for FO

The forward osmosis process depends on the different concentrations of the solutions as a driving force to regulate the process and the transfer of water through the semi-permeable membrane and since the process occurs automatically, so the hydraulic pressure is almost zero so the energy used in the process for water transfer across the membrane is low compared to other osmosis processes that need hydraulic pressure **(Chung et al., 2012; Wang et al., 2010)**. In order to make the forward osmosis process efficient and high productivity, requires the presence of an ideal semi-permeable membrane capable of transporting water and expulsion of salts and other impurities and reducing internal concentration polarization (ICP). As for the draw solution, provides good quality of it enhances the efficiency of the forward osmosis process and facilitate separation it from water or reuse **(Ge et al., 2013)**. There are many factors that adversely affect the performance of the FO process, which limits its use and application in broad areas and some of these challenges membranes are fouling and reverse diffusion of solutes, concentration polarization, controlled by many factors such as membrane orientation, membrane types and configuration, concentration, and the draw/feed solutions content as well temperature for both solutions **(Phuntsho et al., 2012; Akther et al., 2015)**.

2.3.1. Concentration polarization

It is a common phenomenon of osmosis process related to the membrane and is one of the challenges that are necessary to overcome and occur when the solution concentration at the membrane–feed interface is higher than the bulk solution concentration due to depletion of water from the boundary layer

(Klaysom et al., 2013). CP significantly reduces the membrane layer performance due to the reduced concentration gradient across the rejection layer of membrane. Most of the membranes in the forward osmosis process are considered to be asymmetric, consist of dense active and a porous support layers, and the solutions on both surfaces of the membrane always have concentration, the CP appears on both sides of the membrane and can be classified to internal concentration polarization (ICP) in the membrane support layer and external concentration polarization (ECP) on the membrane active layer. **(Wang et al., 2016)**. Generally, CP decreases water flux and induce fouling. The CP influence can be controlled with cross flow velocity and hydrodynamics **(Devia et al., 2015).** Below, these two concentration polarization phenomena are described.

2.3.1.1 Internal Concentration Polarization (ICP)

ICP is one of the problems related to forward osmosis process in particular and closely related to it, which reduces the flux of water through the membrane and increases the probability of reverse transfer of solute due to the reduction in the osmotic pressure gradient across the active layer of the membrane and a corresponding reduction in water flux. Studies in the membrane support layer showed different concentrations of solutes at transversal boundaries of that layer. Which critically reduces the water flow by 80% because it occurs within the membrane and it is difficult to mitigate the decline of water flux by altering the hydrodynamic conditions **(Lutchmiah et al., 2014; Gray et al., 2006).** When the feed solution (FS) flowing into contacting with the supporting layer of the semi-permeable membrane (such as in PRO mode) the water passes through the membrane porous layer to the

active layer which containing the draw solution (DS). The feed solution salt can easily move through the open pores of the membrane as it is transferred to this layer through convective water flow. For the membrane active layer, it is difficult to penetrate by the salt from support layer side that leads to increase the concentration of salt in porous layer. So this phenomenon is called concentrative ICP **(Yang et al ., 2016)**. While the feed solution (FS) flow on the active layer and the draw solution (DS) at the supporting layer of membrane, as is known in the forward osmosis process, Since the draw solution (DS) is diluted within the membrane porous support layer by the permeate water, the ICP phenomenon now occurs on the permeate side and that is the dilutive ICP **(Su et al., 2011).**

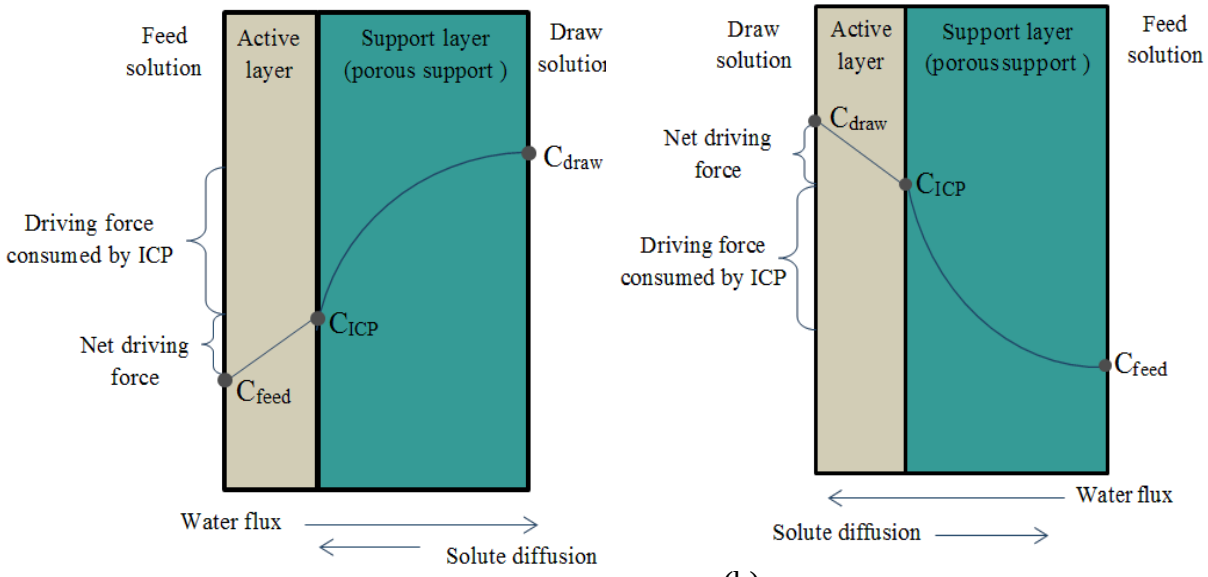

Figure 2.8 schematic descriptions of: (a) dilutive internal concentration polarization, and (b) concentrative internal concentration polarization.

2.3.1.2 External Concentration Polarization (ECP)

ECP is a phenomenon that has a noticeable effect in the membrane processes which use pressure as a driving force. Depending on the direction of the membrane either concentrative ECP or dilutive ECP occur. Concentrative external concentration polarization (CECP) ECP occurs in the forward osmosis process at the dense active layer surface of the membrane due to rejected molecules of salt near the active layer of membrane on the FS region. It increases the effective feed osmotic pressure from π_{FB} to π_{Fm}. In forward osmosis process, the dilutive external concentration polarization (DECP) found in the draw solution (DS) region, which can Contributes to decrease the effective osmotic pressure of draw solution. Generally, this is insignificant compared to the internal concentration polarization (ICP) **(Darwish et al., 2016; 3 Hawari et al., 2016)**. The effect of the ECP is less severe than the effect of the ICP due to the ability to control the ECP to reduce the damage by causing disturbance near the surface of the membrane thus facilitating the diffusion of the concentrated solute back into the bulk solution. The ICP cannot be alleviated by in the shear stress due to the nature of the porous support layer is stagnant **(Choi et al., 2018)**.

2.3.1.3 Impacts of Concentration Polarization

The flux in an osmotic driven membrane such as FO depends on osmotic pressure difference ($\Delta\pi$) across the membrane thin active layer according to equation (2.2) . However, the osmotic pressure is lower across the active layer compared to bulk osmotic pressure in the feed and DS. This results in lower water flux which is often attributed to several phenomena **(Cath et al., 2006)**. In FO, the transmembrane osmotic pressure is chiefly

responsible for controlling the water flux and recovery. Based on the extensive research conducted on CP, it was found that the occurrence of CP on both sides of FO membrane greatly reduces the effective transmembrane osmotic pressure; therefore, it is one of the major factors that contributes to declining water flux and recovery across the semi-permeable membranes **(Gao et al., 2014)**. As in any other membrane separation significant mass transfer resistances occur in FO due to concentration polarization (CP) effects. However here, the CP effects occur not only within the boundary layers on and around the membrane surface, due to non-ideal hydrodynamics, usually referred to as external concentration polarization (ECP), but also within the membrane itself.

The latter concentration polarization effect is unique for conventional forward osmosis membranes and is known as internal concentration polarization or ICP. These effects, being usually the main mass transfer resistance in membrane separations of course have to be minimized. Since ECP is hydrodynamic related it is usually mitigated by suitable membrane module design and use of spacers. Improved hydrodynamics influence ICP as well **(Gray et al., 2006)**, but the phenomenon is mainly related to the membrane structure (porosity, thickness, pore tortuosity) and membrane orientation, i.e. whether the porous support side of an asymmetric membrane is contacting the feed (AL-FS orientation, or FO mode) or the draw (AL-DS orientation, or PRO mode). The three mentioned main membrane structural characteristics are therefore summarized by a membrane structural parameter (S), which is related to the flux of a FO membrane.

2.3.2. Membrane Fouling

Surface fouling of membranes considered one of the main constraints generated by mass transport, which cause the adhesion and accumulation or penetration of particles to the surface or inside the membrane pores **(Chun et al., 2017)**. FO membranes are usually at a lower hazard of membrane fouling due to the absence of hydraulic pressure. Eventually fouling leads to an additional hydraulic resistance lowering the effective osmotic pressure and water permeability **(Lutchmiah et al., 2014)**. Although good types of polymer materials are used in the production of membranes and attention to the operation conditions and cleaning of the system to reduce the fouling of the membrane, but the containment of the feed solution on some of the compounds requires the pre-cleaning of its, which later attains the fouling of membranes, so the pretreatment of the feed is necessary to reduce the fouling which in turn decreases the cost **(Klaysom et al., 2013).** There are many classifications for fouling but the main ones are colloidal fouling due to inorganic fouling from crystallization/scaling of sparingly soluble salt, particle deposition, organic fouling duo to organic compounds such as protein, biofouling due to adhesion/deposition of microorganisms and the natural organic matters **(Chun et al., 2017)**.

2.3.3. Reverse Solute Flux

The flux of solute in the reverse direction of water flow causes a reduction in the osmotic pressure driving force of process which results in flux decline and the need for changing draw solution over time. It also has an undesirable effect on fluids streams in some applications **(Klaysom et al., 2013).** This problem is considered to be the predominant concept in the forward osmosis

process because of the different concentration between the feed and draw solutions, so it is important to determine it accurately to minimize its damage to the efficiency of the process and control it **(Akther et al., 2015)**. The reverse transfer of the salt does not only reduce osmotic pressure across the membrane but also complicate concentrate management which causes accumulation of DS solutes in the feed solution may induce toxicological challenges for sensitive receiving environment or influence adjacent treatment processes. If contaminants such as nitrate, phosphate or heavy metals present in the feed concentrate **(Chekli et al., 2012)**. The water flow in the membrane at forward direction is combined with the draw solute diffusion in the reverse direction as illustrated in Figure (2.9).

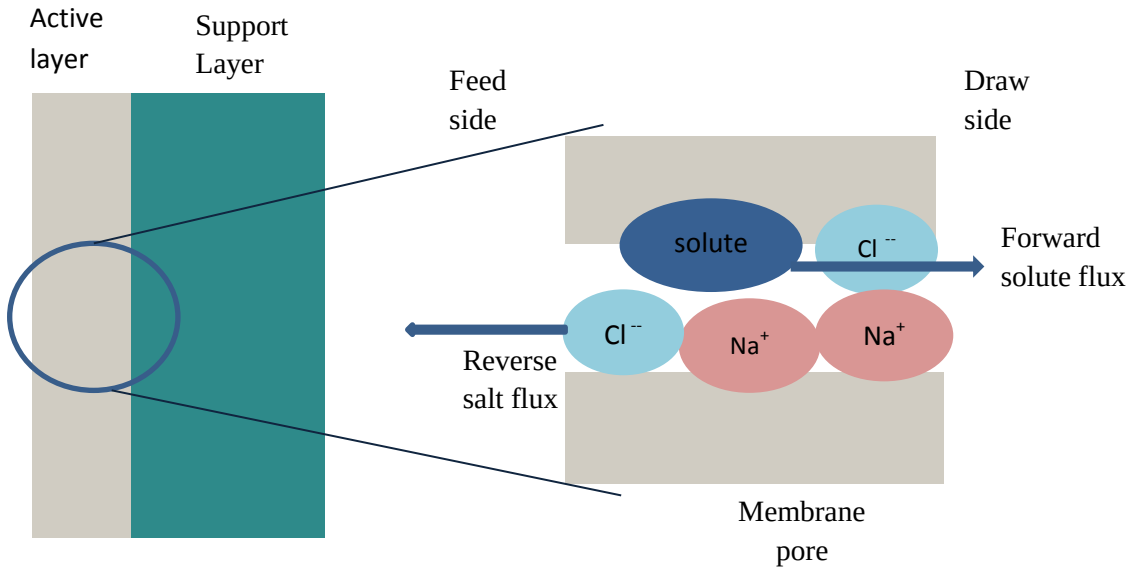

Figure 2.9 The retarded forward diffusion of feed solutes in the forward osmosis process by the reverse draw Solutes.

2.3.4. Membrane Cleaning Strategies

In order to obtain a continuous and constant flux rate in the membrane systems, a suitable cleaning method must be provided. Fouling and declined flux in forward osmosis process is more reversible than other pressure-driven membrane processes. So, there are some cleaning strategies reconnoitered such as hydraulic backwash, osmotic backwash, and surface flushing. **(Chun et al., 2017; Arkhangelsky et al., 2012).** Some research has applied physical cleaning to restore the normal flux of water through the semi-permeable membrane through using DI water on both the draw and feed solutions side of the membrane at a particular cross-flow velocity **(Zhao et al., 2015).**

2.3.5 FO membranes

Studies conducted on the forward osmosis process since the 1960s, using the reverse osmosis membranes special process significantly hindered the progress and expansion of the FO process and its applications. Therefore, special hydrophilic for enhanced water flux and decrease the fouling of membranes have been developed for the forward osmosis process which must be of high efficiency characterized by thin support layer of membrane with small porosity to reduce ICP, active layer with high density for high solute rejection, which causes higher water flux (low resistance of transport), high mechanical strength to save the membrane from the hydraulic pressure when used in PRO mode **(Darwish et al., 2016)**. Depending on the configuration

method, the FO membranes are divided into three types phase inversion-formed cellulosic membranes, thin film composite (TFC) membranes, and chemically manufactured membranes **(Kim et al., 2015; Nasr et al., 2015)**.

2.3.6 Draw solutions

Draw solution represents the main driving force source for forward osmosis process for the water transportation across FO semi-permeable membrane, so the selection of the appropriate type of it is a major factor affecting the performance of the FO process **(Chekli et al., 2012)**. Therefore, the use of suitable types of draw solution are very important to enhance the forward osmosis process (FO) performance and also reduce the cost of next step to separate the solution from water and return it. One of the characteristics that must be available for ideal draw solution is the ability to produce high osmosis pressure since the osmotic pressure is the driving force of the FO process between the feed and the draw solutions. Therefore, the osmotic pressure of the draw solution should be higher than for the feed solution to reach a suitable high flux. This reduces the cost and toxicity of the process **(Ge et al., 2013)**. The osmotic pressure of the draw solution is calculated according to the proposed theory Van't Hoff **(Chekli et al., 2012),** as shown in equation (2.1). There are other criteria that affect the performance of the forward osmosis process besides osmotic pressure such as diffusion coefficient as shown in the following equation **(Chekli et al., 2012)**:

$$K = \left(\frac{t\,\tau}{\varepsilon\, D_S}\right) \qquad 2.3$$

where K is the solute resistance to diffusion in the semi-membrane support layer, t, τ, and ε represent the thickness, tortuosity and porosity of the

membrane porous support layer, respectively, and Ds is the diffusion coefficient of the solute. The K value is an opposite function of the Ds value. That represents when solutes with higher diffusion coefficient will have lower resistance and can more easily diffused through the membrane support layer and therefore have lower ICP influence **(Low et al., 2015).** Various types of draw solutions have been discovered in the mid-1960s which are considered different and varied such as organic and inorganic-based draw solutes, as well as other emerging compounds such as magnetic nanoparticles (MNPs) and RO brines. When these solutions are consisting of charged ions or if it is neutrally charged solutes so can be sub-classified them into non-ionic (non-electrolyte) and ionic (electrolyte) solutions **(Kim et al., 2015)**.

2.4 Literature survey

McCutcheon., (2006) studied FO utilizing semipermeable polymeric membranes. FO driving force was supplied by a DS involving highly soluble carbon dioxide and gases—ammonia. Their experiments carried out in the cross-flow cell of membrane filtration by utilizing commercial membrane of Flat Sheet that available for FO, resulted fluxes between 1 and 10μm/s (2.1 to 21.2 gal ft^{-2} d^{-1} or 3.6 to 36.0 L m^{-2} h^{-1}) with using a wide range of FS and DS concentrations. However, the water fluxes that obtained from experiments were so lower than those expected based on the difference in bulk Osmotic Pressure and membrane permeability data of Pure water. ICP decided to be the fundamental reason for lower than the expectant flux of water via the available data analysis for water flux as well as the membrane SEM images of exhibited a porous support layer. The concentration of (DS) played a key role in this process. The reject of NaCl salts was investigated to be 95–99% for the most

of tests, in which found that under higher conditions of water flux, the rejections become higher.

Chou., (2010) described the potential applications and characteristics of a recently developing HFFO membrane that manufactured via interfacial polymerization upon the internal surface of a polyethersulfone (PES) HF. Separation properties of this FO membrane were intrinsic, in which a J_W was 42.6 (L m^{-2} h^{-1}) by employing (0.5 M) of sodium chloride as the DS and deionized water as FS with PRO mode at 23 °C. The RSF was just 0.094 g/L. To assess different scenarios applications, several solutions of various NaCl (500 ppm (8.6 mM), 1 wt.% (0.17 M) and 3.5 wt.% (0.59 M)) were applied as FS to test the performance of forward osmosis membrane. J_W of 12.4 (L m^{-2} h^{-1}) can be achieved by FO membrane with the solution of (3.5 wt.%) NaCl as FS and (2 M) of NaCl as DS, therefore this indicated to the potential of FO for desalination of seawater.

Su., (2010) fabricated Cellulose acetate (CA) nanofiltration (NF) HF membranes and examined in (FO) process. The heat treatment of fabricated membrane achieved by two steps of 60 min at 60 °C as well as 20 min at 95 °C, the radius of the pore was shrinks from (0.63 nm) to (0.30 nm). MWCO of the fabricated CA membrane was 186 Da. The permeability of pure water (PWP) was 0.47 (L m^{-2} h^{-1} bar^{-1}) when 1.0 bar transmembrane pressure used in the experiments while the levels of rejection were (90.17% for NaCl) and (96.67% for $MgCl_2$). In which the flux was increased with increment the concentration of DS. Where at (2.0M) of $MgCl_2$ for DS (≈258.3 bar) that flowing into membrane shell side, which has obtained the J_w and the RSF, was 7.3 (L m^{-2} h^{-1}) and 0.53 (g m^{-2} h^{-1}), respectively. Osmotic Pressure efficiency

reduced by raising the concentration of FS owing to the more of concentration polarization.

Setiawan.,(2011) fabricated nanofiltration (NF) membranes that has positively charged as selective layer via utilizing asymmetric micro-porous hollow fibers manufactured from the material of Torlon polyamide–imide (PAI) as the porous substrate that followed by polyelectrolyte posttreatment employing polyethyleneimine (PEI). By experiments has been estimated the reaction between PAI and PEI. FO system was applied to test the salt rejection as well as permeability. HF membranes of PAI exhibited a permeability of pure water between 2.19–2.25 (L m^{-2} h^{-1} bar^{-1}) and the salt rejection of NaCl as well as $MgCl_2$ reached to the acceptable level of (49% and 94%) at 1bar, respectively. It was also investigated that in processes of FO, when applying (0.5M) of $MgCl_2$ as a DS and DI water as FS at the active layer that facing feed in configuration of (AL-facing-FS) at 23◦C, 8.36 and 9.74L/m^2 h were the water fluxes that obtained from the two PAI HFFO membranes, respectively. The ration of (J_S/J_W) of two membranes was smaller than (0.4 g/L). This value was lower than the data of 0.85 g/L for a commercial membrane of FO from Hydration Technologies Inc. (HTI).

Wang., (2011) developed a new scheme to manufacture FO membranes for high performance by reaction of interfacial polymerization on porous supports of polymeric. p-Phenylenediamine, as well as 1,3,5-trimesoylchloride, adopted as the monomers for the in-situ polycondensation reaction to manufacture a thin selective layer of an aromatic polyamide has a thickness of 150 nm on the substrate surface, a lab-made polyether- sulfone (PES)/sulfonated polysulfone (SPSf)-alloyed porous membrane with promoted

hydrophilicity. By applied FO system to test the membrane, higher (J_W) of 69.8 LMH was achieved when utilize DI water and 25.2 (L m^{-2} h^{-1}) when utilize (3.5 wt %) of NaCl solution under (5.0 M) of NaCl solution as DS in PRO mode. The structural parameter (S) of PES/SPSf (TFC)-FO membrane was small of 238 µm.

Ren., (2014) reported on FO membrane that recently launched from Hydration Technology Innovations (HTI). This composite membrane of a thin film was an exit from their platform of cellulose acetate. The composite membrane tested, where displayed mechanical strength was good and high permeance of water relative to other membranes. Under forward osmosis tests, high flux of water of 46.4 and 22.9 (L m^{-2} h^{-1}) have achieved by the membrane with a modest RSF of 24.9 as well as 6.4 (g m^{-2} h^{-1}) utilizing (1 M) of NaCl draw solution against DI water in (PRO) as well as FO methods, respectively.

Hamdan., (2015) investigated the binary as well as ternary hydrous systems performance, which may be utilized in the criteria for choosing the DS to employ in applications of FO systems. Characteristics of the chosen binary, as well as ternary hydrous of NaCl solutions, magnesium chloride ($MgCl_2$), maltose and sucrose, were examined. Osmotic Pressures determined from the activities of water that have obtained from measuring the relative humidity of the solutions that have concentrations ranged about 0.5- 6.0 (mol kg^{-1}) at 298.15 K. The behaviors of osmotic of ternary systems in compared together with their binary counter parts; yields indicated the impacts of osmotic synergic either positive or negative. This may be utilized besides the

properties of transport, taking into account the chosen of favorable agents of draw solution from those that shown synergy was positive, i.e. the sum of pressures of the corresponding solutions of the binary was lower than the osmotic pressure of a ternary solution. Results indicated that the ternary hydrous solutions of $MgCl_2$ and NaCl demonstrated considerable positive synergy and hence were possible appropriate candidates as DS.

Sahebi., (2016) developed the high performance of (TFC), FO membranes by improving the hydrophilic nature of support layer by sulphonated polyethersulfone (SPES). Sulphonated substrate not just influenced on the performance of membrane where also alter the morphology of membrane from a finger to a sponge structure for morphology with a high grade of sulphonation where thus impacting on the mechanical characteristics of the membrane of FO. Non- sulphonated of TFC-FO membrane with a concentration of polymer of (12wt.%) displayed a faint finger-like structure whereas sampled that sulphonated at the same concentration of polymer exhibited a fully sponge-like structure with performance was so higher. Sulphonated TFC-FO membrane by applying FO system by utilizing feed of (2 M) of NaCl solution as DS and DI water has achieved J_W of $35 Lm^{-2} h^{-1}$ and 0.28 g L^{-1} flux of specific reverse solute was obtained at a sample (50 wt.% SPES).

Nasr., (2016) selected ammonium sulfate as a DS. Three types of commercially FO membranes were tested for flux. The sample of brackish from Egyptian groundwater was employed as FS. The Performance of membrane has investigated by water flux, reverse salt flux, and the salt rejection of forward of the FS. Commercial Porifera's membrane of FO

exhibited the best membrane relative to flux, in which it has chosen for experimentation. The increment in the concentration of ammonium sulfate led to decrease water flux gradually owing to increase the impact of concentration polarization that happens at high concentration of DS. The values of Specific Reverse Solute Flux (SRSF) didn't reach above 0.18 g/l for each ions of (NH_4^+) as well as (SO_4^{-2}) showing high selectivity of the membrane. The values SRSF at flux reaching to above 20 ($Lm^{-2}\ h^{-1}$) for (NH_4^+) ion was found to be higher than that for (SO_4^{-2}) ion, where that may be imputed to the influence of the thermodynamics. Whereas the rising of DS concentration results in increasing the rejection of (Na^+) ion, it resulted in a significant drop in the rejection of (Cl^-) ion. It was found that the ammonium sulfate was an effective draw solution for (FDFO) process by utilizing Commercial Porifera's membrane of FO were displaying a high value of osmotic pressure, suitable rejection of FS, low RSF.

Ghanbari., (2016) studied the treating of low performance that caused by internal concentration polarization (ICP) for solutes in porous substrates by fabrication hydrophilic halloysite nanotubes (HNTs) into the substrate that made of polysulfone (PSF). The membranes of thin film nanocomposite (TFN) were manufactured by interfacial polymerization upon the top surface for nanocomposite of PSF-HNT, where this was suitable for applications of forward osmosis. The results that obtained from experiments exhibited high J_W and low J_S for the manufactured membrane of TFN with (0.5 wt.%) of HNTs. The membrane of TFN0.5 also showed higher J_W than that of TFC membrane in both FO (27.7 vs 13.3 L $m^{-2}\ h^{-1}$) and PRO(42.3 vs 2 L $m^{-2}\ h^{-1}$) when they examined with FS of NaCl solution of (10 mM) and NaCl solution

of (2 M) as DS. This enhancement may be attributed to the parameter of structural of TFN0.5 was so lower in compared to the membrane of TFC (0.37 vs 0.95mm), where this resulting to reduce the influence of internal concentration polarization.

Long., (2016) studied the synthesize set of carboxyethyl amine sodium salts (CASS) with various group numbers of carboxyl as draw solutions for application of forward osmosis. The performances of forward osmosis were tested as well as compared in terms of various properties of physicochemical. Impact of the concentration of (CASS) on the osmotic pressure as well as the viscosity of DS, and performance of forward osmosis also investigated. J_W of 23.07 (L m^{-2} h^{-1}) and a reasonable RSF of 0.75 (g m^{-2} h^{-1}) has obtained with 0.5 (g/mL) of TTHP-Na DS via the mode of PRO. DS of Triethylenetetramine hexapropionic acid sodium (TTHP-Na) has estimated as DS to recycle the red solution of Congo by forward osmosis method to test its possible to apply it for treatment of wastewater.

Zou., (2016) tested the draw solutions consisting of three commercial solid fertilizers classified as (F1, F2, and F3) in the system of forward osmosis for extraction of water either from wastewater that treated or from (DI) water. Some organized optimizations were resulted to promote the performance of water extraction, in which it involved operation conditions, initial concentrations of draw and control on the chemical fouling. By employing the mode of FO, water has been obtained of 324 mL by utilizing (1-M F1). From between the three types of fertilizers, the content of urea of F1 was low where this was the most favored owing to a higher flux of water and lower (RSF) of fundamental nutrients. The used of treated wastewater as FS produced to

achieve a comparable performance of water extraction of (317 mL) to that achieved of DI water at (72 h) and (J_W) of 4.2 LMH.

Leong., (2016) studied the estimate of the feasibility of apply process of FO for desalination of seawater as well as the boron leak from the seawater to the draw solution was also studied. The application of FO membrane has resulted to 60-70% rejection of boron. The minimal membrane fouling of forward osmosis was noticed in the experimental work that spanning through 70 days. The flux of 1.4 ($L.m^{-2}.h^{-1}$) has obtained throughout the work and there was no great drop in the flux. The recovery of flux has reached to 40 % which was similar to that obtained from the process of (RO), potentially applied FO for applications of seawater desalination.

Shibuya., (2017) investigated the development of a thin-film composite (TFC) of the membrane of hollow fiber forward osmosis (HFFO) by utilizing a hollow fiber membrane of polyketone as a support. To test the diameter impact of hollow fiber membranes that utilized as support on the performance of FO of the (TFC-HFFO) membrane, which has employed a two samples of hollow fiber membrane with different internal diameters, which named as (HF-A: 347 μm and HF-B: 609 μm). The performance of TFC-FO membranes was determined and then tested via applying intrinsic parameters of the membrane that obtained by the technique of FO fitting. The smaller diameter (HF-A) of manufactured TFC-HFFO membrane has exhibited higher flux of FO and best properties of mechanical than those have a bigger diameter (HF-B), whereas higher consumption of energy of operational pumping was necessary owing to a higher drop in bore-side pressure.

Trung., (2017) utilized three composite of draw solution with various concentrations like ammonium iron (II) sulfate, ammonium iron (III) sulfate, and ammonium iron (III) citrate. The physical characteristics were investigated like conductivity, Total Dissolved Solids (TDS), as well as pH. An increase of DS concentrations resulted to the pH of complexes of Ammonium was decreased while TDS increased. Obtained that the water flux of complexes of iron was high of 8.88–11.24 (L m^{-2} h^{-1}) where was higher than DS of the ammonium bicarbonate. Furthermore, the recovered of DS of iron complexes was more than 90% via the membrane of NF-90, where this played a very important role in the process of forward osmosis to produce the freshwater. In which this provided an indication for the capability of applications of iron complexes in process of FO.

Zhang, (2017) studied the effect of adding a small quantity of perfluorosulfonic acid (PFSA) that was hydrophilic blended with the PVDF substrate to promote the performance of membrane of thin-film composite (TFC) for applications of FO. PFSA did not just promote the wettability of the manufactured membrane, where also enhanced the size of the pore through changing the morphology of PVDF/PFSA membrane owing to the hydrophilicity as well as the excellent compatibility within PVDF. Accordingly, the membrane of PVDF/PFSA-TFC the best (J_w) that achieved was 54.4 (L m^{-2} h^{-1}) and a RSF (J_S) was 10.9 (g m^{-2} h^{-1}) in the mode of AL-DS, while a (J_w) was 27.0 (L m^{-2} h^{-1}) with (J_S) was 8.4 (g m^{-2} h^{-1}) in the mode of AL-FS by utilizing deionized water (DI) and NaCl solution of (1M) as FS and DS respectively.

Shokrollahzadeh, (2018) investigated the influence of a new polymeric blend of polysulfone/polyacrylonitrile (PSf/PAN) nanofibers prepared via the electrospinning process as a substrate to produce (TFC-FO) membrane. The solvents in the electrospinning process were optimized. A polyamide (PA) thin layer fabricated on the electrospun nanofibrous substrate via interfacial polymerization. The membranes performance of the nanofiber that based on thin film composite (NTFC) compared with the in-house-made (PSf/PAN) TFC membrane, in which its substrate fabricated via Phase Inversion. The membrane of NTFC established important improvement in hydrophilicity and water permeability, and (RSF) reduced. Thus, the structural parameter (S) value of the made-up NTFC decreased considerably which represented the reduction of Internal Concentration Polarization (ICP) during the process of FO. These achieved results were due to nanofiber structural characteristics such as high porosity as well as interconnected open structure of pore. The effects of different salts as DS (NaCl, KCl, $MgCl_2$, $MgSO_4$) on the performance of osmotic of membranes of NTFC and TFC estimated. Among the tested DS with the same osmotic pressure, NTFC membrane exhibited higher J_W (38.3 LMH) than that of the TFC membrane (14.3 L m^{-2} h^{-1}) for KCl DS.

Table 2.2 Summary of notable FO membrane developments

Membrane	Feed solution	Draw solution	Water flux (LMH)	Revers salt flux (gMH)	FS flow rate	DS flow rate	Temp.	Water permeability coefficient (A) [LMH/bar]	Salt permeability coefficient (B) [LMH]	Membrane porosity ε %	Structural parameter (S)	Salt rejection (%)	Ref.
PPSU 25% HF	0.5 M	3 M	13.48	7.30	0.1 L/ min	0.1 L/ min	25 ± 5˚C.	2.25	0.37	85.72	467 µm	85.1	This work
PPSU 29% HF	0.5 M	3 M	12.82	6.58	0.1 L/ min	0.1 L/ min	25 ± 5˚C.	1.59	0.25	82.02	567 µm	86.2	This work
PPSU 30% HF	0.5 M	3 M	7.81	3.89	0.1 L/ min	0.1 L/ min	25 ± 5˚C.	0.99	0.99	79.55	601 µm	89.8	This work
PPSU (non-sulfonated) HF	DI water	2 M NaCl).	10	2.3	8.33 cm/s	8.33 cm/s	22 ± 0.5˚C.	6529	5.78	65	2.94×10^{-3} m	81.71	[Widjojo et al., 2013]
sPPSU-2,5 (2.5 mol% sDCDPS) HF	DI water	2 M NaCl).	48	7.6	8.33 cm/s	8.33 cm/s	22 ± 0.5˚C.	846.4	1.05	83.41	6.52×10^{-4} m	84.10	[Widjojo et al., 2013]
sPPSU-5 (5 mol% sDCDPS) HF	DI water	2 M NaCl).	62.8	14.9 - 35	8.33 cm/s	8.33 cm/s	22 ± 0.5˚C.	241.3	–	84.18	–	–	[Widjojo et al., 2013]
TFC PPSU	DI water	0.5M NaCl	12.37 ± 1.2	2.69 ± 0.21	0.1 L/min	0.2 L/min	23 °C	3.15 ± 0.07	0.0952 ± 0.003	–	7.46×10^{-4} m	86.8 ± 0.7	[Zhong et al., 2013]
TFC 1.5 mol % sPPSU	DI water	0.5M NaCl	22.51 ± 2.3	5.49 ± 0.35	0.1 L/min	0.2 L/min	23 °C	1.99 ± 0.02	0.0399 ± 0.002	–	1.63×10^{-4} m	90.9 ± 0.3	[Zhong et al., 2013]
TFC 2.5 mol % sPPSU	DI water	0.5M NaCl	17.98 ± 0.17	2.63 ± 0.32	0.1 L/min	0.2 L/min	23 °C	1.80 ± 0.11	0.0490 ± 0.011	–	2.40×10^{-4} m	87.9 ± 0.9	[Zhong et al., 2013]
CA with an acylation degree of 39.2%	0.2 M NaCl	1.5 M glucose	3.47	–	0.33 m/sec,	0.33 m/sec,	25 °C	–	–	–	–	95.48	[Li et al., 2016]
(CA) nanofiltration HF	saline water	2.0M MgCl2	7.3	0.53	50 mL/min	100 mL/min	25 °C	0.47	–	–	–	90.17	[Su et al., 2010]
CA Double-Skinned Membranes	DI water	5.0 M MgCl2	27.4	3.9	–	0.2 L/min	22 ± 0.5 °C	0.78 ± 0.11	0.46 (1.7×10^{-7})	–	–	58	[Wang et al., 2010]

Table 2.2 (Continued)

PVDF/PFSA TFC (MT-0)	DI water	1 M NaCl	2.5	12.0	0.3 L/min	0.3 L/min	ambient temperature	0.11±0.01	0.93±0.02	72.4±0.3	1606.51± 37.31 µm	15.18±0.29	[Zhang et al., 2017]
PVDF/PFSA TFC (MT-1)	DI water	1 M NaCl	7.5	6.1	0.3 L/min	0.3 L/min	ambient temperature	0.57±0.12	0.16±0.09	81.8±0.4	858.75± 17.04 µm	83.20±8.10	[Zhang et al., 2017]
PVDF/PFSA TFC (MT-2)	DI water	1 M NaCl	12.4	6.9	0.3 L/min	0.3 L/min	ambient temperature	1.49±0.09	0.31±0.05	85.8±0.5	706.93± 16.12 µm	87.75±1.94	[Zhang et al., 2017]
PVDF/PFSA TFC (MT-3)	DI water	1 M NaCl	27.0	8.4	0.3 L/min	0.3 L/min	ambient temperature	2.97±0.06	0.39±0.13	86.7±0.6	334.62± 3.50 µm	92.23±2.36	[Zhang et al., 2017]
PVDF/PFSA TFC (MT-5)	DI water	1 M NaCl	22.2	5.1	0.3 L/min	0.3 L/min	ambient temperature	2.31±0.16	0.38±0.01	88.4±0.1	410.13± 0.67 µm	92.86±1.82	[Zhang et al., 2017]
single-skinned (TFC)	DI water	0.5 M NaCl	12.8	3.43	27 cm/s	27 cm/s	23 ± 2 °C	1.37	0.66	_	_	88.0	[Duong et al., 2014]
double-skinned (TFC and Nexar copolymer) in PRO mode	DI water	0.5 M NaCl	17.2	4.85	27 cm/s	27 cm/s	23 ± 2 °C	1.29	0.63	_	_	88.3	[Duong et al., 2014]
Dope formula A (PES) single skinned	DI water	0.5M NaCl	5	2.12	_	_	23 ◦C.	0.95	0.29	84	1.37×10−3 m	78	[Wang et al., 2010]
Dope formula B (PES) double skinned	DI water	0.5M NaCl	14	1.75	_	_	23 ◦C.	2.22	0.20	75	5.95×10−4 m	91	[Wang et al., 2010]
PES/SPSf TFC FO	DI water	0.5 M NaCl	13.0	3.6	100 mL/min	100 mL/min	20–25◦C	0.77	0.11	0.833	2.38 ×10−4 m	93.5	[Wang et al., 2012]
PBI hollow fiber (original) in PRO mode	DI water	5M MgCl2	36.5	_	_	0.08 m/s	23 ◦C	2.43	_	_	_	_	[Wang et al., 2009]
PBI hollow fiber (2 h cross-linking) in PRO mode	DI water	5 M MgCl2	32.4	_	_	0.08 m/s	23 ◦C	1.53	_	_	_	_	[Wang et al., 2009]
ST#1 PAI hollow fiber	DI water	0.5 M MgCl2	4.15	1.909	450 mL/min	1500 mL/min	23 ◦C	1.74	0.065	51	_	94.4	[Setiawan et al., 2011]
ST#2 PAI hollow fiber	DI water	0.5 M MgCl2	11.7	3.861	450 mL/min	1500 mL/min	23 ◦C	2.25	0.113	70	_	92.7	[Setiawan et al., 2011]

Table 2.2 (Continued)

ST#3 PAI hollow fiber	DI water	0.5 M MgCl2	12.9	4.773	450 mL/min	1500 mL/min	23 ◦C	2.19	0.138	85	_	91.1	[Setiawan et al., 2011]
TFC PSf (9 wt %)	DI water	1.0M NaCl	20.5±3.8	_	21.4 cm/s	21.4 cm/s	25±0.5 ◦C	1.63±0.18	0.84±0.19	_	389±150 µm	95.8±1.3	[Tiraferri et al., 2011]
TFC PSf (12 wt %)/ DMF (25 wt %)	DI water	1.0M NaCl	10.8±2.4	_	21.4 cm/s	21.4 cm/s	25±0.5 ◦C	0.93±0.37	0.52±0.29	_	676±111 µm	97.3±1.0	[Tiraferri et al., 2011]
Flat-sheet TFC-1 (Polyamide polysulfone)	10 mM NaCl	0.5 M NaCl	18.1	6.3	500 ml/min	500 ml/min	23 ◦C	1.15 ± 0.16	4.7 ± 1.4	77 ± 3	_	94.5	[Wei et al., 2011]
Flat-sheet TFC-2 (Polyamide polysulfone)	10 mM NaCl	0.5 M NaCl	20.5	5.9	500 ml/min	500 ml/min	23 ◦C	1.78 ± 0.23	9.4 ± 1.9	82 ± 2	_	93.4	[Wei et al., 2011]
TFC PK(25/75)(70)-1	DI water	0.6 M NaCl	13.8	0.047	500 ml/min	500 ml/min	25 ± 2˚C	1.21	0.2	_	364 µm	_	[Yasukawa et al., 2015]
TFC PK(25/75)(150)-1	DI water	0.6 M NaCl	12.6	0.032	500 ml/min	500 ml/min	25 ± 2˚C	1.15	0.15	81.9	449 µm	_	[Yasukawa et al., 2015]
TFC PK(25/75)(70)-2	DI water	0.6 M NaCl	19.7	0.059	500 ml/min	500 ml/min	25 ± 2˚C	1.84	0.21	80.6	287 µm	_	[Yasukawa et al., 2015]
TFC PK(25/75)(70)-3	DI water	0.6 M NaCl	24.4	0.057	500 ml/min	500 ml/min	25 ± 2˚C	2.5	0.18	_	280 µm	_	[Yasukawa et al., 2015]
TFC PK(35/65)(80)-3	DI water	0.6 M NaCl	29.3	0.065	500 ml/min	500 ml/min	25 ± 2˚C	_	_	84.5	_	_	[Yasukawa et al., 2015]
TFC PSf90(0/100)-1	DI water	0.6 M NaCl	5.0	0.021	500 ml/min	500 ml/min	25 ± 2˚C	1.14	0.25	70.2	1975 µm	_	[Yasukawa et al., 2015]
SPPO/PSf (50:50)	DI water	1.0 M MgCl2	29 ± 3	1.4 ± 0.2	0.26 L/min	0.26 L/min	25˚C	3.55	0.74	0.86	293 ± 22 µm		[Zhou et al., 2014]
SPPO/PSf (25:75)	DI water	1.0 M MgCl2	16 ± 2	1.1 ± 0.1	0.26 L/min	0.26 L/min	25˚C	3.22	0.95	0.84	562 ± 149 µm		[Zhou et al., 2014]
SPPO/PSf (0:100)	DI water	1.0 MMgCl2	5 ± 1	1.0 ± 0.2	0.26 L/min	0.26 L/min	25˚C	3.29	0.285	0.80	3680 ± 431 µm		[Zhou et al., 2014]

Table 2.2 (Continued)

hydrophilic cellulose-based polymer (CA)	sodium chloride	ammonia–carbon dioxide	3.6 – 36..0	-	30 cm/s	30 cm/s	50±1 ◦C	5.69×10−12 $mPa^{-1} s^{-1}$	-	-	-	95–99	[Low et al., 2015]
(PES) hollow fiber	DI water	0.5 M NaCl	42.6	4.0	-	-	23 °C	3.50	6.22×10−8 m/s	82	5.50×10−4 m	~95	[Chou et al., 2010]
TFC (Sulphonated polyethersulfone (SPES))	DI water	2.0 M NaCl	35	9.9	200 mL/min	200 mL/min	25˚C	2.9 ± 0.25	5.1 ± 0.1.3	79 ± 3	245 µm	91.1	[Sahebi et al., 2016]
Cellulose acetate (TFC) membrane	DI water	2.0 M NaCl	22.9	6.4	0.25 m/s	0.25 m/s	20 ± 0.5 °C	~1.8	~1.25	-	620 µm	~93	[Ren et al., 2014]
Polyamide (PA) & polysulfone (TFC) membrane	5 g/L	2.5 M ammonium sulphate	21.67	-	400 mL/min	400 mL/min	25 °C	3.036	1.968	-	-	85.2	[Nasr et al., 2016]
The thin film nanocomposite TFN0.5	10 mM NaCl	2M NaCl	27.7	14.62	0.35 L/min	0.35 L/min	0.35 L/min	2.00	9.34	77 ± 0.45	0.37 ± 0.05	93.7	[Ghanbari et al., 2016]
CTA FO membrane	DI water	0.5 g/mL TTHP-Na	23.07	0.75	300 mL/min	300 mL/min	25±1 °C	-	-	-	-	85.3-93.5	[Long et al., 2016]
Cellulose triacetate (CTA)	DI water	1 M Fertilizers (f1)	4.2	-	10 to 100 mL min^{-1}	10 to 100 mL min^{-1}	20 ± 2 °C	0.6 - 1.0	-	-	-	81	[Zou et al., 2016]
FO flat sheet membrane	32,500 ppm Surface seawater	1.15 M Sodium sulphate	1.4	-	-	-	-	-	-	-	-	60-70	[Ong et al., 2016]
TFC polyketone HF -A	DI water	sodium chloride	-	-	1.0 L/h	1.0 L/h	25 ± 1 ℃	1.2	0.265	73.6	250 µm	-	[Shibuya et al., 2017]
TFC polyketone HF -B	DI water	sodium chloride	-	-	1.0 L/h	1.0 L/h	25 ± 1 ℃	0.9	0.125	78.0	521 µm	-	[Trung et al., 2017]
NF-90 membrane	DI water	0.05-1.0 M iron complexes	8.88–11.24	-	1.2 L/m	1.2 L/m	25 ± 5 ℃	-	-	-	-	93	[Zhang et al., 2017]
polysulfone/polyacrylonitrile (PSf/PAN) nanofibers	DI water	79.27 g/L KCl	38.3	10.1	-	-	25 ℃	3.68 ± 0.23	0.32 ± 0.12	84.3	0.34 mm	97.12 ± 0.92	[Shokrollahzadeh et al., 2018]

CHAPTER THREE

EXPERIMENTAL WORK

3. Experimental work

The current chapter study (lab scale) concerns the treatment of saline water by using a hollow FO membrane module. the hollow fiber membrane prepared by using PPSU polymer with different concentration to investigate the change in membrane properties, water and salt permeability, water flux, salt rejection with using a different concentration of draw solution.

3.1 Materials

PPSU, Radel R-5000 with average Mw = 50 KDa, and specific gravity = 1.28 was provided by Solvay Advanced Polymers (Belgium). N-methyl-2-pyrrolidone (NMP), 99.5% was used as the polymer solvent, and was purchased from Sigma–Aldrich (St. Louis, MO). The sodium chloride (NaCl) chemical analysis is given in the Table 3.1.

Table 3.1 Sodium chloride (NaCl) solutions chemical specification.

Sodium chloride (Assay 99.5%min)	
Impurities Maximum limits	%
Ammonia (NH3)	<0.002 %
Iron (Fe)	<0.003 %
Lead (Pb)	<0.0005%
Potassium (K)	<0.02%
Sulphate (SO4)	<0.02 %
NaCl molecular weight	58.44
NaCl solubility in H_2O gm/l	355

3.1.1. Membranes

The membrane used was Three Poly (phenyl sulfone) PPSU hollow fiber membrane prepared from different concentration ((PPSU 25%, PPSU 29%, and PPSU 30%). These percentages were selected in order to distinguish the difference in the polymer content to the properties of membranes at this increase from 25 to 29 and 30 wt%. This membrane was prepared using phase inversion method with solvent of N-methyl-2-pyrrolidone in the laboratories of Membrane Technology Research Unit/Chemical Engineering Department/ University of Technology. All the spinning parameters are shown in Table 3.2 with more details are shown elsewhere **(Alobaidy et al., 2017; Alsalhy et al., 2011; Alsalhy et al., 2012)**.

Table 3.2 Spinning parameters of PPSU hollow fiber membranes.

Membrane code	Dope composition (wt%)	Bore fluid composition NMP/water	Coagulation bath temperature (◦C)	Extrusion pressure (bar)	Bore fluid flow rate (ml/min)	Air gap length (cm)
PPSU-25	PPSU/NMP; (25:75)	0/100	36	2.5	3	3.5
PPSU-29	PPSU/NMP; (29/71)	0/100	36	3	3	3.5
PPSU-30	PPSU/NMP; (30:70)	0/100	36	2.5	3	3.5

3.1.1.1 Membrane characterization

- **SEM analysis**

Scanning electron microscope was used for investigating the physical structures and the microscopy of surface and the structure of cross-sectional for the HFFO membranes were imaged with scanning electron microscopy (SEM). To show the membranes cross-sections, the HFFO membrane samples were immersed in liquid nitrogen and cut with a razor blade to maintain the pore structure. This analysis was done in laboratories of production engineering and metallurgy department / University of Technology by SEM model (ZEISS-EVO MA10) at the institute membrane technology, and scrutinizing.

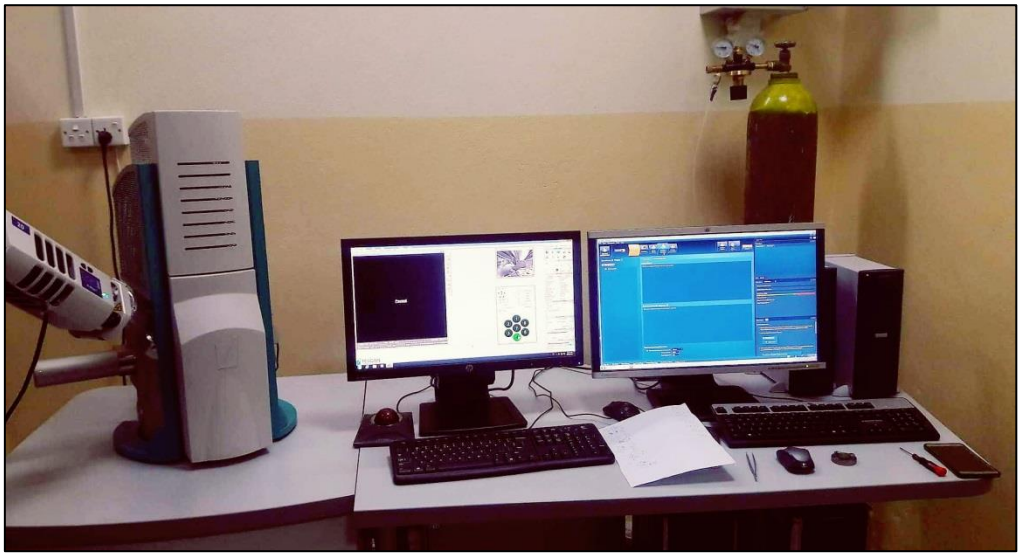

Figure 3.1 The Scanning Electron Microscope (SEM) device used in membrane characteristics study.

- **AFM analysis**

Atomic Force Microscope (AFM) analysis was used to investigate the roughness membranes surface under the dynamic mode, which was evaluated by the average surface roughness (R_a), the root mean square roughness (R_q) , mean pore size and pore size distribution. This analysis was done in laboratories of College of science/chemistry department /Baghdad University by AFM (Angstrom Advanced Inc., (USA), model AA3000).

- **Porosity**

The HFFO membrane porosity (PPSU 25 %, PPSU 29 %, and PPSU 30%) was determined using the volumetric weight for three pieces of HFFO membrane with 4 cm long which was measured by an electronic balance. And then the HFFO membrane porosity calculated using the following equation **(Shibuya et al., 2017)** :

$$\text{Porosity} = \left[1 - \frac{G}{1.41 \times 4}\left\{\frac{4}{(d_{out}^2 - d_{in}^2)\times 10^{-8}\ \pi}\right\}\right] \qquad 3.1$$

where G is the measured weight of the dried HFFO membrane piece. The quantities d_{in} and d_{out} are the inner and outer diameters of the HFFO membranes as measured by SEM analysis. Here, the Polyphenylenesulfone density was taken to be 1.28 g/cm^3.

3.1.2 Feed and draw solutions properties and characteristics

In operation, deionized water (DI) was utilized to prepare feed and draw solutions. Synthetic saline water samples were prepared by quantifying the required amount of sodium chloride salt NaCl in electrical balance (kern-PLE 310-3N) and then dissolving in deionized water. Some experiments have used distilled water as a feed solution to obtain a good understanding of the

performance of the forward osmosis process (FO) and the effect of the FS on the flux of membranes. In the preparation of the draw solution, sodium chloride salt was used in different concentrations 1, 1.5, 2, 2.5, and 3 M.

Feed and draw solutions are mixed using the stirrer (MR Hei. Standard) at 1000 rpm agitation speed for 30 min. The total feed and draw solution volumes were 1.0 liter. The choice of sodium chloride salt NaCl in the preparation of the draw solution due to several reasons, including a relatively small molecular weight, a low viscosity, high and rapid solubility in water, its solution can generate a high osmotic pressure, nontoxic, easy to separation from water as well as restore and recycle after the end of process.

3.2 Forward Osmosis System

The experimental work has been carried out using a bench scale FO system shown in Figure (3.2) and schematic FO flow diagram is shown in Figure (3.3). The experimental system consists of two feed cylindrical vessels, the first for feed solution (FS) and the second for draw solution (DS). The size of the vessels used in this process was one liter in volume. Two diaphragm pumps were used to pump the draw and feed solutions from vessels to FO osmosis module. Hollow fiber module was prepared using stainless steel tube of 24.56 cm length. PPSU hollow fiber membranes sealed with an epoxy resin (Euxit 50KII-hardener) was inserted in the stainless steel tube as shown schematically in Figure (3.4) and photographically in Figure (3.5).

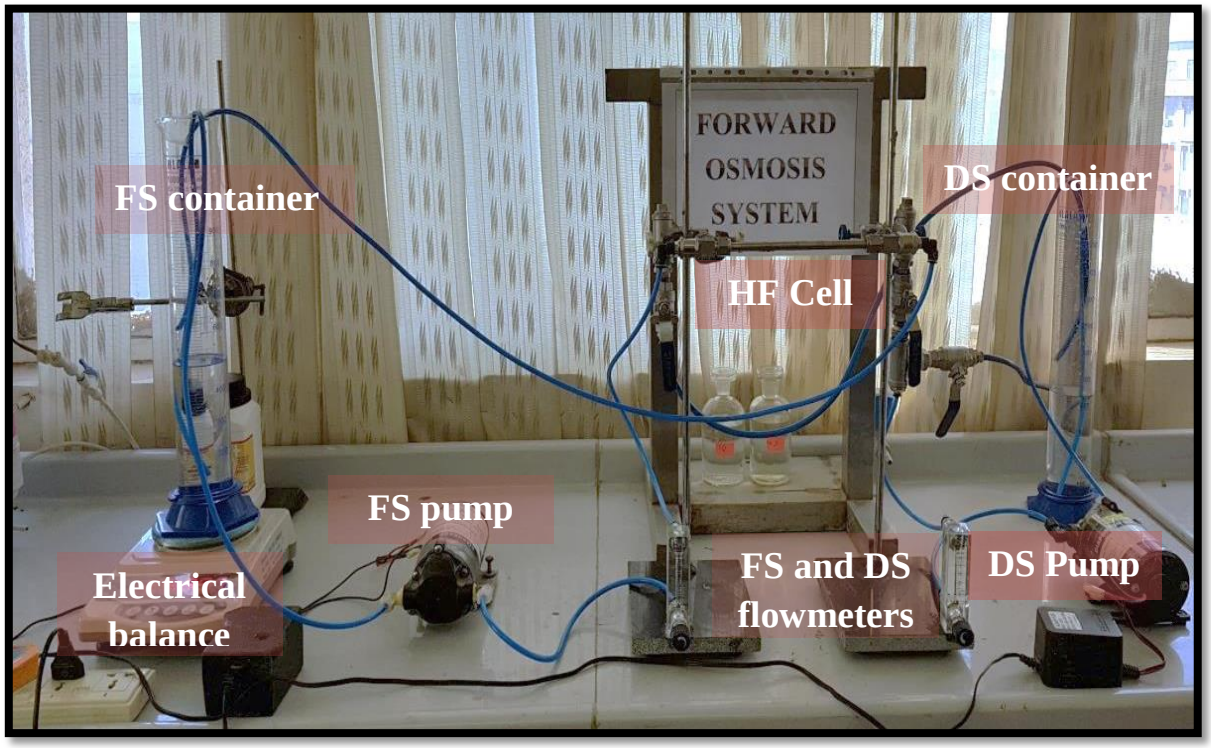

Figure 3.2: Photograph of FO system

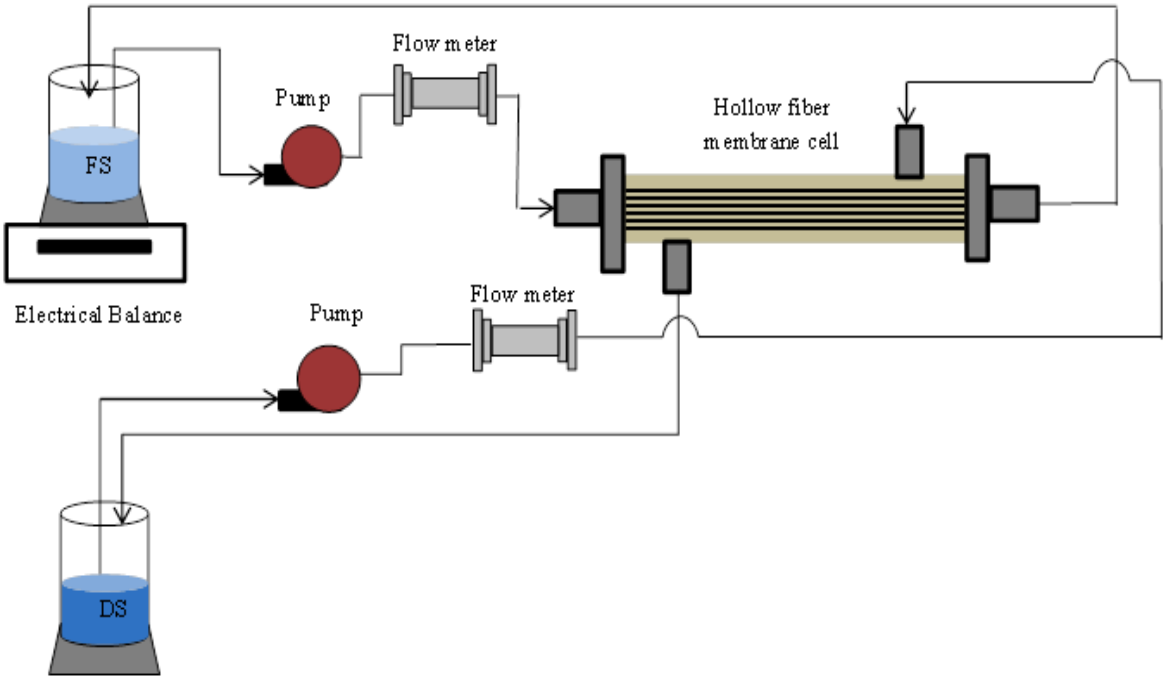

Figure 3.3 The schematic diagram of the experimental bench scale FO process.

The cross-flow (volumetric flow rate) of the feed and draw solutions were measured using two Calibrated flowmeters in the range of (0.1- 1 l/hr). In order to wholly fill of the forward osmosis system pipes, the outlet valves were opened for feed and draw solutions. Feed and draw solutions were run in a counter-current flow mode (feed and draw solution flowing tangential to the membrane surfaces but in opposite direction). FO membrane show slightly higher flux under countercurrent flow arrangements than the co-current cross-flow direction. It is likely because the net driving force is higher at the DS inlet than at the outlet point of the FO module under the counter-current arrangement and made the process more efficient. As for the osmosis cell outlet streams, they were returned to the main vessels of the feed and draw solutions.

The continuous transfer of water from the feed solution led to the dilution of the draw solution in the module over time. When the diluted draw solution out from the module and flew back to the main DS vessel, it would mix with the draw solution in the vessel. But when utilizing a large volume of draw solution the diluted draw solution from the module would not significantly affect the concentration of draw solution in the vessel. All experiments in FO process were carried out at atmospheric pressure and 25 ±5°C temperature of both solutions. The time of experiment was 4 hours, every 0.5 hour the reducing in the volume of the feed solution (FS) was measured and compared with the increase in the draw solution (DS) volume for checking. Also, NaCl concentration in DS and FS outlet was measured using conductivity meter. The forward osmosis process variables of operating conditions in this process are summarized in Table (3.3). The membrane was cleaned at the end of each experiment, using deionized water (DI) at a cross-

flow rate for 1 hr, in order to remove salt particles that accumulated on or in the pores and surfaces of the HFFO membrane.

Table 3.3 Variables of operating conditions for FO process

Variables	Ranges
Concentration of draw solution (DS)	1-3 M
Flow rate of draw solution (Q_{DS})	0.1-1 l/min
Flow rate of feed solution (Q_{FS})	0.1-1 l/min

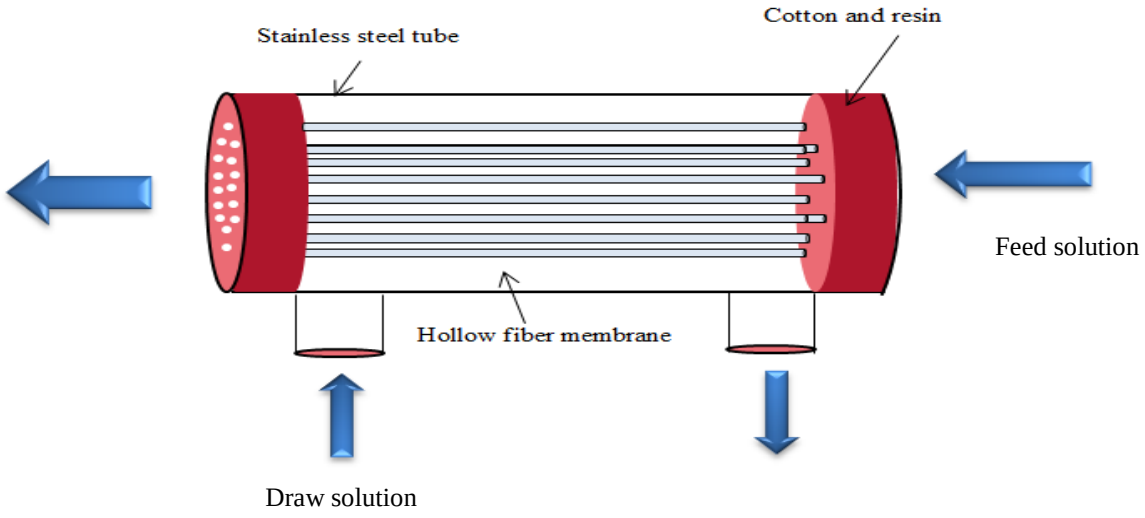

Figure 3.4: Hollow fiber module**.**

Figure 3.5: Picture for Membrane Module.

3.3 Measurement of FO performance

3.3.1 Water permeability coefficient (A)

Pressure-driven permeation test was used to evaluate the HFFO membranes performance of the water permeability. Briefly, the permeation experiment was run in an RO mode. A 24.56 cm-long HFFO membranes were installed in the HF module, and then the inlet pressure of feed solution was increased from 0 to 2 bar. FS was forced to permeate from the shell side of HFFO membrane to the lumen side. The inlet feed solution flow rate was at 1.0 L/h. The PWP was measured using DI water. This permeation experimental was carried out at room temperature (25 °C). The results showed that the increased of pure water flux J_w was linearly with the increased in the transmembrane pressure (TMP, ΔP) in the low-pressure range to avoid membranes damage, as described by equation (3.2) **(Wei et al., 2011):**

$$J_w = A \cdot \Delta P \qquad 3.2$$

Where:

J_w Water flux (LMH).

ΔP Applied pressure (bar).

3.3.2 The salt rejection (Rs)

One of the most important characteristics of hollow fibers membranes is the ability of the membrane to salts rejection and the extent of separation depends on some of the properties of the feed solution and its concentration and the applied pressure. The salt rejection (Rs) was obtained by utilizing a feed solution (FS) with 1000 ppm NaCl concentration at a certain pressure. The NaCl concentrations in the feed (C_f) side and permeate side (C_p) were measured using conductivity meter and then the salt rejection (R_S) was found using **(su et al., 2010)**:

$$R_S = \left(1 - \frac{C_P}{C_F}\right) \times 100\ \% \qquad 3.3$$

Where:

R: Rejection rate (%)

C_P : Concentration of NaCl salt in permeate side (mg/l).

C_F : Concentration of NaCl salt in feed side (mg/l).

3.3.3 Salt permeability coefficient (B)

Accordingly, the salt permeability coefficient (B) was calculated according to the solution-diffusion theory by a linear fitting based on this equation **(Wei et al., 2011)**:

$$\frac{1-R_S}{R_S} = \frac{B}{A(\Delta P - \Delta\pi)} \qquad 3.4$$

3.3.4 The structural parameter (*S*)

The resistance of the membrane surface to the internal polarization (ICP) effect can be evaluated by measuring the structural parameter of the membrane. Structural parameter was an important property of the HFFO membranes based on the support layer characteristic and the porosity (ε), tortuosity (τ) as well as thickness (t) of membranes where (S= t τ / ε), which can be calculated utilizing equation (3.5) which was the classical ICP model advanced by **(Loeb et al., 1997)**:

$$S = \left(\frac{D}{J_W}\right) \ln \frac{B + A\pi_D}{B + J_W + A\pi_{F,m}} \qquad 3.5$$

Where

D is the diffusion coefficient of NaCl salt (D = 1.33×10^{-9} m/s at 25˚C) **(Lobo et al., 1993).**

π_D the osmotic pressure of the bulk draw solution (DS).

$\pi_{F,m}$ the osmotic pressure at the surface of the membrane in the FS.

For high salt rejecting membranes, salt permeability coefficient (B) was ordinarily assumed zero. The structural parameter (S) of the fabricated HFFO membranes was evaluated using 1.0M NaCl solution and (DI) water as draw and feed solutions, respectively. The cross-flow velocity was maintained at 0.1 l/min for both draw and feed solutions, while utilizing (DI) water as feed ($\pi_{F,m}$ = zero) Equation (3.5) can be simplified to:

$$S = \left(\frac{D}{J_W}\right) \ln \frac{A\pi_D}{J_W} \qquad 3.6$$

3.3.5 Water flux

By determining the volume changes for the feed solution (FS), the flux of water for the three HFFO membranes was found using the following equation **(Wei et al., 2011)**:

$$J_W = \frac{\Delta V}{A_m \times \Delta t} \qquad 3.7$$

where:

J_W Water flux (LMH).

ΔV volume changes of feed solution volume (liter).

Δt the measured time interval (hr).

A_m effective membrane area (m^2).

3.3.6 Solute flux

The reverse solute flux is the reversely permeating of salt from the draw solution (DS) side to the feed side (FS) of the membrane. This flux was calculated by measuring the volume and the changing in the conductivity of the feed solution FS **(su et al., 2010)**:

$$J_S = \frac{CtVt\_CoVo}{A_m \times \Delta t} \qquad 3.8$$

Where :

J_S salt flux.

V_t The feed solution volume at time t (liter).

V_o The feed solution volume at time 0 (liter).

C_t is the feed solute concentration in the feed tank at time t (g/l).

C_o is the feed solute concentration in the feed tank at time 0 (g/l).

A_m is the effective area of membrane (m^2).

CHAPTER FOUR
RESULTS AND DISCUSSION

4. General

This chapter discusses the experimental results of the forward osmosis process which explain the influence of various operating conditions such as draw solution (DS) concentration, feed and draw solution flow rate on the performance of hollow fiber forward osmosis HFFO membrane. Also discussing the influence of polymer content of the morphology of the HF membranes, pore size, and pore size distribution as well as water permeability.

4.1. Hollow fiber forward osmosis analysis

4.1.1. Scanning electron microscope (SEM)

Figures (4.2, 4.3) show the structural morphology images of the hollow fibers with different PPSU concentrations i.e., 25, 29, and 30 wt %. It can be seen that the outer surfaces were dense and no pores were appeared at the surface of all hollow fibers, while the pores on the inner surface were decreased in size and density with increasing of the polymer (PPSU) concentration in dope solution. This phenomenon was due to the delay water-DMAC exchange rate during the formation of the nascent hollow fibers with increasing of PPSU concentration **(Alobaidy et al., 2017; Alsalhy et al., 2011; Alsalhy et al., 2012)**. Also, in Figure (4.4) it can be noticed that the structure of the cross-sectional area of the PPSU hollow fibers prepared from 25 wt.% PPSU have composed of one layer finger like shape near the inner surface of the hollow fiber and some finger like shape near the outer surface with full sponge shape in the middle of the cross section area and in between

of the figure shape as shown in Figure (4.4). Further increase in PPSU concentration resulted to change the structure of the fibers to full sponge shape in whole cross section of the fiber with one layer figure like shape near the inner surface as well as increasing of the skin layer of all fibers with increasing of PPSU concentration as shown in Figures (4.5 and 4.6).

Table 4.1 Summary of the Characteristics for three HFFO membranes

Sample membranes	Dimension		
	OD(μm)	ID(μm)	Thickness (µm)
PPSU 25%	809.59	695.57	57.01
PPSU 29%	728.83	603.61	62.61
PPSU 30%	867.25	736.13	65.56

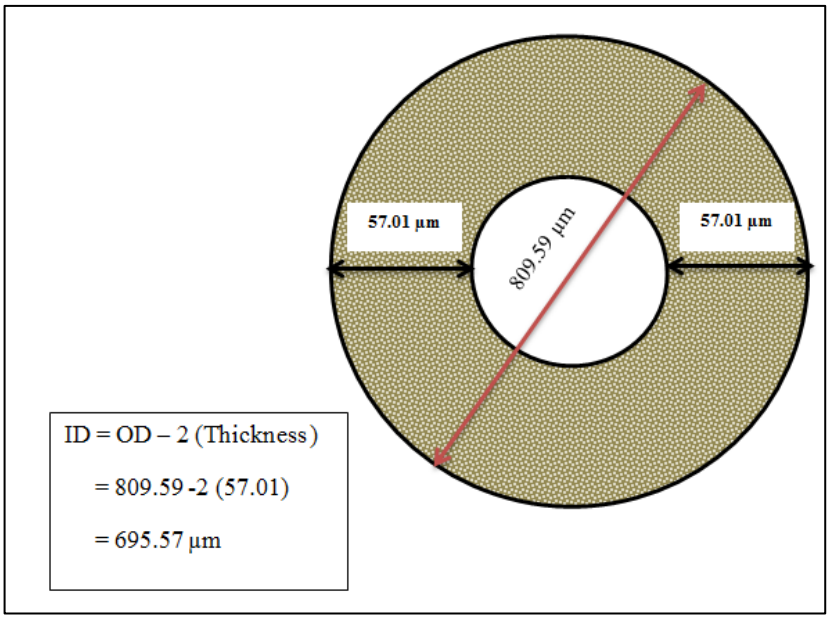

Figure 4.1 Membrane dimensions calculation

(a)

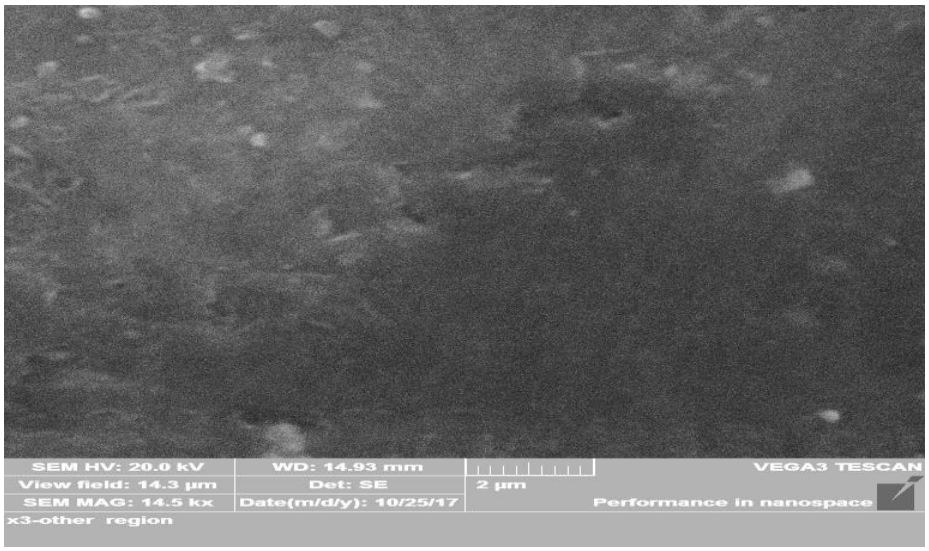

(b)

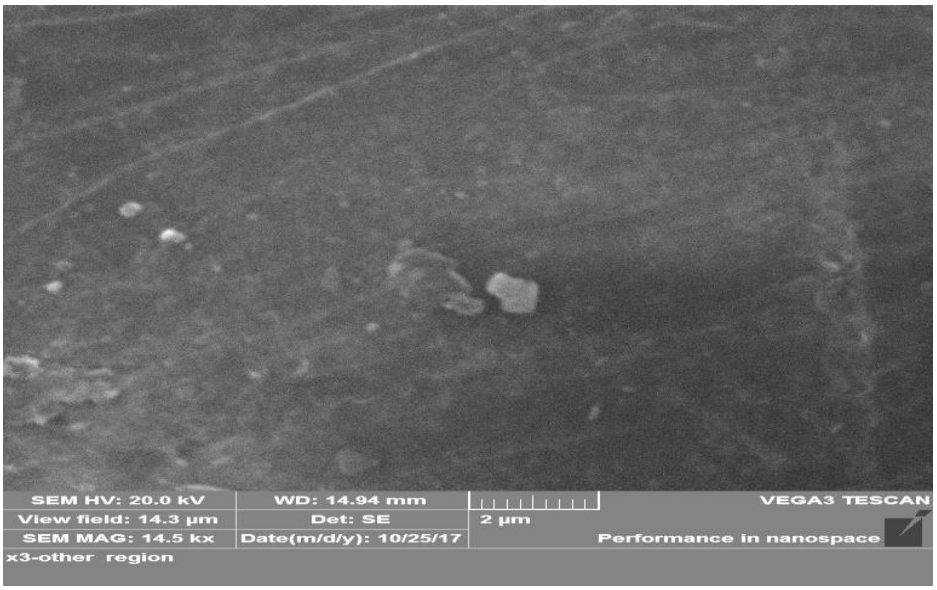

(c)

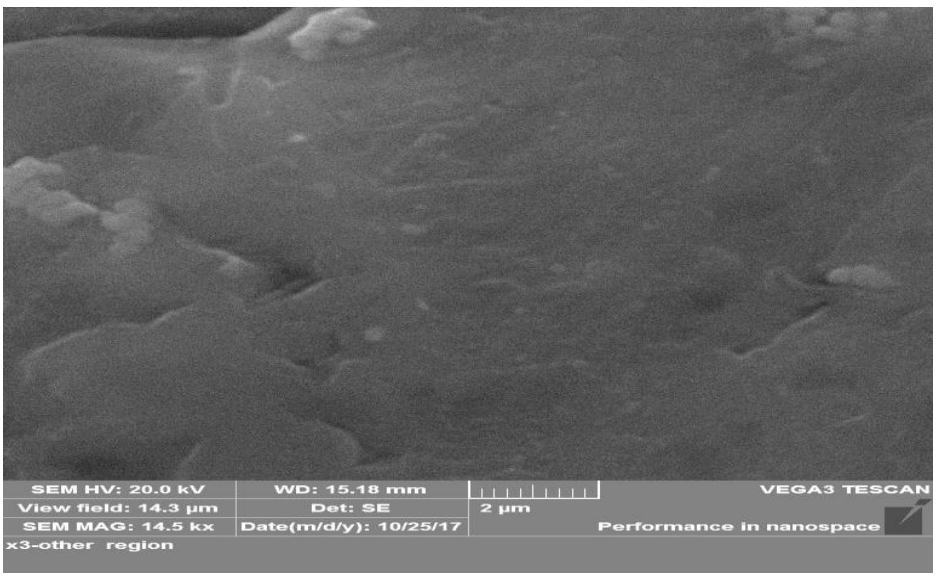

Figure 4.2 The hollow fibers membranes outer surface SEM images with different PPSU concentrations: (a) 25 wt % , (b) 29 wt % , (c) 30 wt %.

(a)

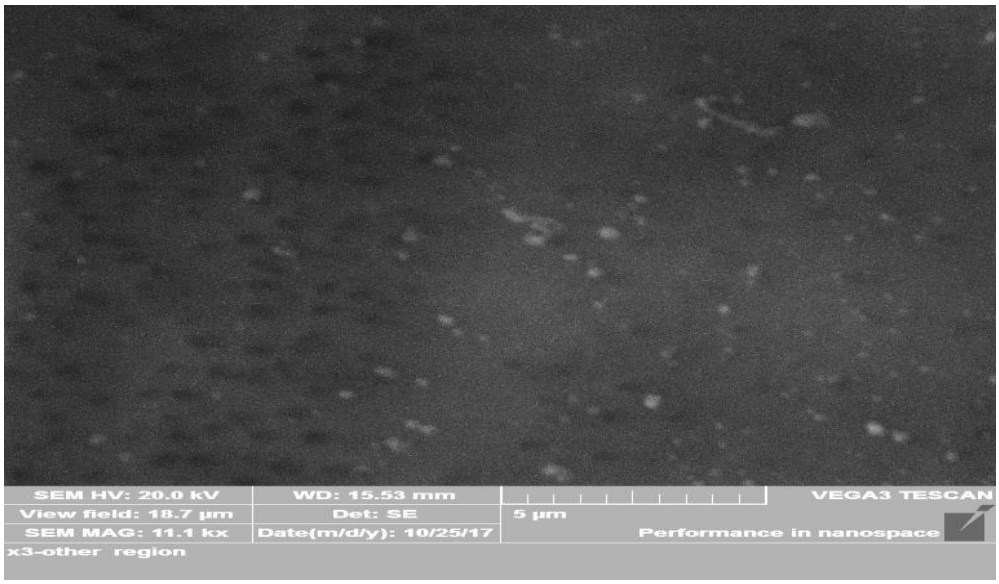

(b)

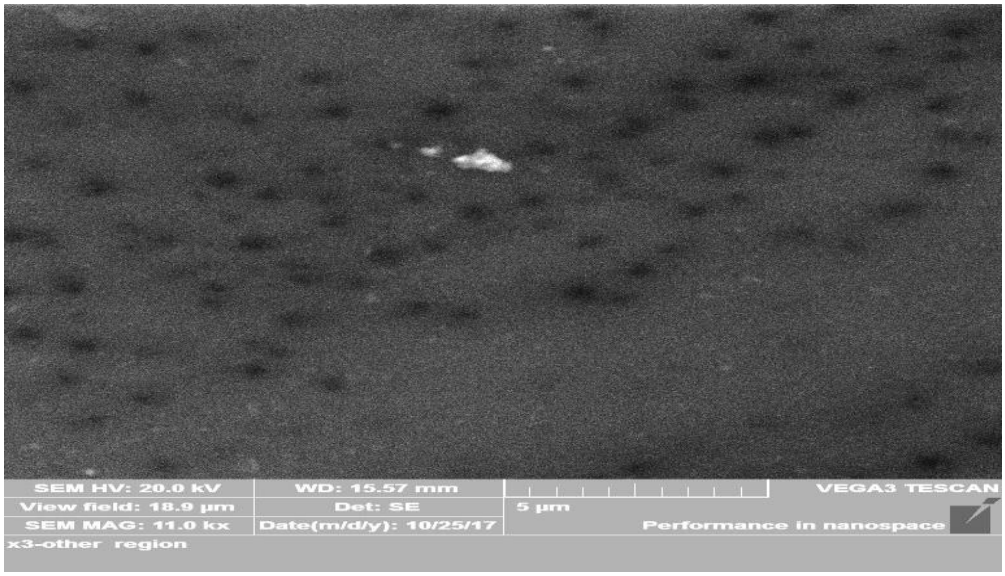

(c)

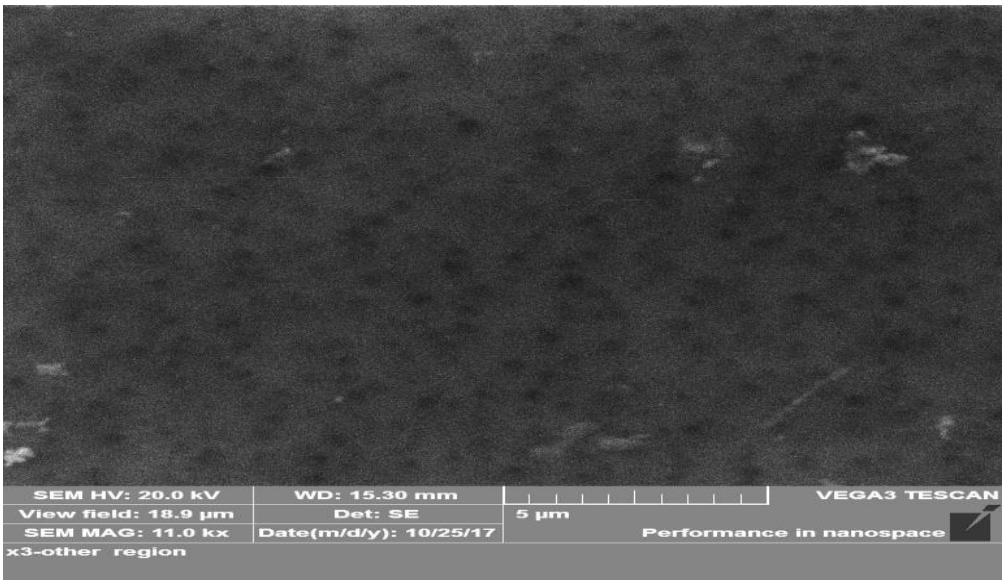

Figure 4.3 The hollow fibers membranes inner surface SEM images with different PPSU concentrations: (a) 25 wt % , (b) 29 wt % , (c) 30 wt %.

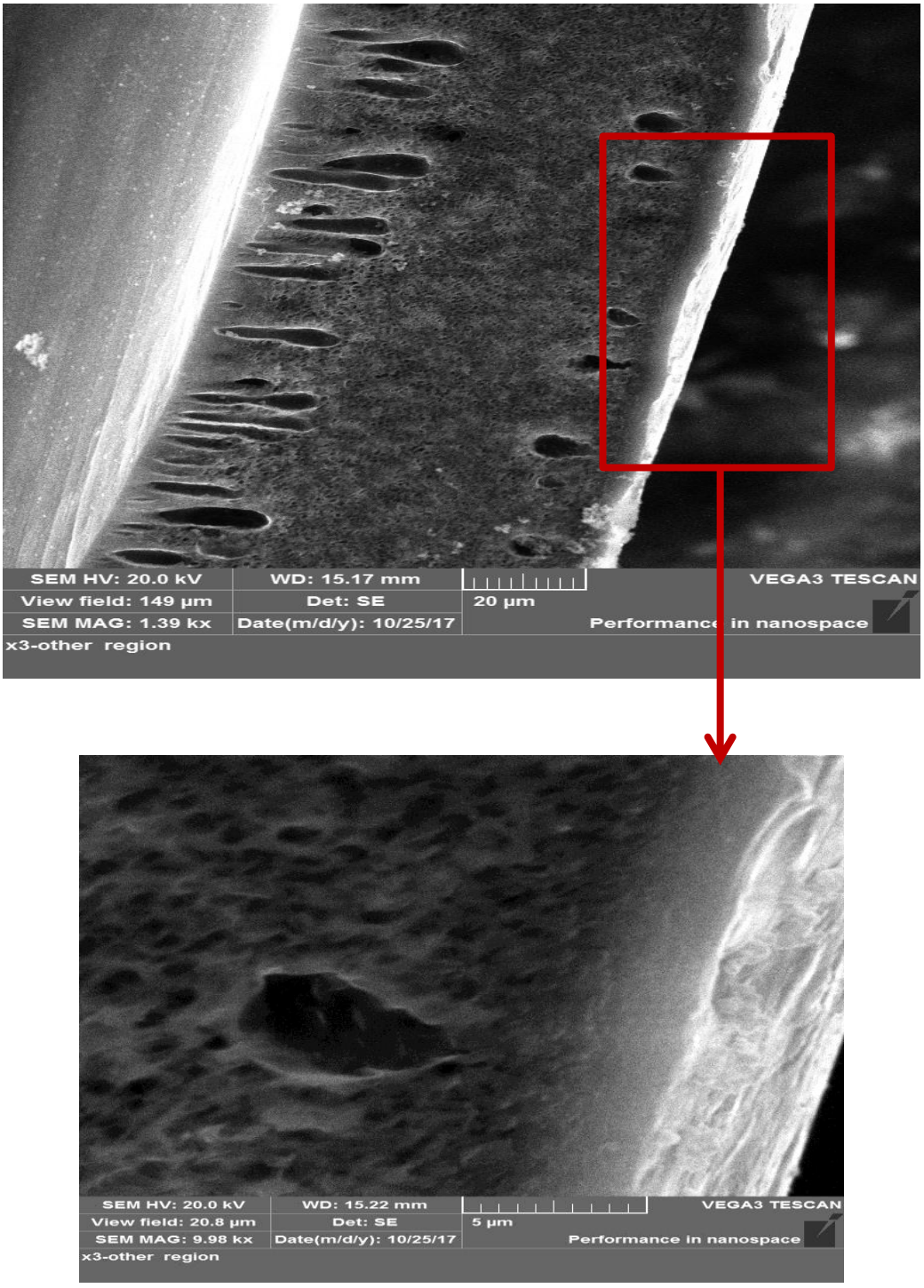

Figure 4.4 The PPSU 25 wt% hollow fiber membrane cross section SEM images.

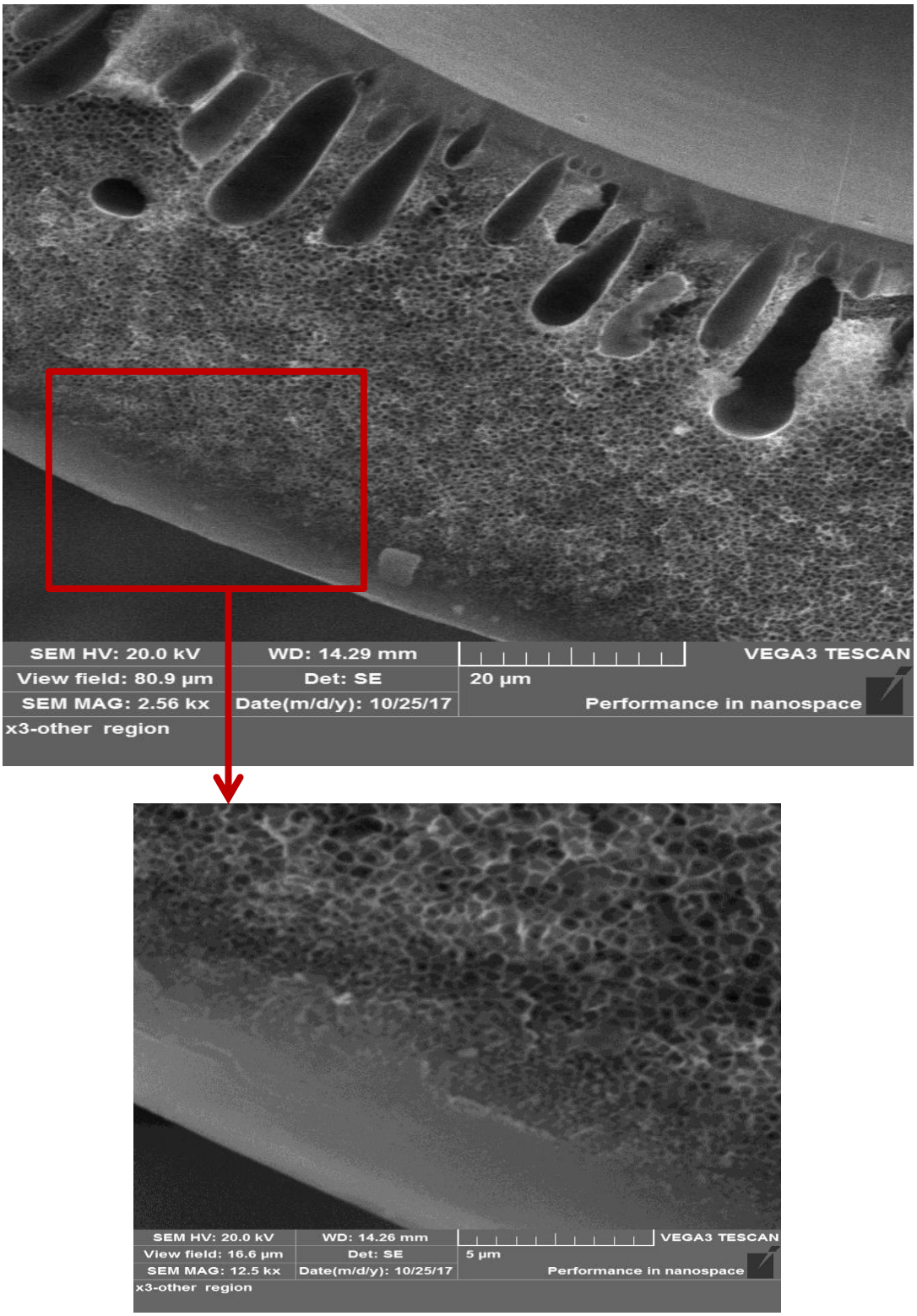

Figure 4.5 The PPSU 29 wt% hollow fiber membrane cross section SEM images.

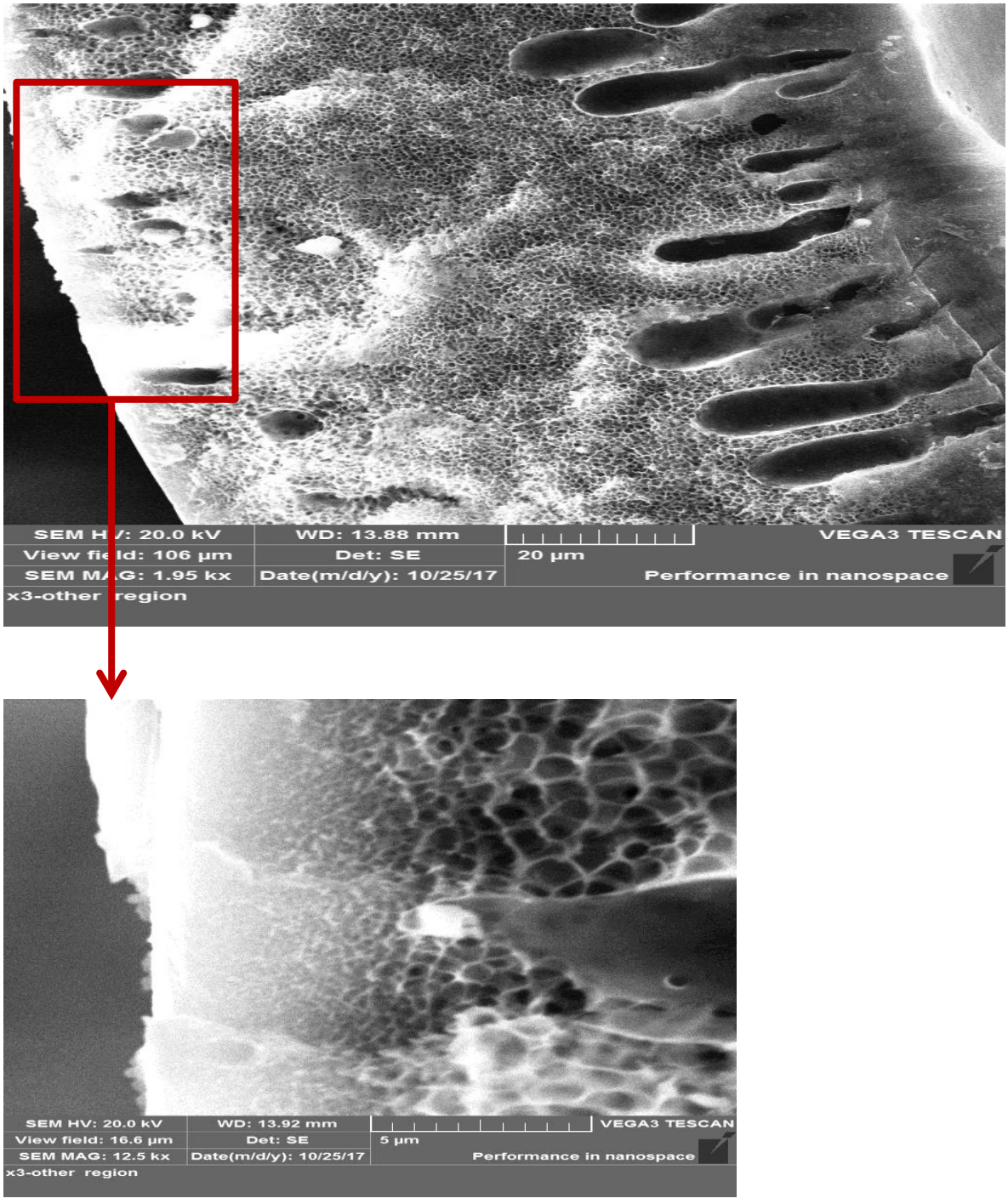

Figure 4.6 The PPSU 30 wt% hollow fiber membrane cross section SEM images.

4.1.2. Atomic Force Microscope (AFM) analysis

Figures (4.7 and 4.8) show 2D and 3D of AFM images for inner and outer surfaces of hollow fiber fabricated from **PPSU** polymer with different concentrations (i.e., 25, 29, and 30 wt.%). It can be observed that the presence of nodules (light zones) and valleys (dark zones) at each inner and outer surfaces of fabricated membrane. For inner and outer surfaces at (25 wt.%) concentration of **PPSU** it can be seen that the sizes of nodules were big with approximately a small density of it as well as of valleys as shown in Figures (4.7 A and B ,4.8 A and B). Whereas more increasing of the concentration of **PPSU** polymer to 29, and 30 wt.% results to smaller sizes of nodules with high nodules density as well as density of valleys were become high (see Figures (4.7 and 4.8; C, D, E and F)). Therefore, it can be concluded that the change of diffusion rate between solvent/nonsolvent during formation of membrane was extremely important in formation of nodules and valleys for inner as well as outer surface of fabricated membrane **(Alsalhy et al., 2013).**

The mean roughness of both surfaces of fabricated membranes is summarized in Tables (4.2 and 4.3), in which it represents the vertical distance between the higher peak of nodules and valleys of fabricated membranes **(Alsalhy et al., 2013)**. From Tables (4.2 and 4.3) for (25 wt.%) concentration of **PPSU** it can be noticed that the outer surface means roughness is (8.04 nm) which was higher than that for inner surface (6.65 nm) at the same concentration. Whereas with increasing the concentration of **PPSU** in dope solution to (29 and 30 wt.%) it can be seen that the mean roughness of outer surface became (3.37 and 4.93 nm) respectively, which was smaller than that observed at inner surface of (24.5 and 7.36 nm) respectively. This may be referred to increased viscosity of dope solution with

increasing the concentration of PPSU polymer, therefore leading to slower rate of coagulation of inner surface where this resulting to increase the mean roughness of inner surface of fabricated membrane through spinning process. In contrary, increasing the viscosity of dope solution may cause elongation stress at outer surface as a result for gravity during the spinning process where this reduces the mean roughness of outer surface of fabricated membrane owing to change the size of the nodules as well as pore size of membrane **(García-Payo et al., 2010).**

In Figure (4.9) and Table (4.2) of inner surface of membrane fabricated from (25 wt.%) concentration of **PPSU** polymer it can be seen that the mean pore size is (106.89 nm) with pore size distribution of (70-150 nm) (see Figure 4.9A), and with increasing the **PPSU** concentration in dope solution to (29 wt.%) we noticed that the pore size reduced to (83.07 nm) without change in distribution of pore size according to Figure (4.9 B). Whereas increasing the concentration of **PPSU** polymer to (30 wt.%) the pore size decreased to (76.16 nm) with narrow pore size distribution (i.e., 65-115 nm) as shown in Figure (4.9 C).

Regarding the outer surface pore size and pore distribution, from Figure (4.9) of outer surface and Table (4.3) it can be seen that the pore size of fabricated membrane that fabricated with (25 wt.%) concentration of **PPSU** polymer was (98.02 nm) with distribution of pore size ranged between (75 and 120nm) according to Figure (4.9 A), and with increasing the **PPSU** concentration to (29 wt.%) the membrane pore size reduced to (71.67 nm) with approximately wide range of pore size distribution of (i.e., 60-120) as shown in Figure (4.9 B), whereas further increasing of the concentration of **PPSU** polymer to (30 wt.%) the size of pore has reduced to (60 nm) with

wider pore size distribution ranged between (45 and 125 nm) as shown in Figure (4.9 C).

It is worth to conclude that the pore size was reduced by about (22.28 and 28.75%) of inner surface, whereas for outer surface was reduced by about (26.88 and 38.78%) with increasing the **PPSU** polymer concentration from 25 wt.% to 29 and 30 wt.%, respectively. It was obvious that increasing concentration of polymer resulting to increase the dope solution viscosity, which this in turn delays the exchange rate of solvent/nonsolvent of polymer solution during the membrane formation, therefore was found lower size of pores **(Alsalhy, 2012).**

Through the AFM analysis of membranes, the mean pore size and pore size distribution were taken results in consideration and reliance on the diagnosis of properties of the three membranes and the differences in the composition of the outer and internal surfaces with the increase in the polymer content, which is the important in this analysis and were more logical and identical with the results to be obtained . And the results of the surface roughness were uneven and cannot be compared.

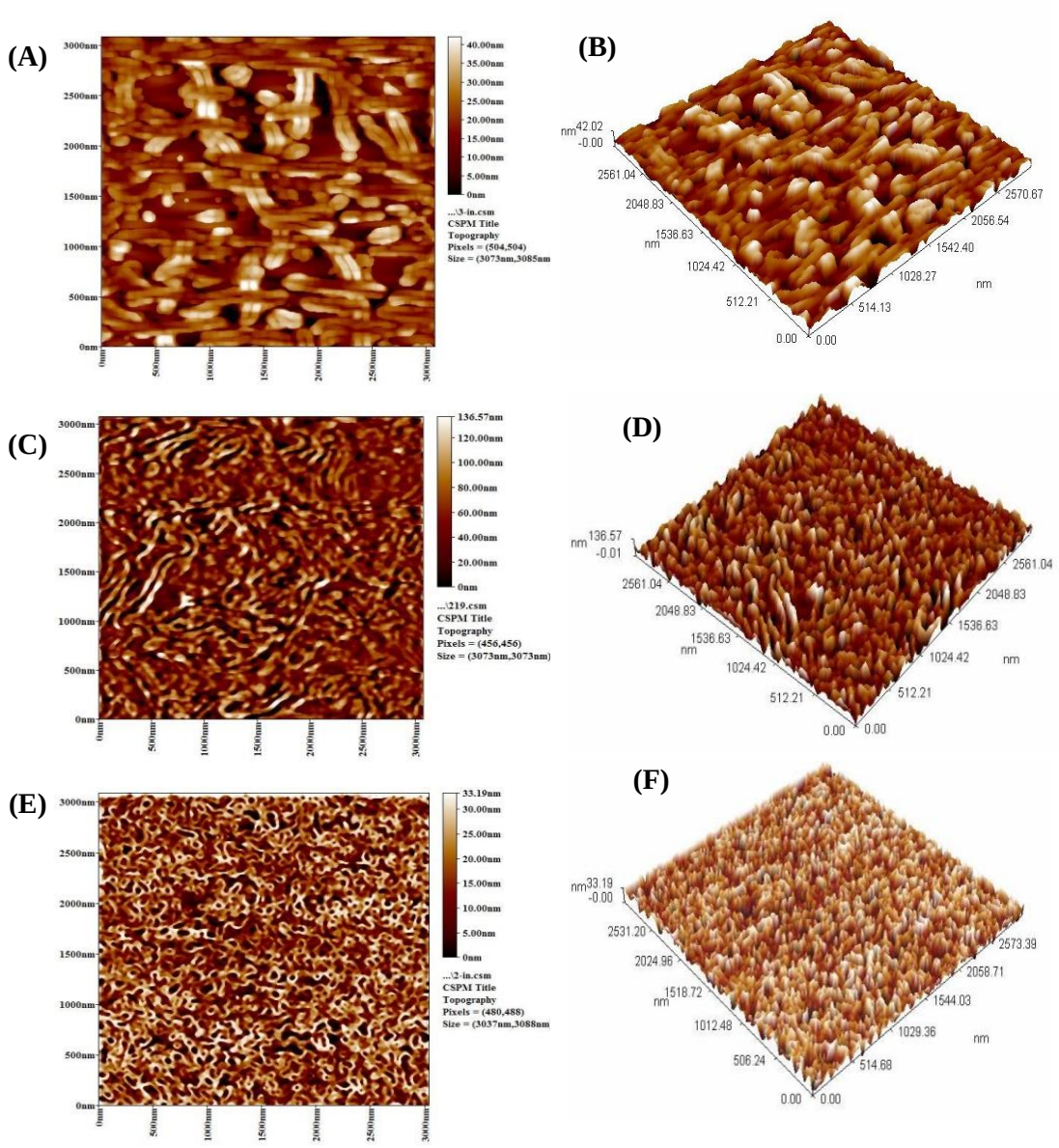

Figure 4.7. The inner surfaces of the PPSU hollow fibers topography and three-dimensional AFM images with different PPSU concentrations: (A) PPSU 25% (B) PPSU 25 % 3D, (C) PPSU 29 %, (D) PPSU 29% 3D, (E) PPSU 30%, and (F) PPSU 30% 3D.

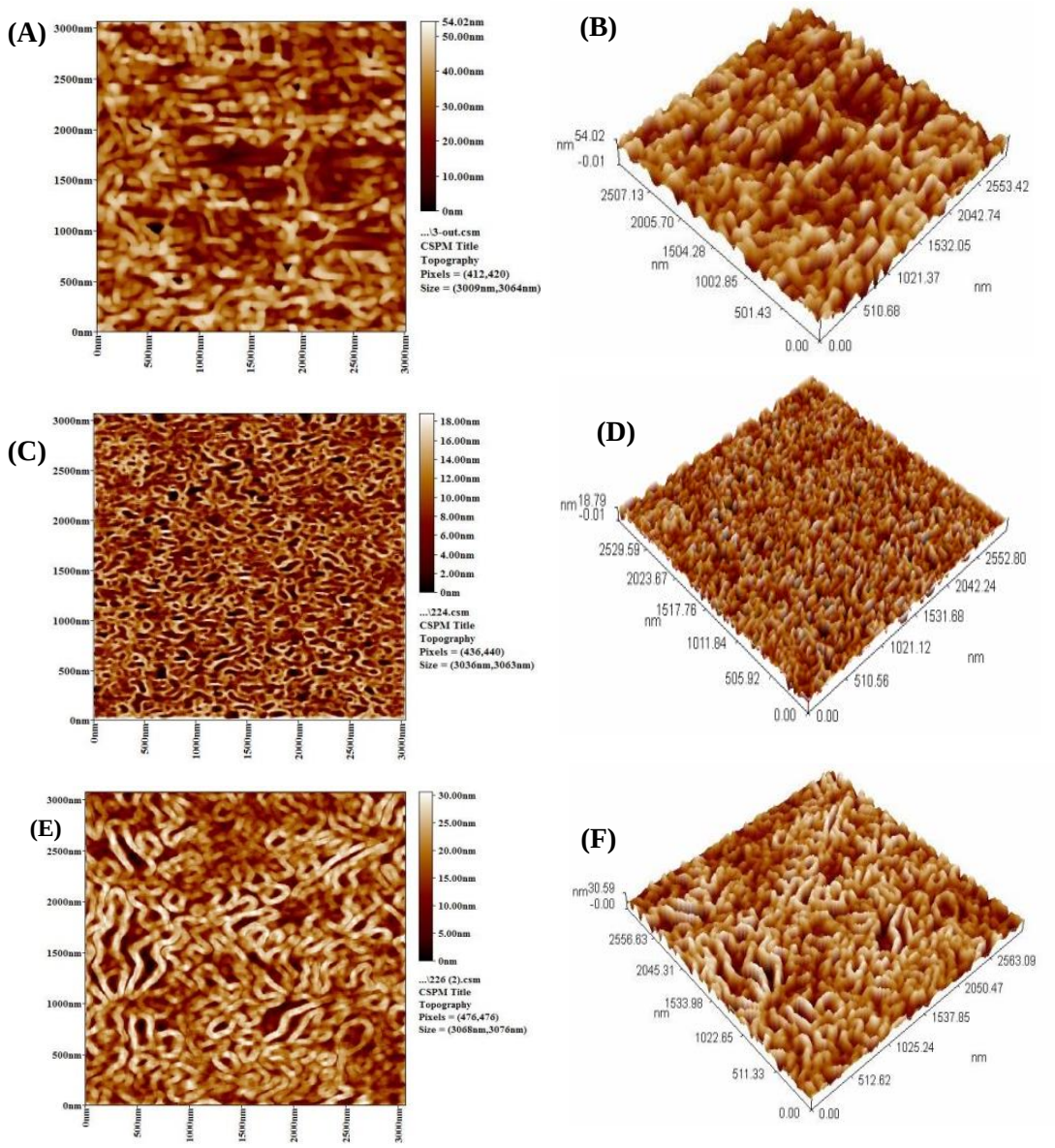

Figure 4.8 The outer surfaces of the PPSU hollow fibers topography and three-dimensional AFM images with different PPSU concentrations: (A) PPSU 25% (B) PPSU 25 % 3D, (C) PPSU 29 %, (D) PPSU 29% 3D, (E) PPSU 30%, and (F) PPSU 30% 3D.

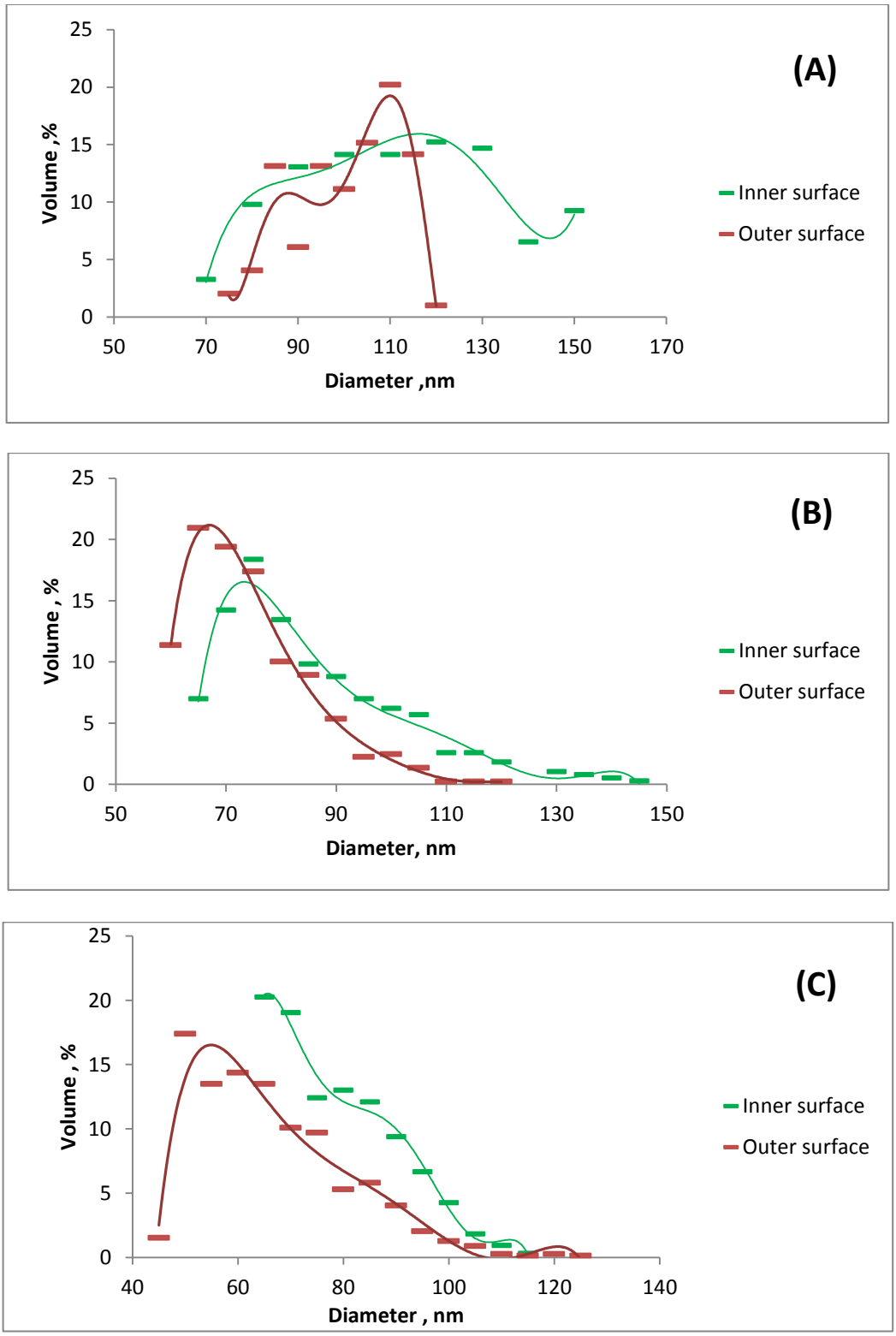

Figure 4.9 The normal distribution chart of pores for the inner and outer surfaces of the PPSU hollow fibers: (A) PPSU 25 % , (B) PPSU 29 % ,and (C) PPSU 30 %.

Table 4.2 Mean Pore Size and pore size distribution, and Roughness of the inner surface of PPSU Hollow Fiber Membranes.

Membranes	Inner Surface			
	Mean pore size D^*(nm)	Surface roughness (nm)		Pore size distribution (nm)
		Mean roughness (R_a)	The root mean square of Z values (R_{rms})	
PPSU 25%	106.89	6.64	8.44	70 - 150
PPSU 29%	83.07	24.5	29.7	65 - 145
PPSU 30%	76.16	7.36	8.65	65 - 115

Table 4.3 Mean Pore Size and pore size distribution, and Roughness of the outer surface of PPSU Hollow Fiber Membranes.

Membranes	Outer surface			
	Mean pore size D^*(nm)	Surface roughness (nm)		Pore size distribution (nm)
		Mean roughness (R_a)	The root mean square of Z values (R_{rms})	
PPSU 25%	98.02	8.04	9.68	75 - 120
PPSU 29%	71.67	3.37	4.05	60 - 120
PPSU 30%	60.00	4.93	6	45 - 125

4.2 Parameters Affected Membrane Performance

4.2.1 Porosity and thickness

The porosity of the HFFO membranes can be obtained by measuring the weight. Figure (4.10) illustrates the change of porosity values for three HFFO membranes (PPSU 25% , PPSU 29% , and PPSU 30%) with polymer content were PPSU 25% showing higher porosity than two other membranes that indicates when increasing polymer percentage in fabricated membrane porosity reduced which agreeing well with previous studies **(Wei et al., 2011;**

Darvishmanesh et al., 2011). The porosity data in Table (4.4) support the above observations by showing that the porosity of PPSU 30% was only 79.87 %, of less than PPSU 29% (82.45 %) and PPSU 25% (83.72%).

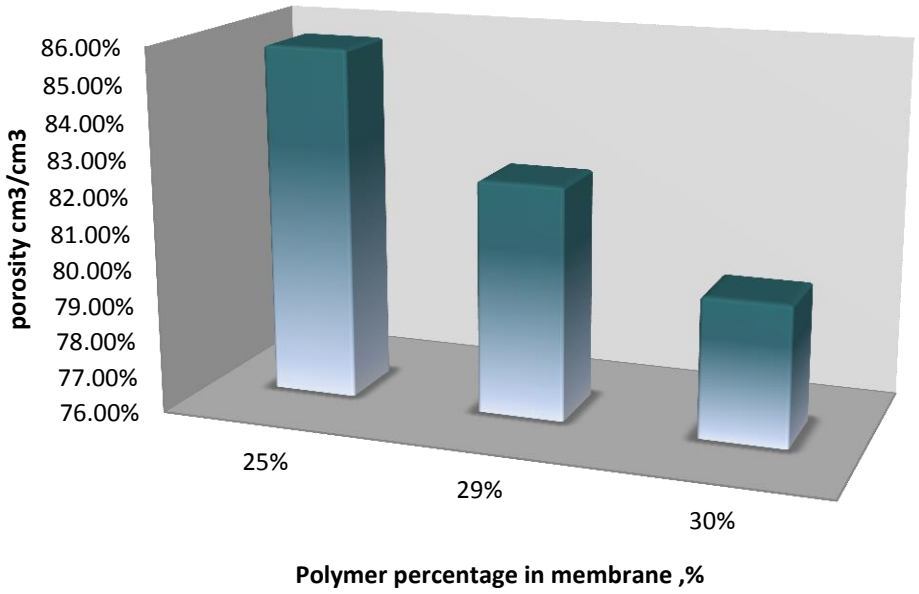

Figure 4.10 Relationship between polymer percentage in membrane and porosity.

As shown in Table (4.1), it can be observed that the thickness of the PPSU 25% HFFO membrane was small compared with the thicknesses of PPSU 29% and PPSU 30 %. Small membrane thickness is a preferred characteristic for high flux across the membrane and this explains the PPSU 25% membrane achieving the expect highest flux between the others membranes. It is expected that the higher the thickness of the membrane, the more it contributes to the internal concentration polarization (ICP) development that resulting in reduced driving force and thus reduce the flux

rate produced **(McCutcheon et al., 2005)**. Hence a thin membrane is preferred for the purpose of minimizing ICP. Figure (4.11) shows the increase of membrane thickness with increasing polymer percentage. Generally, this small membranes thickness (57.01~65.56 µm) in FO process can effectively minimize the transport resistance and internal concentration polarization (ICP).

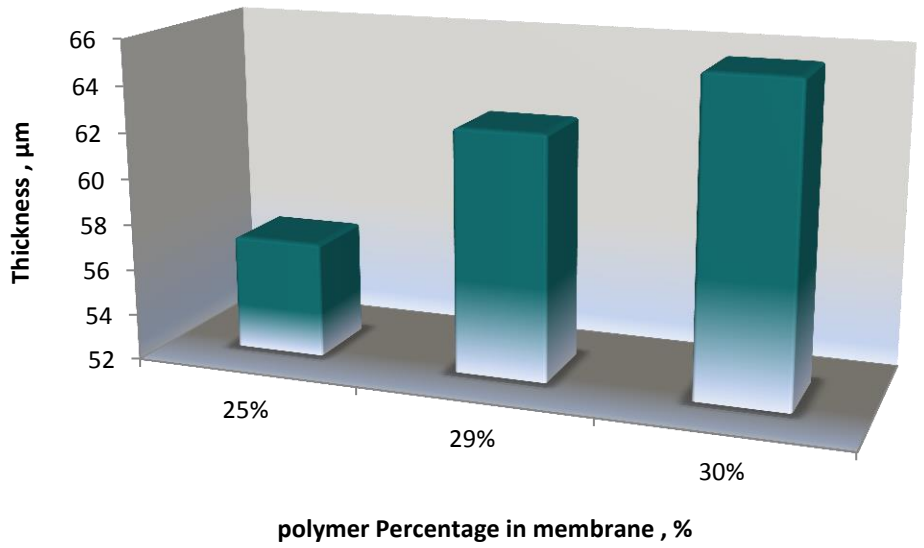

Figure. 4.11. Relationship between polymer percentage in membrane and thickness.

4.2.2 Structural parameter (*S*)

The membrane structural parameter is an intrinsic important property that shows the extent to which the membrane is affected by internal concentration polarization. In the membranes of the forward osmosis process, the small value of the structure parameter shows its positive performance mainly due to reducing the tortuosity according to ($S= t \tau / \varepsilon$) the resulting in decreased ICP. Experiments in the FO test apparatus were employed to calculate S, following the protocol described in earlier studies **(Tiraferri et al., 2011; Yip et al.,**

2010). As shown in the Table (4.4), the increase in water flux for PPSU 25% can be attributed to the decrease in structural parameter (S value = 467 µm). In general, other membranes have relatively low S values (i.e., 567, and 601 µm) respectively. This is a good indication to evaluate the membrane efficiency.

4.3 Mass Transport Characteristics of HFFO Membranes.

4.3.1 Water permeability coefficient (A)

Pure water permeability (PWP) for the three types of membranes was measured by using cross-flow filtration process by applying transmembrane pressure (TMP, ΔP) between 0 – 2 bar and using DI water as feed solution. PPSU 25% membrane showed PWP value (2.25 LMH/bar) higher by 29% and 56% respectively than PPSU 29% (PWP 1.59 LMH/bar) and PPSU 30% (PWP 0.99 LMH/bar), as shown in Table (4.4). It can be noted that the water permeability increased with the decreasing of polymer content (which led to increase membrane pore size) and thickness. Figure (4.12, 4.13 & 4.14) graphically describes how to determine water permeability (A) of the hollow fibers. The results indicate that pure water flux Jw for the HFFO membranes increased linearly with the increase in transmembrane pressure (TMP, ΔP).

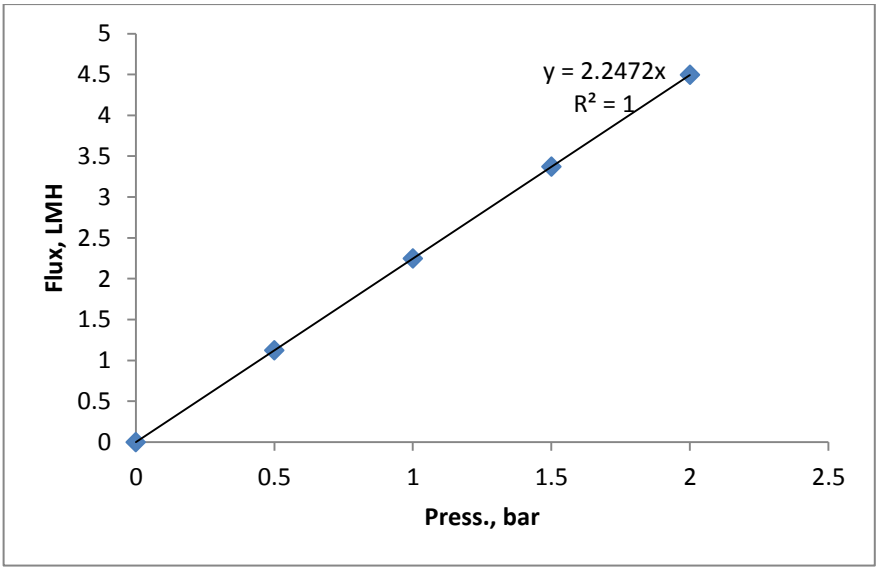

Figure. 4.12 Water Flux Change with pressure (Temp. 25±5˚C, DI water used as feed , 0.1 l/m flow rate ,for PPSU 25%).

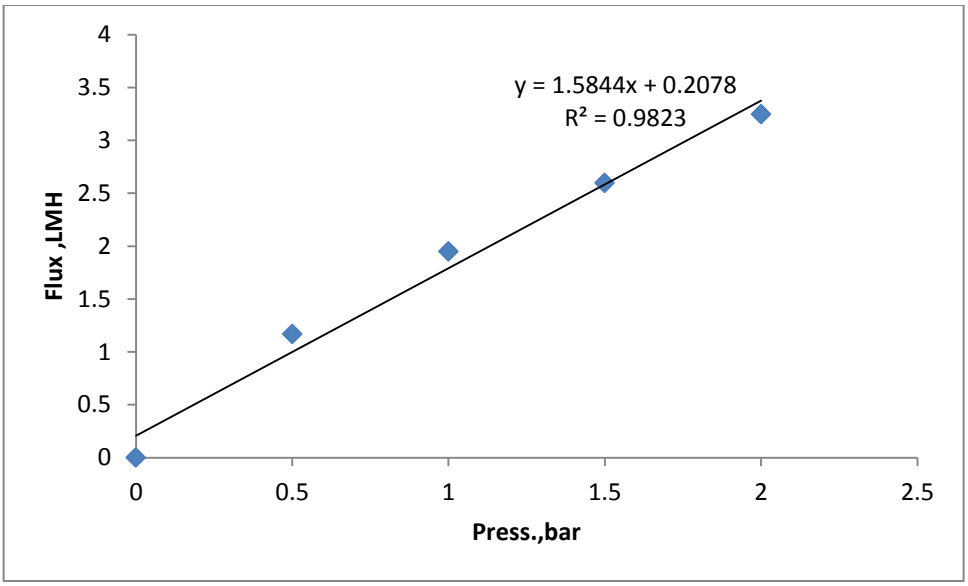

Figure. 4.13 Water Flux Change with pressure (Temp. 25±5˚C, DI water used as feed , 0.1 l/m flow rate ,for PPSU 29%).

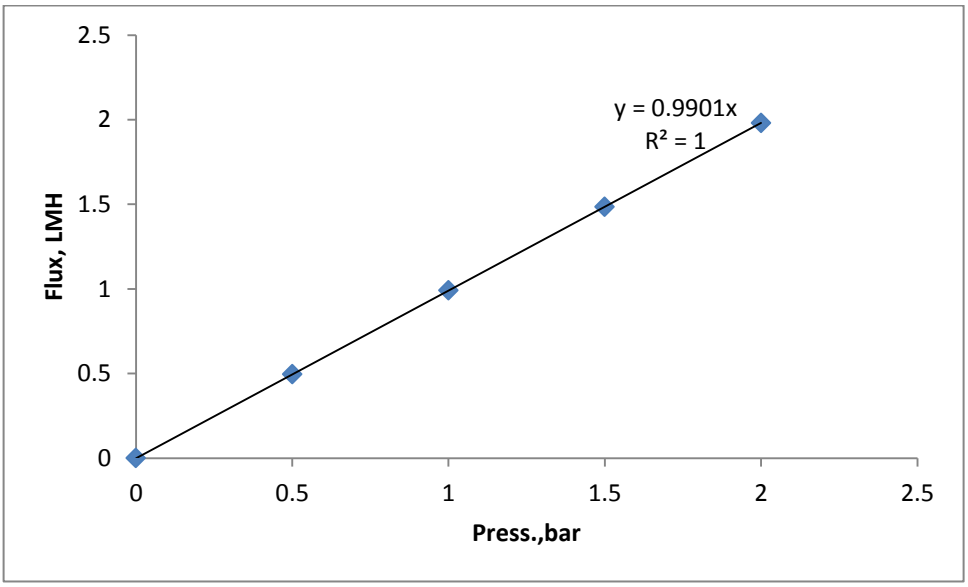

Figure. 4.14 Water Flux Change with pressure (Temp. 25±5˚C, DI water used as feed , 0.1 l/m flow rate ,for PPSU 30%).

4.3.2 Salt rejection (Rs)

The salt rejection of the membranes tested at room temperature and 1.0 bar transmembrane hydraulic pressure to avoid fiber damage and 1000 ppm NaCl solution was used as feed, as in previous research **(Zhong et al., 2013)**. As shown in the Table (4.4) the three membranes show various salt rejections of NaCl, where PPSU 25 % was the smallest rejection among the others hollow fibers (i.e., 85.1%). PPSU 30% higher salt rejection (Rs) by about 5.5% and 4% than PPSU 25% and PPSU 29%, respectively. Higher rejection can lower salt reverse flux in the FO process.

4.3.3 Salt permeability coefficient (B)

The salt permeability coefficient (B) represents an intrinsic property of a membrane, and it was found based on the solution-diffusion theory (**Emadzadeh et al., 2013)**. PPSU 25% show higher salt permeability coefficient (B) (0.371 LMH) than PPSU 29% (0.250 LMH) and PPSU 30% (0.105 LMH).

Table 4.4 Summary of the calculated transport parameters A, B, R_S and S, with porosity, and length for three HF membranes.

Sample membranes	Length (cm)	Water permeability coefficient, A [LMH/bar]	Salt permeability coefficient, B [LMH]	Porosity ε (%)	salt rejection R_S%	structural parameter S (µm)
PPSU 25%	24.56	2.25	0.371	85.72%	85.1 @1.0 bar	467
PPSU 29%	24.56	1.59	0.250	82.02 %	86.2 @1.0 bar	567
PPSU 30%	24.56	0.99	0.105	79.55 %	89.8 @1.0 bar	601

4.4. Effect of Operating Conditions

The operating conditions have a direct impact on the performance of the forward osmosis operation. This has been tested by conducting a number of experiments to investigate the results.

4.4.1 Flux variation with time

In order to measure the change of flux with time, experiments were carried out for the three types of hollow fiber membranes (PPSU 25% ,PPSU 29% and PPSU 30%) using 1.0 M NaCl as draw solution and DI water as feed solution, while the cross flow for both sides stabilized at 0.1 l/ min. The FS was flowing tangled with the membrane active layer and the DS flowing at the membrane support layer. The temperature was at 25 ±5°C, for both sides and the water flux changed with the experiment time were measured for the three types of membranes. As shown in the Figure 4.15 the PPSU 25% membrane shows much higher water flux than each of PPSU 29% and PPSU 30% membranes. In general, it can be observed that all three membranes showed water flux decline with time during the test, the decline in water flux at the first hour and half of experiment was high, about 40% for PPSU 25% , 52% for PPSU 29% while it was 36% for concentration of 30% PPSU. The flux became fewer declines and after four hours of operation became more stable with time. The flux difference among these membranes was due to the PPSU polymer content difference in the membranes in which changes their properties, where the PPSU 25% membrane thickness was 57.01 µm, which was less than thickness of PPSU 29% and PPSU 30% membranes 62.61 and 65.56 µm, respectively. That explains the thick support layers of PPSU 29% and PPSU 30% membranes may have an influence on the development of internal concentration polarization (ICP) and that reduced the effective driving force of process and hence the water flux with time.

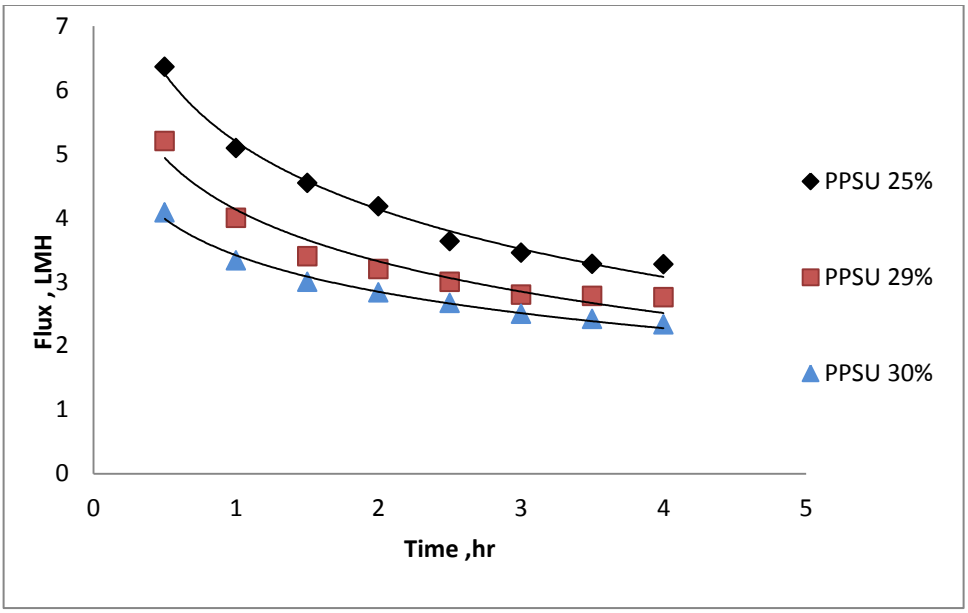

Figure .4.15. Water Flux Change with time (Temp. 25±5˚C, DI water & 1 M draw solution conc. , 0.1 l/m feed & draw solution flow rate, and for three type of PPSU HF Membrane).

4.4.2 Effect of draw solution concentration on water flux

Experiments were conducted to study the effect of changing the concentration of the draw solution on the flux. The results showed that increasing in the water flux when the draw solution concentration was changed in the range between 1.0 and 3.0 M NaCl, as a result of the osmotic driving force increasing across the HFFO membranes (while the osmotic pressure difference ($\Delta\pi$) was the driving force in FO process). These results were confirmed with several previous studies **(Holloway et al., 2015; Ong et al., 2015; Widjojo et al., 2013)**. Some deviation from the linearity due to the effect of ICP can be observed in the Figure (4.16), **(Cath et al., 2006)**. And the order of water flux increased according to membrane type as: PPSU25% > PPSU29% > PPSU30%.

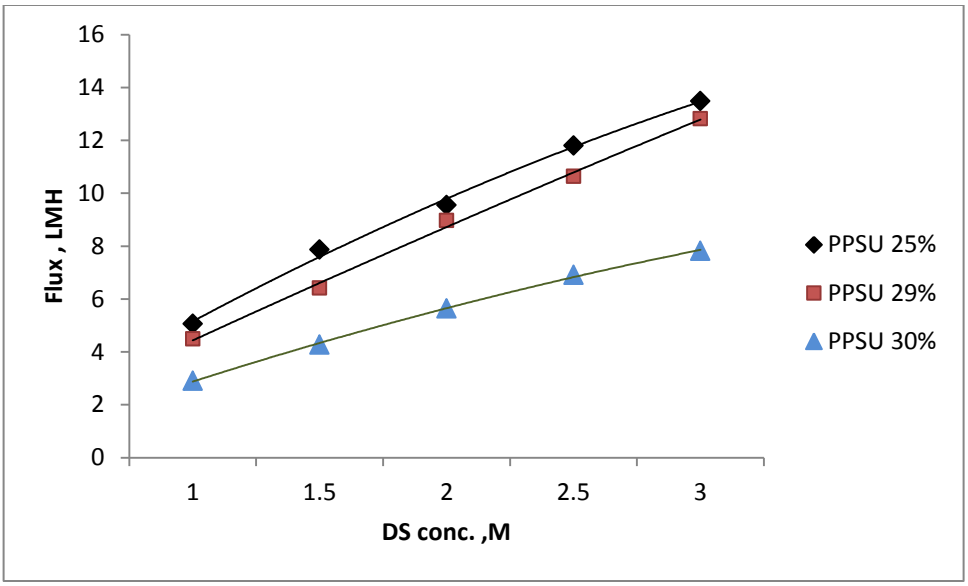

Figure 4.16 Water Flux Change with Draw Solution Concentration (Temp. 25±5˚C, Feed & Draw Flow Rate 0.1 l/min, 0.5 M FS concentration and for three types of PPSU Membranes).

This Figure shows that the increasing in the water flux for the concentration 1.0−1.5 M is between 43− 55%, while for concentration 1.5−2.0 M, 2.0−2.5 M, and 2.5−3.0 M were 21−39%, 24− 23%, and 18− 23% respectively for three HFFO membranes. This outcome reveals that higher water flux obtained with concentration of 1.0−1.5 M, because at these concentrations the probability of salt transportation (RSF) is less than if the concentrations are high and lead to the decrease of the osmotic pressure across the membrane.

4.4.3 Effect of draw solution flow rate on water flux

The effect of draw solution flow rate (Q_{DS}) on water flux at the same concentration of draw solution (1.0 M) for the three types of HFFO membranes is shown in Figure (4.17). The results show that the increase in the DS flow rate was adversely affected on the flux. For PPSU 25%, PPSU 29%, and PPSU 30% membranes, the decrease in water flux with draw solution

flow rate (0.1− 0.5 l/min) was approximately 24%, 20%, and 21% respectively, and from (0.5− 1.0 l/min) was 5.2%, 6% and 3.9% respectively. It can be noticed from Figure (4.17) that the decreasing in the water flux with draw solution flow rate (Q_{DS}) was approximately linear and PPSU 30% membrane was the less affected membrane among them. It was found that increasing the flow rate of the DS on the support side of the HFFO membranes has no any effect on reducing the ICP when it was facing the support layer but caused the reducing in flux with a concomitant increase in the pumping energy cost.

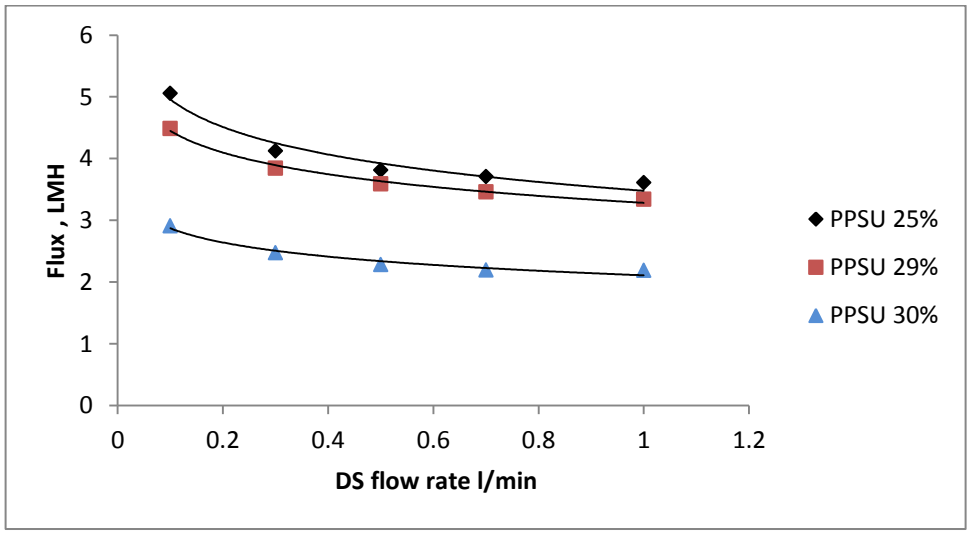

Figure 4.17 Water Flux Change with DS flow rate (Temp. 25±5˚C, 0.5M Feed solution conc. & 1M draw solution conc., 0.1 l/m feed solution flow rate, and for three types of PPSU Membranes).

4.4.4 Effect of Feed Solution Flow Rate on water flux

The forward osmosis unit was operated under different feed solution flow rates (Q_{FS}) (0.1, 0.3, 0.5, 0.7 and 1.0 l / min). The effect of these flow rates on the flux for the three types of HFFO membranes was observed as shown in Figure (4.18), the increase in the water flux proportionally with increasing the FS flow rate. Increasing the flow rate of FS caused lowering the concentration

accumulated near the active layer of HFFO membrane surface (i.e. reducing the concentrative external concentration polarization), results in decreasing the osmotic pressure in the feed solution region and thus increased the driving force which in term leading to increase the water flux. These observations are well agreed with **(Roy et al., 2016)** which illustrated that the flux decline with lower FS flow rate due to ECP was limited by the flow velocity**.** For PPSU 25% membrane, the increase in water flux with feed flow rate 0.1−0.5 l/min was 24% (5.05 – 6.74 LMH) while the flux increase was 24% (6.74 – 8.42 LMH) for feed flow rate 0.5−1.0 l/min. With respect to PPSU 29% and PPSU 30% membranes, the increase in water fluxes for flow rate 0.1−0.5 l/min were 28% (4.48 – 5.76 LMH) and 31% (2.90 – 3.81 LMH) respectively. And, when the flow rate increased 0.5−1.0 l/min, the water fluxes increased about 22% (5.76– 7.05 LMH) for PPSU 29% and 24% (3.81 – 4.76LMH) for PPSU 30%. These results prove the preference of PPSU 25% membrane than others. Figure (4.18) shows that PPSU 30% membrane was less influenced by Q_{FS} variation.

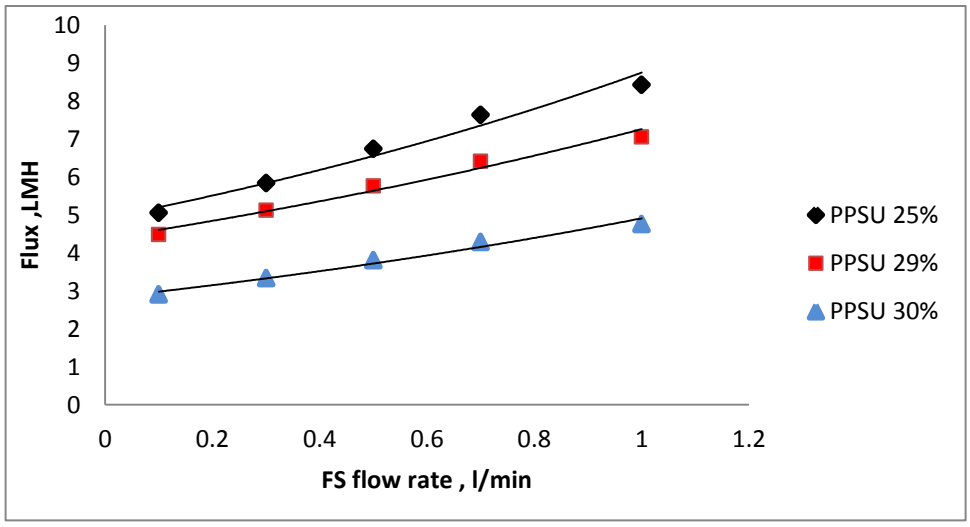

Figure .4.18. Water Flux Change with FS flow rate (Temp. 25±5 ˚C, 0.5M Feed solution conc.& 1M draw solution conc. , 0.1 l/m draw solution flow rate, and for three types of PPSU Membranes)

4.4.5 Reverse Salt Flux variation with time

Figure (4.19) shows the difference in the reverse salt flux between the three types of membrane (PPSU 25%, PPSU 29%, and PPSU 30%). This difference was mainly due to the structure and composition of the membranes by different polymer ratios. It was clearly observed that the reverse salt flux was decreased with time. For PPSU 25% membrane, the decrease was 21% at the first half hour of the experiment, while for PPSU 29% and PPSU 30% membranes, the decrease was 20% and 17% respectively. The decrease in the reverse salt flux was severe in the first hour of the experiment and then the decline becomes stable.

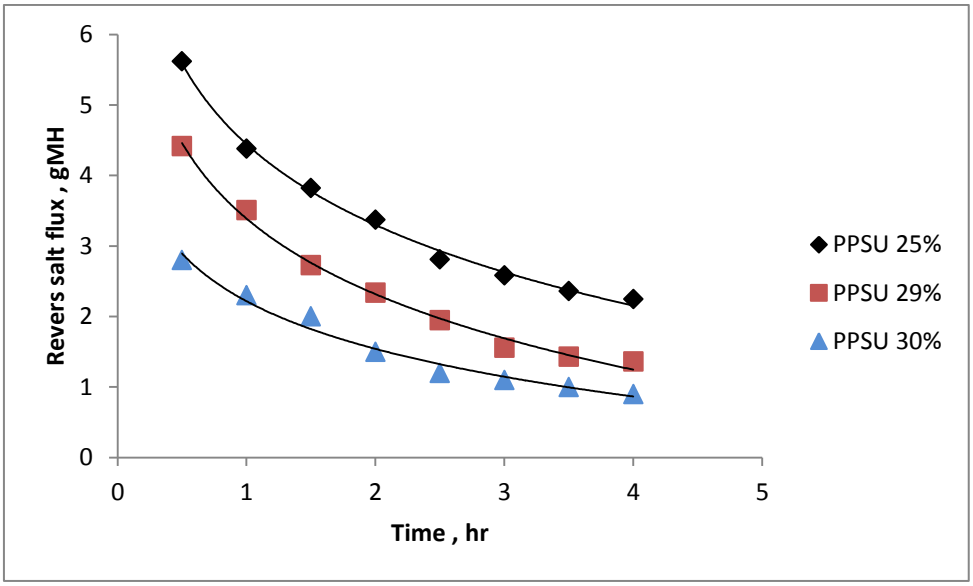

Figure 4.19. Reverse Salt Flux with Time (Temp. 25±5˚C, DI water & 1 M draw solution conc. , 0.1 l/m feed & draw solution flow rate, and for three types of PPSU HF Membranes).

4.4.6 Reverse draw solute flux as function of draw solution concentration.

To study the effect of the draw solution concentration on the reverse solute flux, several experiments were conducted using NaCl salt with different

concentrations changed from 1 to 3 M for all of three types of HFFO membranes. The results of the experiments are shown in Figure 4.20. As expected, increasing the concentration of the draw solution increased the reverse solute flux as a result of increasing the driving force of the process as mentioned in previous research **(Al-aibi et al., 2016; Phillip et al., 2010)** which showed that reverse salt flux (Js) increased with an increase in the osmotic pressure difference (i.e. an increase in the sodium chloride draw solution concentration). Figure 4.20 indicates that the higher reverse salt flux for PPSU 25% than other membranes. The increase in the reverse salt flux (RSF) for PPSU 25% was 67% for concentration (1.0−1.5 M), while for PPSU 29% and PPSU 30%, were 80% and 70% respectively. The increase in salt flux with concentration (2.0−3.0 M) were 78% , 55% and 18% for PPSU 25% ,PPSU 29% and PPSU 30% respectively.

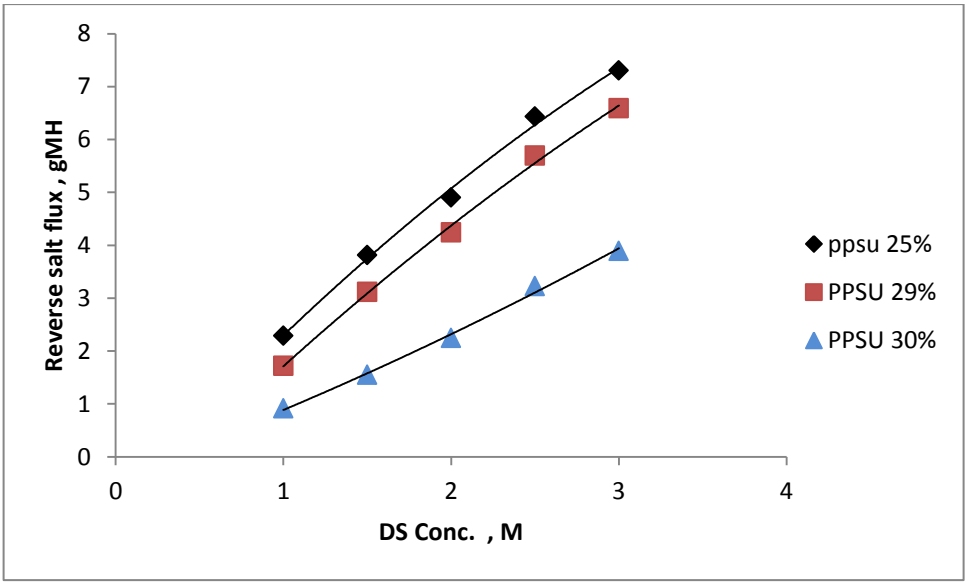

Figure. 4.20. Effect of Draw Solution Concentration on the reverse salt flux (Temp. 25±5˚C, Feed & Draw Flow Rate 0.1 l/min, 0.5 M FS conc. and for three types of PPSU Membranes).

4.4.7. Specific revers salt flux with draw solution concentration

Specific Reverse Salt Flux (SRSF, Js/Jw) measurement is an important and well-known method for assessing the performance of a membrane and the draw solution. The specific salt flux (Js/Jw) for the draw solutions used in this study is demonstrated in Figure (4.21), where Js is the reverse salt flux and Jw represent the water flux. The average Js/Jw for PPSU 25%, PPSU 29%, and PPSU 30% were 0.5, 0.47, and 0.40 g/l respectively. PPSU 25% has higher Js/Jw than PPSU 29% and PPSU 30% with a percent of 6% and 25% respectively.

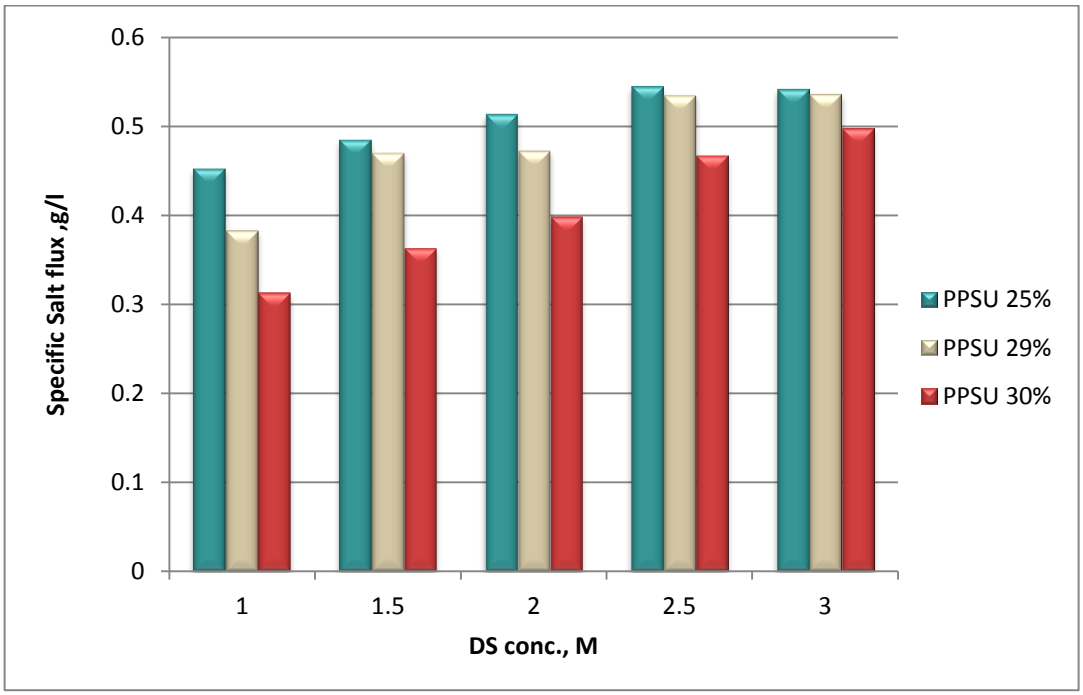

Figure 4.21. Comparison of Specific Salt Flux with Different concentration of Draw Solutions for three types of membranes. (Temp. 25±5˚C, Feed & Draw Solution Flow Rate 0.1 l/min and 0.5 M FS conc.).

4.4.8. Specific Salt Flux variation with time

Figure (4.22) shows changing of the specific salt flux with time of HF membranes when using high DS concentration of 1M NaCl and deionized

water (DI) as FS. The result indicated the decrease of the specific RSF with time, PPSU 25% shows higher J_s/J_w (0.88 g/l) than PPSU 29% (0.84 g/l) and PPSU 30% (0.68 g/l) at the first half hour of the experiment. The J_s/J_w at four hours for PPSU 25%, PPSU 29%, and PPSU 30% are 0.78, 0.67, and 0.52 g/l respectively. The specific RSF was an important parameter in FO because it provided a quantitative measure of the mass of solutes lost from the DS per volume of water recovered from the feed.

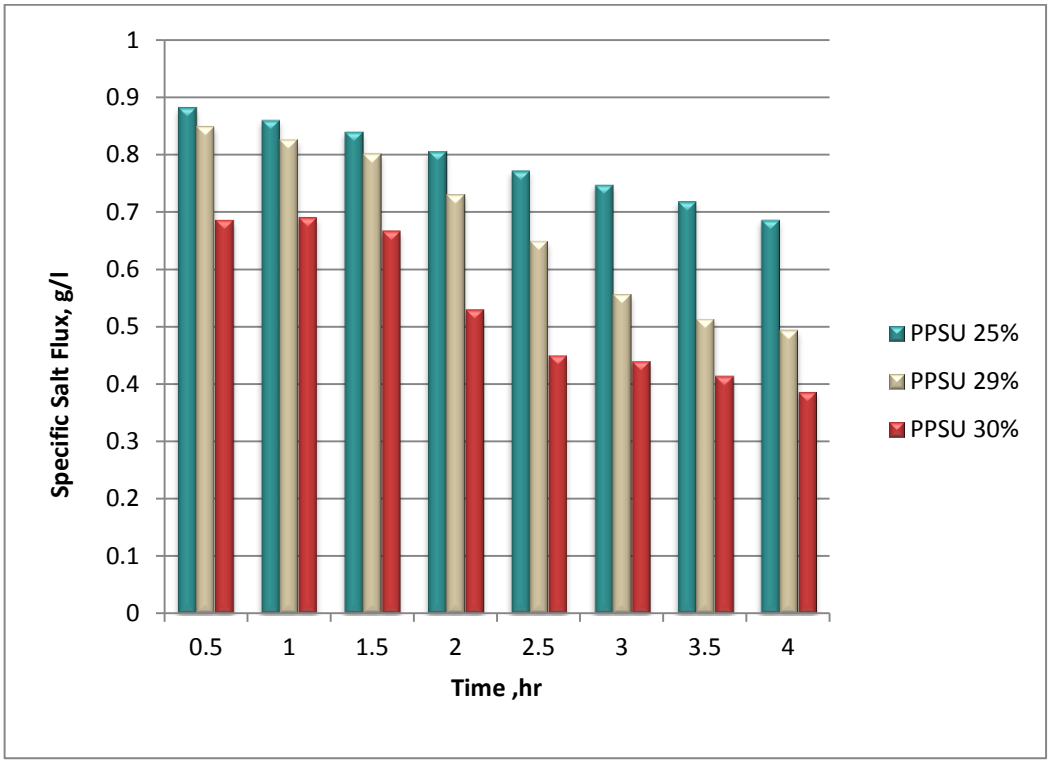

Figure.4.22. Specific salt flux with Time (Temp. 25±5˚C, DI water & 1 M draw solution conc. , 0.1 l/m feed & draw solution flow rate, and for three types of PPSU HF Membranes).

4.5 Comparison the FO performances in the present work with previous researches

This work investigates a new approach to fabricate hollow fiber membrane by using high percentage of Poly (phenyl sulfone) PPSU reached 30% (to the

best of our knowledge have not previously been used), to illustrate the effect of polymer concentration on the properties of the membranes used in forward osmosis process. The hollow fiber membranes PPSU 25, 29% in this work showed higher water flux and salt rejection than other PPSU flat sheet membrane used (at the FO and RO mode) in previous study **(Widjojo et al., 2013)** with much lower salt permeability (B). And in spite of the lower water flux of PPSU 30% as compared with PPSU hollow fiber membrane used by- **(Zhong et al., 2013)** but it showed higher rejection of salt and lower structural parameters that was good indication of the membrane ability to internal concentration polarization resistant and it is worth noting that the PPSU 25% and PPSU 29% have shown a much lower value than them. And when discussing the other HF membrane properties as compared with membrane fabricated by different materials such as polyketone as reported in the three PPSU hollow fiber membranes have lower thickness that help to reduce the accumulation of salts on the surface of the membranes and PPUS 30% showing higher water permeability coefficient and lower salt permeability coefficient than TFC-FO (HF-B) used by **(Shibuya et al., 2017)**. However, when considering the diameter of the membrane used in FO process, the small diameter produces higher water flux, and that got through comparison with **(Wang et al., 2010)** which used a large lumen with an inner diameter of >1mm and a wall thickness of 0.17–0.215mm.

With the variation of the polymer concentration used in the manufacture of membranes in this research, it can be observed that low polymer content led to improved properties and performance of membranes in most respects. **(Zhang et al., 2017)** used concentrations range from (16-21 wt%) of polyvinylidene fluoride (PVDF) that exhibited an improvement in membrane performance in

porosity, water and permeability coefficient, structural parameter, water flux, and with reduced of reverse salt flux. The PPSU- HFFO membranes showed higher porosity lower structural parameter (S), and higher water flux than PVDF 21% HF membrane despite using higher PPSU polymer concentration. Most of the research that was being investigated in the field of membrane testing and its efficiency in the forward osmosis process was limited to the use of distilled water as a feed solution within it and that the use of synthetic saline water in this work gave practical application to membrane and the forward osmosis process efficiency in saline water desalination at the same time

CHAPTER FIVE

CONCLUSIONS AND RECOMMENDATIONS

5. Conclusions

The following conclusions can be derived from this study:

1. The forward osmosis process is able to extract water from saline water with high efficiency.
2. The membrane manufactured using polyphenylsulfone (PPSU) polymer was appeared to have high efficiency to reject the salts with high water flux. The water flux of 25% PPSU HFFO membrane was higher than PPSU 29% and PPSU 30% flux. The water flux order for the three membranes were :

   PPSU 25% > PPSU 29% > PPSU 25%

   The reverse salt flux for PPSU 25% membrane was the higher one.
3. The flux of water produced from the osmosis module increased with the increase of the concentration of the draw solution and the flow rate of the feed solution. While, decreased with the increase of feed solution concentration and the flow rate of the draw solution.
4. The reverse salt flux amount increased with increasing draw solution concentration while it decreased over the time of experiments.
5. The PPSU 30% showed higher salt rejection percentage.

6. the concentration of draw solution was the higher effected parameter on flux than other parameters.
7. PPSU 25% has high porosity, low thickness and structural parameter values which increased with increasing polymer content in the membrane. While has a high pore size which was decreased with increasing polymer content. So the water and salt permeability coefficient for PPSU 25% hollow fiber membrane were higher than for PPSU 29% and PPSU 30%.

5.1 Recommendations for Further Work

1. Using other types of draw solution to choose the best and least expensive, such as hydrogels and nanoparticles materials. to examine the performance of forward osmosis process.
2. Testing another boundary conditions such as the changing in temperature, feed solution concentration, and pH. And study their effect on PPSU hollow fiber membrane and forward osmosis process generally.
3. Studying the fouling and internal and external concentration polarization on forward osmosis process.
4. Developing the forward osmosis process by connecting it with other systems such as reverse osmosis and membrane distillation or ultrafiltration to separate the draw solution after dilution. And calculating the efficiency and the economic feasibility of the process.

- Akther, N., Sodiq, A., Giwa, A., Daer, S., Arafat, H. A., & Hasan, S. W. (2015). Recent advancements in forward osmosis desalination: a review. Chemical Engineering Journal, 281, 502-522.
- Al-aibi, S., Mahood, H. B., Sharif, A. O., Alpay, E., & Simcoe-Read, H. (2016). Evaluation of draw solution effectiveness in a forward osmosis process. Desalination and Water Treatment, 57(29), 13425-13432.
- Alkaisi, A., Mossad, R., & Sharifian-Barforoush, A. (2017). A review of the water desalination systems integrated with renewable energy. Energy Procedia, 110, 268-274.
- Alobaidy, A. A., Sherhan, B. Y., Barood, A. D., & Alsalhy, Q. F. (2017). Effect of bore fluid flow rate on formation and properties of hollow fibers. Applied Water Science, 7(8), 4387-4398.
- Alsalhy, Q. F. (2012). Hollow fiber ultrafiltration membranes prepared from blends of poly (vinyl chloride) and polystyrene. Desalination, 294, 44-52.
- Alsalhy, Q. F., Rashid, K. T., Ibrahim, S. S., Ghanim, A. H., Van der Bruggen, B., Luis, P., & Zablouk, M. (2013). Poly (vinylidene fluoride-co-hexafluoropropylene)(PVDF-co-HFP) hollow fiber membranes prepared from PVDF-co-HFP/PEG-600Mw/DMAC solution for membrane distillation. Journal of Applied Polymer Science, 129(6), 3304-3313.
- Alsalhy, Q. F., Rashid, K. T., Noori, W. A., Simone, S., Figoli, A., & Drioli, E. (2012). Poly (vinyl chloride) hollow-fiber membranes for

ultrafiltration applications: Effects of the internal coagulant composition. Journal of Applied Polymer Science, 124(3), 2087-2099.

- Alsalhy, Q. F., Salih, H. A., Melkon, R. H., Mahdi, Y. M., & Abdul Karim, N. A. (2014). Effect of the preparation conditions on the morphology and performance of poly (imide) hollow fiber membranes. Journal of Applied Polymer Science, 131(12).

- Alsalhy, Q., Algebory, S., Alwan, G. M., Simone, S., Figoli, A., & Drioli, E. (2011). Hollow fiber ultrafiltration membranes from poly (vinyl chloride): preparation, morphologies, and properties. Separation Science and Technology, 46(14), 2199-2210.

- Altaee, A., Zaragoza, G., & van Tonningen, H. R. (2014). Comparison between Forward Osmosis-Reverse Osmosis and Reverse Osmosis processes for seawater desalination. Desalination, 336(1), 50–57.

- Arkhangelsky, E., Wicaksana, F., Chou, S., Al-Rabiah, A. A., Al-Zahrani, S. M., & Wang, R. (2012). Effects of scaling and cleaning on the performance of forward osmosis hollow fiber membranes. Journal of membrane science, 415, 101-108.

- Blandin, G., Verliefde, A. R., Comas, J., Rodriguez-Roda, I., & Le-Clech, P. (2016). Efficiently combining water reuse and desalination through forward osmosis—reverse osmosis (FO-RO) hybrids: a critical review. Membranes, 6(3), 37.

- Cath, T. Y., Childress, A. E., & Elimelech, M. (2006). Forward osmosis: principles, applications, and recent developments. Journal of membrane science, 281(1-2), 70-87.

- Chekli, L., Phuntsho, S., Shon, H. K., Vigneswaran, S., Kandasamy, J., & Chanan, A. (2012). A review of draw solutes in forward osmosis process and their use in modern applications. Desalination and Water Treatment, 43(1-3), 167-184.

- Choi, Y., Hwang, T. M., Jeong, S., & Lee, S. (2018). The use of ultrasound to reduce internal concentration polarization in forward osmosis. Ultrasonics sonochemistry, 41, 475-483.

- Chou, S., Shi, L., Wang, R., Tang, C. Y., Qiu, C., & Fane, A. G. (2010). Characteristics and potential applications of a novel forward osmosis hollow fiber membrane. Desalination, 261(3), 365-372.

- Chun, Y., Mulcahy, D., Zou, L., & Kim, I. S. (2017). A short review of membrane fouling in forward osmosis processes. Membranes, 7(2), 30.

- Chung, T. S., Li, X., Ong, R. C., Ge, Q., Wang, H., & Han, G. (2012). Emerging forward osmosis (FO) technologies and challenges ahead for clean water and clean energy applications. Current Opinion in Chemical Engineering, 1(3), 246-257.

- Clayton, R. (2015). A review of Current Knowledge : Desalination for Water Supply. Foundation for Water Research.

- Darvishmanesh, S., Tasselli, F., Jansen, J. C., Tocci, E., Bazzarelli, F., Bernardo, P., ... & Van der Bruggen, B. (2011). Preparation of solvent stable polyphenylsulfone hollow fiber nanofiltration membranes. Journal of membrane science, 384(1-2), 89-96.

- Darwish, M. A., Abdulrahim, H. K., Hassan, A. S., Mabrouk, A. A., & Sharif, A. O. (2014). The forward osmosis and desalination. Desalination and Water Treatment, 3994,1–27.

- Darwish, M. A., Abdulrahim, H. K., Hassan, A. S., Mabrouk, A. A., & Sharif, A. O. (2016). The forward osmosis and desalination. Desalination and Water Treatment, 57(10), 4269-4295.

- Devia, Y. P., Imai, T., Higuchi, T., Kanno, A., Yamamoto, K., & Sekine, M. (2015). Effect of Operating Conditions on Forward Osmosis for Nutrient Rejection Using Magnesium Chloride as a Draw Solution. World Academy of Science, Engineering and Technology, International Journal of Environmental, Chemical, Ecological, Geological and Geophysical Engineering, 9(6), 691-696.

- Duong, P. H., Chung, T. S., Wei, S., & Irish, L. (2014). Highly permeable double-skinned forward osmosis membranes for anti-fouling in the emulsified oil–water separation process. Environmental science & technology, 48(8), 4537-4545.

- Duranceau, S. J. (2012). Emergence of Forward Osmosis and Pressure-Retarded Osmotic Processes for Drinking Water Treatment. PDF). Florida Water Resources Journal, 32-36.

- Emadzadeh, D., Lau, W. J., Matsuura, T., Ismail, A. F., & Rahbari-Sisakht, M. (2014). Synthesis and characterization of thin film nanocomposite forward osmosis membrane with hydrophilic nanocomposite support to reduce internal concentration polarization. Journal of Membrane Science, 449, 74-85.

- Feng, Y., Han, G., Zhang, L., Chen, S. B., Chung, T. S., Weber, M., ... & Maletzko, C. (2016). Rheology and phase inversion behavior of polyphenylenesulfone (PPSU) and sulfonated PPSU for membrane formation. Polymer, 99, 72-82.

- García-Payo, M., Essalhi, M., & Khayet, M. (2010). Effects of PVDF-HFP concentration on membrane distillation performance and structural morphology of hollow fiber membranes. Journal of Membrane Science, 347(1-2), 209-219.

- Ge, Q., Ling, M., & Chung, T. S. (2013). Draw solutions for forward osmosis processes: developments, challenges, and prospects for the future. Journal of membrane science, 442, 225-237.

- Ghanbari, M., Emadzadeh, D., Lau, W. J., Riazi, H., Almasi, D., & Ismail, A. F. (2016). Minimizing structural parameter of thin film composite forward osmosis membranes using polysulfone/halloysite nanotubes as membrane substrates. Desalination, 377, 152-162.

- Gray, G. T., McCutcheon, J. R., & Elimelech, M. (2006). Internal concentration polarization in forward osmosis: role of membrane orientation. Desalination, 197(1-3), 1-8.

- Hawari, A. H., Kamal, N., & Altaee, A. (2016). Combined influence of temperature and flow rate of feeds on the performance of forward osmosis. Desalination, 398, 98-105.

- Holloway, R. W., Maltos, R., Vanneste, J., & Cath, T. Y. (2015). Mixed draw solutions for improved forward osmosis performance. Journal of membrane science, 491, 121-131.

- Jacob, A. (2006). A critical review of the history, development and future prospects for Forward Osmosis.
- Jacques Andrianne ,& FClix Alardin.(2002) Thermal and membrane process economics: optimized selection for sea water desalination . Desalination (153) 305-3 11.
- Kim, B., Lee, S., & Hong, S. (2014). A novel analysis of reverse draw and feed solute fluxes in forward osmosis membrane process. Desalination, 352, 128-135.
- Kim, J. E., Phuntsho, S., Lotfi, F., & Shon, H. K. (2015). Investigation of pilot-scale 8040 FO membrane module under different operating conditions for brackish water desalination. Desalination and Water Treatment, 53(10), 2782-2791.
- Kim, J., Jeong, K., Park, M. J., Shon, H. K., & Kim, J. H. (2015). Recent advances in osmotic energy generation via pressure-retarded osmosis (PRO): a review. Energies, 8(10), 11821-11845.
- Klaysom, C., Cath, T. Y., Depuydt, T., & Vankelecom, I. F. (2013). Forward and pressure retarded osmosis: potential solutions for global challenges in energy and water supply. Chemical society reviews, 42(16), 6959-6989.
- Korenak, J., Basu, S., Balakrishnan, M., Hélix-Nielsen, C., & Petrinic, I. (2017). Forward Osmosis in Wastewater Treatment Processes. Acta Chimica Slovenica, 64(1), 83-94.
- Lee, J. Y., Wang, Y., Tang, C. Y., & Huo, F. (2015). Mesoporous Silica Gel–Based Mixed Matrix Membranes for Improving Mass Transfer in

Forward Osmosis: Effect of Pore Size of Filler. Scientific reports, 5, 16808.

- Li, G., Wang, J., Hou, D., Bai, Y., & Liu, H. (2016). Fabrication and performance of PET mesh enhanced cellulose acetate membranes for forward osmosis. Journal of Environmental Sciences, 45, 7-17.
- Li, N. N., Fane, A. G., Ho, W. W., & Matsuura, T. (Eds.). (2011). Advanced membrane technology and applications. John Wiley & Sons.
- Linares, R. V., Li, Z., Sarp, S., Bucs, S. S., Amy, G., & Vrouwenvelder, J. S. (2014). Forward osmosis niches in seawater desalination and wastewater reuse. Water research, 66, 122-139.
- Linders, J. T. M. (1992). Patai's 1992 Guide to the Chemistry of Functional Groups, S. Patai, John Wiley, Chichester, 1992, vi+ 524 pp.,£ 39.95. ISBN 0-471-93022-9. Recueil des Travaux Chimiques des Pays-Bas, 111(10), 458-458.
- Lobo, V. M. M. (1993). Mutual diffusion coefficients in aqueous electrolyte solutions (technical report). Pure and applied chemistry, 65(12), 2613-2640.
- Loeb, S., Titelman, L., Korngold, E., & Freiman, J. (1997). Effect of porous support fabric on osmosis through a Loeb-Sourirajan type asymmetric membrane. Journal of Membrane Science, 129(2), 243-249.
- Long, Q., & Wang, Y. (2016). Novel carboxyethyl amine sodium salts as draw solutes with superior forward osmosis performance. AIChE Journal, 62(4), 1226-1235.

- Low, Z. X., Liu, Q., Shamsaei, E., Zhang, X., & Wang, H. (2015). Preparation and characterization of thin-film composite membrane with nanowire-modified support for forward osmosis process. Membranes, 5(1), 136-149.

- Lutchmiah, K., Verliefde, A. R. D., Roest, K., Rietveld, L. C., & Cornelissen, E. R. (2014). Forward osmosis for application in wastewater treatment: a review. Water research, 58, 179-197.

- Malak, H., Adel, O. S., Ghazi, D., Sami, A., & Ali, A. (2015). Draw solutions for Forward Osmosis process: Osmotic pressure of binary and ternary aqueous solutions of magnesium chloride, sodium chloride, sucrose and maltose. Journal of Food Engineering, 155, 10-15.

- McCutcheon, J. R., & Elimelech, M. (2006). Influence of concentrative and dilutive internal concentration polarization on flux behavior in forward osmosis. Journal of membrane science, 284(1-2), 237-247.
- McCutcheon, J. R., McGinnis, R. L., & Elimelech, M. (2005). A novel ammonia—carbon dioxide forward (direct) osmosis desalination process. Desalination, 174(1), 1-11.

- McCutcheon, J. R., McGinnis, R. L., & Elimelech, M. (2006). Desalination by ammonia–carbon dioxide forward osmosis: influence of draw and feed solution concentrations on process performance. Journal of membrane science, 278(1-2), 114-123.
- Mi, B., & Elimelech, M. (2010). Organic fouling of forward osmosis membranes: fouling reversibility and cleaning without chemical reagents. Journal of membrane science, 348(1-2), 337-345.

- Nasr, P., & Sewilam, H. (2015). Forward osmosis: an alternative sustainable technology and potential applications in water industry. Clean Technologies and Environmental Policy, 17(7), 2079-2090.

- Nasr, P., & Sewilam, H. (2016). Investigating the performance of ammonium sulphate draw solution in fertilizer drawn forward osmosis process. Clean Technologies and Environmental Policy, 18(3), 717-727.

- Ong, R. C., & Chung, T. S. (2012). Fabrication and positron annihilation spectroscopy (PAS) characterization of cellulose triacetate membranes for forward osmosis. Journal of membrane science, 394, 230-240.

- Ong, R. C., Chung, T. S., de Wit, J. S., & Helmer, B. J. (2015). Novel cellulose ester substrates for high performance flat-sheet thin-film composite (TFC) forward osmosis (FO) membranes. Journal of Membrane Science, 473, 63-71.

- Phillip, W. A., Yong, J. S., & Elimelech, M. (2010). Reverse draw solute permeation in forward osmosis: modeling and experiments. Environmental science & technology, 44(13), 5170-5176.

- Phuntsho, S., Vigneswaran, S., Kandasamy, J., Hong, S., Lee, S., & Shon, H. K. (2012). Influence of temperature and temperature difference in the performance of forward osmosis desalination process. Journal of membrane science, 415, 734-744.

- Ren, J., & McCutcheon, J. R. (2014). A new commercial thin film composite membrane for forward osmosis. Desalination, 343, 187-193.

- Roy, D., Rahni, M., Pierre, P., & Yargeau, V. (2016). Forward osmosis for the concentration and reuse of process saline wastewater. Chemical Engineering Journal, 287, 277-284.

- Sagle, A., & Freeman, B. (2004). Fundamentals of membranes for water treatment. The future of desalination in Texas, 2(363), 137.

- Sahebi, S., Phuntsho, S., Woo, Y. C., Park, M. J., Tijing, L. D., Hong, S., & Shon, H. K. (2016). Effect of sulphonated polyethersulfone substrate for thin film composite forward osmosis membrane. Desalination, 389, 129-136.

- Setiawan, L., Wang, R., Li, K., & Fane, A. G. (2011). Fabrication of novel poly (amide–imide) forward osmosis hollow fiber membranes with a positively charged nanofiltration-like selective layer. Journal of Membrane Science, 369(1-2), 196-205.

- Shibuya, M., Yasukawa, M., Mishima, S., Tanaka, Y., Takahashi, T., & Matsuyama, H. (2017). A thin-film composite-hollow fiber forward osmosis membrane with a polyketone hollow fiber membrane as a support. Desalination, 402, 33-41.

- Shokrollahzadeh, S., & Tajik, S. (2018). Fabrication of thin film composite forward osmosis membrane using electrospun polysulfone/polyacrylonitrile blend nanofibers as porous substrate. Desalination, 425, 68-76.

- Shon, H. K., Vigneswaran, S., Kandasamy, J., & Cho, J. (2002). Membrane technology for organic removal in wastewater.

- Su, J., & Chung, T. S. (2011). Sublayer structure and reflection coefficient and their effects on concentration polarization and membrane performance in FO processes. Journal of membrane science, 376(1-2), 214-224.

- Su, J., Yang, Q., Teo, J. F., & Chung, T. S. (2010). Cellulose acetate nanofiltration hollow fiber membranes for forward osmosis processes. Journal of membrane science, 355(1-2), 36-44.

- Subramani, A., & Jacangelo, J. G. (2015). Emerging desalination technologies for water treatment: a critical review. Water research, 75, 164-187.

- Tiraferri, A., Yip, N. Y., Phillip, W. A., Schiffman, J. D., & Elimelech, M. (2011). Relating performance of thin-film composite forward osmosis membranes to support layer formation and structure. Journal of Membrane Science, 367(1-2), 340-352.

- Trung, N. Q., & Thao, P. T. P. (2017). Novel draw solutes of iron complexes easier recovery in forward osmosis process. Journal of Water Reuse and Desalination, jwrd2017150.

- Wallace, M., Cui, Z., & Hankins, N. P. (2008). A thermodynamic benchmark for assessing an emergency drinking water device based on forward osmosis. Desalination, 227(1-3), 34-45.
- Wang, K. Y., Chung, T. S., & Amy, G. (2012). Developing thin-film-composite forward osmosis membranes on the PES/SPSf substrate through interfacial polymerization. AIChE journal, 58(3), 770-781.

- Wang, K. Y., Ong, R. C., & Chung, T. S. (2010). Double-skinned forward osmosis membranes for reducing internal concentration polarization within the porous sublayer. Industrial & Engineering Chemistry Research, 49(10), 4824-4831.

- Wang, K. Y., Yang, Q., Chung, T. S., & Rajagopalan, R. (2009). Enhanced forward osmosis from chemically modified polybenzimidazole (PBI) nanofiltration hollow fiber membranes with a thin wall. Chemical Engineering Science, 64(7), 1577-1584.

- Wang, R., Shi, L., Tang, C. Y., Chou, S., Qiu, C., & Fane, A. G. (2010). Characterization of novel forward osmosis hollow fiber membranes. Journal of membrane science, 355(1-2), 158-167.

- Wang, Y., Zhang, M., Liu, Y., Xiao, Q., & Xu, S. (2016). Quantitative evaluation of concentration polarization under different operating conditions for forward osmosis process. Desalination, 398, 106-113.

- Wei, J., Qiu, C., Tang, C. Y., Wang, R., & Fane, A. G. (2011). Synthesis and characterization of flat-sheet thin film composite forward osmosis membranes. Journal of Membrane Science, 372(1-2), 292-302.

- Widjojo, N., Chung, T. S., Weber, M., Maletzko, C., & Warzelhan, V. (2013). A sulfonated polyphenylenesulfone (sPPSU) as the supporting substrate in thin film composite (TFC) membranes with enhanced performance for forward osmosis (FO). Chemical engineering journal, 220, 15-23.

- Xiong, S., Zuo, J., Ma, Y. G., Liu, L., Wu, H., & Wang, Y. (2016). Novel thin film composite forward osmosis membrane of enhanced

water flux and anti-fouling property with N-[3-(trimethoxysilyl) propyl] ethylenediamine incorporated. Journal of Membrane Science, 520, 400-414.

- Yang, Q., Lei, J., Sun, D. D., & Chen, D. (2016). Forward osmosis membranes for water reclamation. Separation & Purification Reviews, 45(2), 93-107.
- Yang, X., Wang, R., Fane, A. G., Tang, C. Y., & Wenten, I. G. (2013). Membrane module design and dynamic shear-induced techniques to enhance liquid separation by hollow fiber modules: a review. Desalination and Water Treatment, 51(16-18), 3604-3627.
- Yasukawa, M., Mishima, S., Shibuya, M., Saeki, D., Takahashi, T., Miyoshi, T., & Matsuyama, H. (2015). Preparation of a forward osmosis membrane using a highly porous polyketone microfiltration membrane as a novel support. Journal of Membrane Science, 487, 51-59.
- Yip, N. Y., Tiraferri, A., Phillip, W. A., Schiffman, J. D., & Elimelech, M. (2010). High performance thin-film composite forward osmosis membrane. Environmental science & technology, 44(10), 3812-3818.
- Zhang, X., Shen, L., Lang, W. Z., & Wang, Y. (2017). Improved performance of thin-film composite membrane with PVDF/PFSA substrate for forward osmosis process. Journal of Membrane Science, 535, 188-199.
- Zhao, P., Gao, B., Yue, Q., & Shon, H. K. (2015). The performance of forward osmosis process in treating the surfactant wastewater: The

rejection of surfactant, water flux and physical cleaning effectiveness. Chemical Engineering Journal, 281, 688-695.

- Zhao, S., Zou, L., & Mulcahy, D. (2012). Brackish water desalination by a hybrid forward osmosis–nanofiltration system using divalent draw solute. Desalination, 284, 175-181.

- Zhao, S., Zou, L., Tang, C. Y., & Mulcahy, D. (2012). Recent developments in forward osmosis: opportunities and challenges. Journal of membrane science, 396, 1-21.

- Zhong, P., Fu, X., Chung, T. S., Weber, M., & Maletzko, C. (2013). Development of thin-film composite forward osmosis hollow fiber membranes using direct sulfonated polyphenylenesulfone (sPPSU) as membrane substrates. Environmental science & technology, 47(13), 7430-7436.

- Zhou, Z., Lee, J. Y., & Chung, T. S. (2014). Thin film composite forward-osmosis membranes with enhanced internal osmotic pressure for internal concentration polarization reduction. Chemical Engineering Journal, 249, 236-245.

- Zou, S., & He, Z. (2016). Enhancing wastewater reuse by forward osmosis with self-diluted commercial fertilizers as draw solutes. Water research,99,235-243.

Appendix–A

Experimental Results

Table B.1 Water Flux Change with Concentration Draw Solutes (Temp. 25±5 ˚C, Feed & Draw Flow Rate 0.1 l/min, and for three type of PPSU Membrane).

Conc., M	Water flux, LMH		
	PPSU 25%	PPSU 29%	PPSU 30%
1	5.05	4.48	2.90
1.5	7.86	6.41	4.27
2	9.55	8.97	5.63
2.5	11.79	10.64	6.90
3	13.48	12.82	7.81

Table B.2 Water Flux Change with DS flow rate (Temp. 25±5˚C, 0.5M Feed solution conc.& 1M draw solution conc. , 0.1 l/m feed solution flow rate, and for three type of PPSU Membrane).

DS flow rate (l/min)	Water flux, LMH		
	PPSU 25%	PPSU 29%	PPSU 30%
0.1	5.056	4.48	2.90
0.3	4.12	3.84	2.47
0.5	3.81	3.58	2.28
0.7	3.71	3.46	2.19
1	3.61	3.33	2.19

Table B.3 Water Flux Change with FS flow rate (Temp. 25±5˚C, 0.5M Feed solution conc.& 1M draw solution conc. , 0.1 l/m draw solution flow rate, and for three type of PPSU Membrane).

FS flow rate (l/min)	Water flux, LMH		
	PPSU 25%	PPSU 29%	PPSU 30%
0.1	5.05	4.48	2.90
0.3	5.84	5.12	3.33
0.5	6.74	5.76	3.81
0.7	7.64	6.41	4.28
1	8.42	7.05	4.76

Table B.4 Water Flux Change with time (Temp. 25±5˚C, DI water FS & 1.0 M draw solution conc. , 0.1 l/m feed & draw solution flow rate, and for three type of PPSU Membrane).

Time(hr)	Water flux, LMH		
	PPSU 25%	PPSU 29%	PPSU 30%
0.5	6.36	5.18	4.08
1	5.09	3.99	3.33
1.5	4.54	3.39	3.01
2	4.18	3.19	2.83
2.5	3.63	2.99	2.66
3	3.45	2.79	2.50
3.5	3.28	2.77	2.41
4	3.27	2.75	2.33

Table B.5 Reverse salt flux change with Draw Solution Concentration (Temp. 25±5˚C, Feed & Draw Flow Rate 0.1 l/min, 0.5 M FS conc. and for three types of PPSU Membranes).

Conc., M	Reverse salt flux, gMH		
	PPSU 25%	PPSU 29%	PPSU 30%
1	2.28	1.72	0.91
1.5	3.81	3.11	1.55
2	4.90	4.24	2.24
2.5	6.43	5.69	3.22
3	7.30	6.58	3.89

Table B.6 Reverse Salt Flux change with Time (Temp. 25±5˚C, DI water & 1.0 M draw solution conc. , 0.1 l/m feed & draw solution flow rate, and for three types of PPSU HF Membranes).

Time(hr)	Reverse salt flux, gMH		
	PPSU 25%	PPSU 29%	PPSU 30%
0.5	5.61	4.41	2.80
1	4.38	3.50	2.30
1.5	3.82	2.72	2.00
2	3.37	2.33	1.51
2.5	2.80	1.94	1.20
3	2.58	1.55	1.10
3.5	2.35	1.42	1.00
4	2.24	1.36	0.90

Table B.7 Specific Salt Flux with Different concentration of Draw Solutions for three types of membranes. (Temp. 25±5˚C, Feed & Draw Flow Rate 0.1 l/min and 0.5 M FS conc.).

Conc., M	Specific Reverse Salt Flux, g/l		
	PPSU 25%	PPSU 29%	PPSU 30%
1	0.45	0.38	0.31
1.5	0.48	0.47	0.36
2	0.51	0.47	0.39
2.5	0.54	0.53	0.46
3	0.54	0.53	0.49

Table B.8 Specific salt flux with Time (Temp. 25±5˚C, DI water & 1 M draw solution conc. , 0.1 l/m feed & draw solution flow rate, and for three types of PPSU HF Membranes).

Time(hr)	Specific Reverse Salt Flux, g/l		
	PPSU 25%	PPSU 29%	PPSU 30%
0.5	0.88	0.84	0.68
1	0.86	0.82	0.69
1.5	0.84	0.80	0.66
2	0.80	0.73	0.52
2.5	0.77	0.64	0.45
3	0.74	0.55	0.44
3.5	0.71	0.51	0.41
4	0.68	0.49	0.38

الخلاصه

في هذه الدراسة تم دراسة كفاءة عملية التناضح الأمامي (FO) لتحلية المياه المالحة والعوامل المؤثرة على أداء العملية من خلال استخدام ثلاثة أنواع من الأغشية المجوفة. تم تصنيع ثلاثة ألياف مجوفه من بوليمر (بولي فينيل سلفون) (PPSU) بنسب مختلفة من البوليمر باستخدام طريقة تحويل الطور وتطبيقها في عملية التناضح الامامي (FO). تم قياس الخصائص المختلفة مثل البنية السطحية والمقطعية ، سمك الغشاء ، خشونة السطح ، متوسط حجم المسام وتوزع المسام باستخدام المجهر الإلكتروني (SEM) ومجهر القوة الذرية (AFM) وكذلك المسامية للألياف الثلاثة المجوفة. ايضا تم تحديد تأثير الظروف التشغيلية للعملية مثل تركيز محلول السحب (DS) بين (1- 3 مولاري) ، تركيز المحلول الحلول الداخل (FS) (الماء منزوع الأيونات و 0.5 مولاري) , تدفق المحلولين بين (0.1 - 1.0 - لتر / دقيقة) و الضغط عند درجة حرارة (25 ±5 درجة مئوية). وقد وجد أن تدفق الماء يزداد بزيادة تركيز محلول السحب ، ومعدل تدفق المحلول الداخل وينخفض مع زيادة معدل تدفق محلول السحب ، وتركيز المحلول الداخل . أظهر غشاء الألياف المجوفة 25٪ PPSU تدفق للماء (13.48 لتر/متر مربع × ساعه) عند اختباره بوضع المحلول الداخل يواجه الطبقة النشطة للغشاء باستخدام 0.5 مولاري و 3 مولاري لكلوريد الصوديوم كمحلول داخل و محلول سحب على التوالي. الزيادة في تدفق المياه للتركيز0.5-1.0 مولاري تتراوح ما بين 43 و 55 ٪ ، في حين أن التركيز 1.5–2.0 مولاري 2.0–2.5 مولاري, و 2.5–3.0 مولاري كانت 21–39 ٪ ، 24 ٪ 23 ٪

، و 18 – 23 ٪ على التوالي لثلاثة أغشية ليفية مجوفة. هذه النتيجة تكشف ان اعلى تدفق المياه التي تم الحصول عليها مع تركيز 1.5–1.0 مولاري .في حين كان تدفق الملح العكسي (7.30غم/ متر مربع × ساعه). بالإضافة إلى ذلك ، أظهرت PPSU 25٪ نفاذية للماء النقي أعلى (2.25 لتر/متر مربع × ساعه × بار) بنسبة 29٪ و 56٪ من PPSU 29% و PPSU 30%على التوالي. ونفاذية الملح (B) PPSU 25٪ كانت (0.37 لتر/متر مربع × ساعه) والتي كانت أعلى أيضًا من الأغشية الأخرى. يقل حجم المسام بحوالي (22.28 و 28.75٪) من السطح الداخلي ، بينما انخفض السطح الخارجي بحوالي (26.88 و 38.78٪) مع زيادة تركيز البوليمرات PPSU من 25٪ إلى 29 و 30٪ بالوزن ، على التوالي. أظهرت المعلمة الهيكلية (S) قيمة أقل لـ PPSU 25٪ من من الأغشية الاخرى (467 مايكرومتر) والتي كانت متوافقة بشكل جيد مع أدائها. في الختام ، أشارت النتائج إلى أن عملية التناضح الأمامي كانت أداء مشجعاً وأن غشاء الألياف المجوفة PPSU كان قادراً على تحلية المياه المالحة بتركيزات ومصادر مختلفة.

وزارة التعليم العالي والبحث العلمي
الجـــامعة التكنـــولوجية
قسـم الهندســة الكيميـــاويـة

تصنيع و اختبار اداء غشاء البولي فينول سلفون في عملية التناضح الامامي لتحلية المياه المالحة

رسالة مقدمة الى

قسم الهندسة الكيمياوية/ الجامعة التكنولوجية/ كجزء من متطلبات الدراسة لنيل درجة ماجستير علوم في الهندسة الكيمياوية / هندسة العمليـات الكيميـاوية

من قبل

مريم جبر جعفر

بأشراف

أ. د قصي فاضل الصالحي **أ.م. د. جنان عبد الكريم النجار**

2018 **1439**